10-28-2008

Compliant Prosthetic Knee Extension Aid: A Finite Elements Analysis Investigation of Proprioceptive Feedback During the Swing Phase of Ambulation

Adam Daniel Roetter
University of South Florida

Compliant Prosthetic Knee Extension Aid: A Finite Elements Analysis Investigation of Proprioceptive Feedback During the Swing Phase of Ambulation

by

Adam Daniel Roetter

A thesis submitted in partial fulfillment
of the requirements for the degree of
Master of Science in Mechanical Engineering
Department of Mechanical Engineering
College of Engineering
University of South Florida

Major Professor: Craig Lusk, Ph.D.
Rajiv Dubey, Ph.D.
Nathan Crane, Ph.D.

Date of Approval:
October 28, 2008

Keywords: compliant mechanisms, proprioception, knee disarticulation, polycentric 4-bar, prosthetic, interface mechanics, design by specialization

Acknowledgments

There are many people who have contributed to my life during the course of this thesis and the road to it, which I would like to recognize. First and foremost, I am truly grateful to my father, who has sacrificed so much my entire life and has been my shining mentor; who has taught me to learn from my mistakes and to love and appreciate everything along the way, who has been my best friend and an irreplaceable part of my world. To my loving step-mother, Bev, for all the support and love she has given to me and for being the piece of my family I had been missing for so long. To my beautiful wife-to-be, Laura, for her constant love, support, admiration and understanding; I love and appreciate all she has done for me and sincerely hope her sacrifices will be well rewarded. To Laura's family, Patty, Glenn, Audrey and Calvin, for their constant interest in my work and my life, and for showing me support whenever they knew I needed it.

I greatly appreciate my fellow peers, whose friendships have kept my life true and meaningful. To Pete for all the times we studied and worked on finite elements and for the great future to-come with our families. To my friends Anthony, Jason, Jeff and Aaron, your friendships' have truly made my life richer.

To my professors who have nourished my desire for learning over these past years I cannot thank you enough. To my committee who has taken so much time to review my work and offer their thoughts and guidance I am forever grateful, I am particularly grateful to my advisor Dr. Lusk, for all his support and encouragement.

Finally, I am eternally grateful for the abundant blessings God has offered me and the strength he has given me to push forward.

Table of Contents

List of Tables

List of Figures

Compliant Prosthetic Knee Extension Aid: A Finite Elements Analysis Investigation of Proprioceptive Feedback During the Swing Phase of Ambulation

Adam Daniel Roetter

ABSTRACT

Compliant mechanisms offer several design advantages which may be exploited in prosthetic joint research and development: they are light-weight, have low cost, are easy to manufacture, have high-reliability, and have the ability to be designed for displacement loads. Designing a mechanism to perform optimally under displacement rather than force loading allows underlying characteristics of the swing phase of gait, such as the maximum heel rise and terminal swing to be developed into a prosthetic knee joint. The objective of this thesis was to develop a mechanical add-on compliant link to an existing prosthetic knee which would perform to optimal standards of prosthetic gait, specifically during the swing phase, and to introduce a feasible method for increasing proprioceptive feedback to the amputee via transferred moments and varying surface tractions on the inner part of a prosthetic socket. A finite elements model was created with ANSYS to design the prosthetic knee compliant add-on and used to select the geometry to meet prosthetic-swing criteria. Data collected from the knee FEA model was used to apply correct loading at the knee in a SolidWorks model of an above-knee prosthesis and residual limb. Another finite element model was creating using COSMOSWorks to determine the induced stresses within a prosthetic socket brought on

by the compliant link, and then used to determine stress patterns over 60 degrees of knee flexion (standard swing). The compliant knee add-on performed to the optimal resistance during swing allowing for a moment maxima of 20.2 Newton-meters (N-m) at a knee flexion of 62 degrees. The moments applied to the prosthetic socket via the compliant link during knee flexion and extension ranged from 5.2 N-m (0 degrees) in flexion, to 20.2 N-m (62 degrees) in extension and induced a varying surface tractions on the inner surface of the socket over the duration, thus posing a possible method of providing proprioceptive feedback via surface tractions. Developing a method for determining the level of proprioceptive feedback would allow for less expensive and more efficient methods of bringing greater control of a prosthesis to its user.

Chapter 1 Overview

The objective of this thesis was to develop a compliant linkage add-on as a design specialization to the Otto Bock 3R21 frame (Figures 1-1 and 1-2) and to test the hypothesis that the extension moments brought about by the compliant extension aid offer a method of providing proprioceptive feedback to the amputee via variable stress patterns on the inner part of the prosthetic socket over the swing phase of the gait cycle. This hypothesis was tested by developing a Computer Assisted Drawing (CAD) and Finite Element (FE) model of the knee with the bistable compliant extension aid (Figure 1-3), a prosthetic socket and residual limb with simplified geometry. Knee flexion (0-90 degrees) and the resulting forces and moments were analyzed with ANSYS, and the resulting tractions on the socket analyzed using SolidWorks (COSMOSWorks).

The criterion we adopted for analyzing proprioception was that the tractions applied to the inner part of the socket showed distinct variation over the swing phase, remained tolerable by the user and did not cause failure of the polypropylene socket. This criterion provided the basis for analytical work but should be refined through clinical testing.

Figure 1-1. Photograph of Otto Bock 3R21 Modular 4-Bar Linkage Knee Joint

Figure 1-2. CAD Model of Otto Bock 3R21 Modular 4-Bar Linkage Knee Joint

Figure 1-3. Otto Bock 3R21 with Bistable Compliant Extension Aid Concept

1.1 Background

The introduction of compliant mechanism technology offers several advantages in prosthetic joint design: low friction and wear, low part count, lighter weight, high reliability and efficient manufacturing and assembly. These advantages, as well as the ability to design for displacement loading, fit compliant mechanisms well into the design of an efficient prosthetic knee during swing.

1.1.1 Background – History of Prosthetics and the Prosthetic Knee

Prosthetics are said to have existed from the times of the ancient Egyptians. Prosthetics were used in many applications: function, cosmetic appearance and most important to the ancient Egyptians, psycho-spiritual sense of being whole. It was feared by many that when an amputation was performed the individual would be left un-whole in the afterlife. Once performed, the amputated limb was buried until the individual passed when it would be placed with the body so as to make them whole for the afterlife. One of the earliest known examples of a cosmetic prosthesis date back to the 18th dynasty of ancient Egypt where a mummy was found with a prosthetic toe made of leather and wood (Figure 1-4). Greek and Roman civilizations are sometimes credited for creating prostheses for rehabilitation aids. [11]

Figure 1-4. Prosthetic Toe in Cairo Museum [11]

Modern prostheses are said to have originated from a man known as Ambroise Paré (Figure 1-5). The French surgeon contributed to the origination and perfection of the amputation procedure itself and among the first to show interest in the design of a *functional* prosthesis. Paré instructed a Parisian armor maker (Le petit Lorrain) to construct a metal above-knee prosthesis which consisted of a locking knee joint as well as an ankle joint. His prosthesis weighed 7 kg and was only suitable for equestrians. Functional prostheses were not used at that time mainly because the distal end of the residual limb could not be loaded without damage; this limited people to using crutches, peg legs or even crawling as means of locomotion. [29]

Figure 1-5. Ambroise Pare: Founder of Prosthetics [11]

After 1816, functional wooden prostheses were built which consisted of a mechanism which synchronized the motion of the knee and ankle joints. This ingenious mechanism was invented by James Potts, who also is credited with the use of the trumpet socket. This Total-Surface-Bearing-type socket along with the joint mechanism was made famous by the Count of Uxbridge, also known as the Marquees of Anglesey who lost his leg in the Battle of Mont St. Jean in 1815. [29]

Over the course of history, large scale wars have directed government interests towards research and development of more efficient and functional prostheses. Following World War I, materials such as aluminum and rubber were being tested as alternative materials which led to the current research on space-age materials and mechanism designed to improve user comfort, mechanical efficiency, and cosmetic symmetry.

1.1.2 Background – Compliant Mechanisms and Current Research

Compliant mechanisms are mechanisms that gain some or all of their motion from the deflection of flexible segments [8]. Compliant mechanisms store and release strain energy as they move. Input forces are required to store strain energy and output forces can be provided when strain energy is released. Most compliant mechanisms have an unstressed (or minimum energy) state which they naturally assume. In a bistable mechanism (a mechanism which contains two stable equilibrium positions), the mechanism has two distinct locally minimum energy states. A bistable mechanism will oppose forces that drive the mechanism from either one of the stable positions. Bistable mechanisms make sense for prosthetic knees because they offer two home positions (straight and bent) for the leg. The straight-leg position is the preferred home position while walking or standing, and the bent-leg position is the preferred home position when sitting. Furthermore, the change in stored strain energy between stable points offers a characteristic moment-rotation profile or 'feel' to leg motion, thus increasing user proprioception over the position of their knee and lower leg. Other potential advantages

of compliant mechanisms are the lower costs of manufacturing and assembly through lower part count as well as the reduction of weight when compared with rigid-body counterparts.

Compliant mechanisms are used by the public everyday, and a few are so commonplace that their compliance is considered unremarkable. The paperclip and shampoo bottle cap are examples of such 'unremarkable' compliant mechanisms. The paperclip utilizes stored strain energy to hold paper together by attempting to return to its original shape. The shampoo bottle incorporates small plastic flexures known as living hinges in the cap. These are some of the simplest forms of compliant mechanisms.

Figure 1-6. Common Compliant Mechanisms

Other more advanced mechanisms can be designed compliant or can be transformed via compliant mechanism synthesis. The crimping device shown in Figure 1-7 (a) is very similar to its rigid-body counterpart (Figure 1-7 b). The locking jaws serve similar functions, while the weaker material used to construct the compliant version limits its applicability. The plastic construction of the compliant crimping device limits its maximum output force, and its compliant members store some of the work provided by the input force in the form of strain energy making less work available for output at the jaws. As shown, the design of the crimping device was based upon a rigid body mechanism which has four separate parts, but is realized using a single monolithic part.

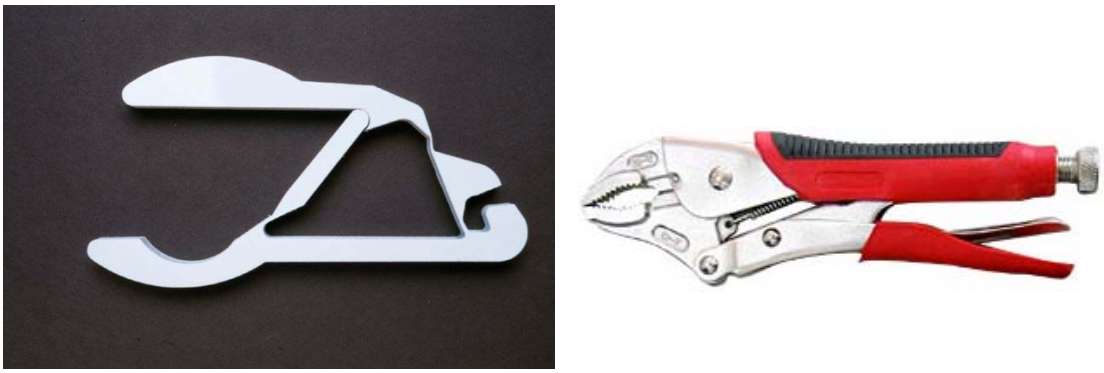

(a) (b)

Figure 1-7. Crimping Mechanism, Compliant & Rigid-Body Counterpart
Courtesy of the Compliant Mechanisms Research Group (CMR) at Brigham Young University

A reduction in part count is one of the most noticeable differences between compliant mechanisms and their rigid-body counterparts. The Compliant Mechanisms Research group at Brigham Young University designed and prototyped an overrunning clutch using only two links and a pin. Figure 1-8 (a) shows the latter, while (b) depicts its rigid-body counterpart which has a significant increase in part count.

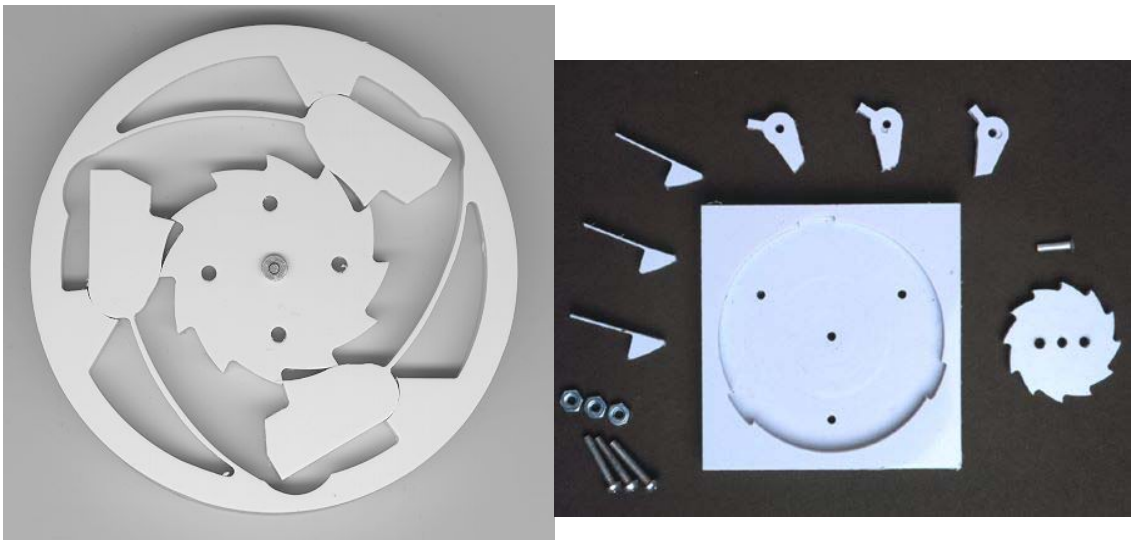

(a) (b)

Figure 1-8. Overrunning Clutch, Compliant & Rigid-Body Counterpart
Courtesy of the Compliant Mechanisms Research Group (CMR) at Brigham Young University

Compliant mechanisms have advantages and disadvantages when compared with their rigid-body counterparts, whose importance depends upon the requirements of a given application. For example, some applications have requirements for high precision, some for high strength, and some require both. Both of these requirements have been demonstrated in compliant mechanism design. For example, the concept of high strength has been demonstrated in High Compression Compliant Mechanisms (HCCMs) by Alexandre Guèrinot in his design of a compliant prosthetic knee [5] (discussed in the next section). High precision mechanisms have been applied to Micro-Electromechanical systems (MEMS). The prosthesis industry is a recent target for compliant mechanism designs, which are discussed in the next section.

1.1.3 Background – Compliant Mechanism Prosthetic Joint Research

Compliant mechanisms have made the transition to prosthetics joint research. For example, compliant prosthetic knees have been researched at The University of South Florida under the direction of Dr. Craig Lusk [10] and at Brigham Young University's CMR under Dr. Larry Howell [5]. A compliant prosthetic ankle was designed and analyzed at BYU by Jason Wiersdorf [32] under Dr. Howell and Dr. Magleby.

The introduction of compliant mechanisms under loading more appropriate to rigid-body mechanisms is a challenging task and must be done under heavy scrutiny. Prosthetic knees and ankles see very large compressive loads which are not suited for compliant mechanisms. Theories have been developed to alleviate these major design issues and are discussed.

Prosthesis design and engineering has made transitions from new materials to exotic mechanism design (including CPU control), and has traditionally been constructed to withstand any and all buckling of members comprising the mechanisms. Compliant mechanism design is counter to the concept of the rigid structure as they gain all of their motion from the bending/buckling of the compliant members. Nature employs compliant structures to provide both movement and strength. Ligaments are made of flexible, fibrous tissue which binds bones together, and helps form the joints necessary for locomotion and movement. A common misperception is that strength and safety necessarily go hand-in-hand with stiffness. This is one reason why the prosthesis industry is dominated by rigid-body mechanisms which use pins and friction rather than compliant parts. The concept that stiffness equals strength is, in fact, incorrect as a healthy biological knee shows. It is quite contrary to the 'stiffness equals safety' argument since as a knee gets stiffer, a decrease in function is noticed (i.e. arthritis). "This design preference can largely be attributed to the long legacy of design for force loads rather than design for displacement loads that has influenced the engineering community" [5].

Prosthetic knees are designed to meet strict safety criteria and must be able to withstand high compressive loading. On the other hand, compliant mechanisms are more typically designed under tensile loads rather than the compressive ones that the knee joint sees. Work done by Alexandre Guèrinot [5,6] with High Compression Compliant Mechanisms (HCCMs) have opened new doors to the applicability of compliant mechanisms to high compression situations similar to those faced in the prosthetic knee

joint. He laid the groundwork for design of compliant mechanisms which can carry high compressive loading by using two design principles: inversion and isolation.

Inversion is the ability of the compliant mechanism to 'invert' a compressive load into a tensile load by the design of the mechanism's geometry. "The concept of inversion builds on the proposition of tensurial pivots, which are flexures loaded in tension" [5]. The geometry of the rigid links invert the top and bottom of the mechanism thus transforming the load more appropriately for a compliant mechanism. Figure 1-9 depicts one of Guèrnot's inversion concepts of a knee prototype. Notice the top and bottom brackets invert the loading and thus allow the compliant segments to see a tensile load rather than compressive.

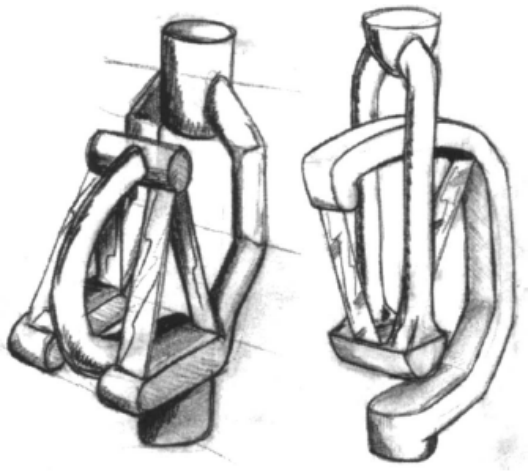

(a) (b)

Figure 1-9. Guèrinot's Inversion HCCM Concept
(a) Compressive Configuration, (b) Inverted Tensile Configuration [5]

The second principle Guèrinot discusses is the concept of isolation. Isolation is the ability to remove the load from the flexible segments and redirect it through the rigid-body segments. Isolation can be applied when compressive loads are in alignment. In prosthetic knees, isolation will allow the compliant knee to withstand the stance loading

while ‘feeling’ rigid and ‘strong’ to the user while at the same time during motion the compliance is unchanged and fully effective as a compliant mechanism. The true advantage of isolation is to harness the stiffness of the rigid body mechanism while still utilizing the flexibility of the compliant mechanism, thus increasing the overall compressive load capability of the compliant mechanism.

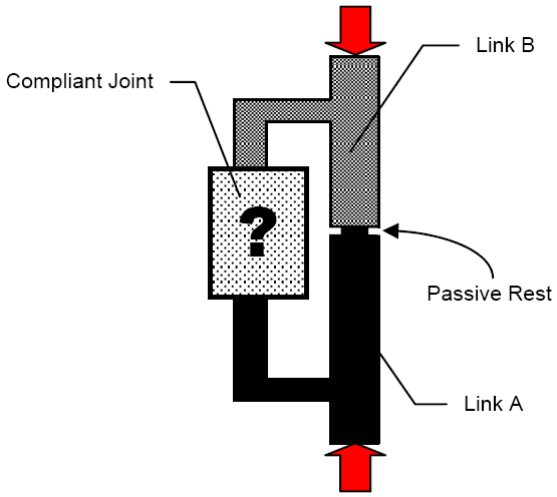

Figure 1-10. Guèrinot’s Isolation HCCM Concept [5]

Guèrinot’s design of a compliant knee joint included these concepts of inversion and isolation and was successful in supporting heavy compressive loads. Under testing, the knee, shown in Figure 1-11, was able to withstand close to 700 lbf in compression with roughly a mere 0.14-0.15 inches of displacement [5]. The success of a compliant mechanism being able to hold such high levels of compressive loads has been tested against the inversion and isolation theories and proved to be highly successful. These HCCM concepts are crucial for a fully compliant knee joint to be able to withstand the loading during the stance phase of gait (discussed later).

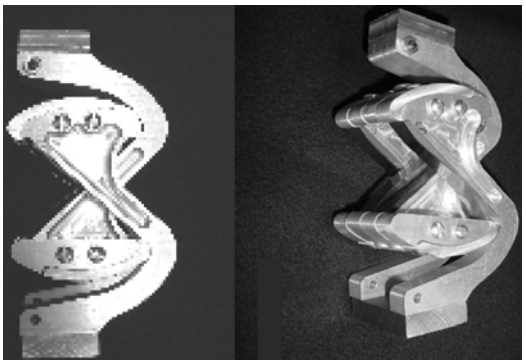

Figure 1-11. Guèrinot's Tested Inverted Cross-Axis Flexural Pivot Knee Prototype [5]

Further compliant knee joint research was conducted at the University of South Florida by Sebastian Mahler, under the direction of Dr. Craig Lusk [10]. Mahler designed and prototyped a pediatric prosthetic knee that introduced compliance into the mechanism shown in Figure 1-12. The major influential factor driving the design of a compliant pediatric prosthetic knee was the overall reduction in weight allowing the child to wear their prosthesis for longer periods of time. Children with above-knee amputations are typically given a peg leg to learn to walk on. The prosthetic leg must be shorter than the sound limb in order to clear the ground during swing, but this creates a gait pattern similar to walking with "one foot constantly in a hole" [10]. These major gait deviations are exacerbated later in life when learned at an early stage. The lighter knee, and thus a lighter prosthesis, allows the child to wear their prosthesis for longer periods of time without the discomfort of heavier prostheses. With longer wear, the child can learn to walk with a standard polycentric knee similar to that of an adult prosthesis, thus lowering or eliminating the gait deviations early.

Figure 1-12. Mahler's Pediatric Prosthetic Knee Prototype [10]

Mahler was able to analyze the motion of the knee prototype by using nonlinear finite elements analysis and the calculation of the mechanisms instant center of rotation. The reaction forces and resultant mechanism's stresses were also analyzed under deflections from 0° to 120°. Mahler's work focussed heavily on the concept of the instantaneous center of rotation. The instantaneous center (IC) of rotation is defined as a 'key point' where the body rotates about at a particular instant in time. This IC is at rest and is the only point at rest in the body at this particular instant. Mahler explains how the instant center of rotation and the stability of a prosthetic knee go hand in hand. A 'well placed' IC can give the prosthesis adequate toe clearance as well as provide the necessary trade-off from stability to control (discussed in detail later in the chapter). The instantaneous center of rotation is crucial point of design when considering polycentric prosthetic knee mechanisms, a mechanism with a varying IC through rotation. For a simpler single axis knee mechanism, the IC is constant and does not lend advantages such as those listed above.

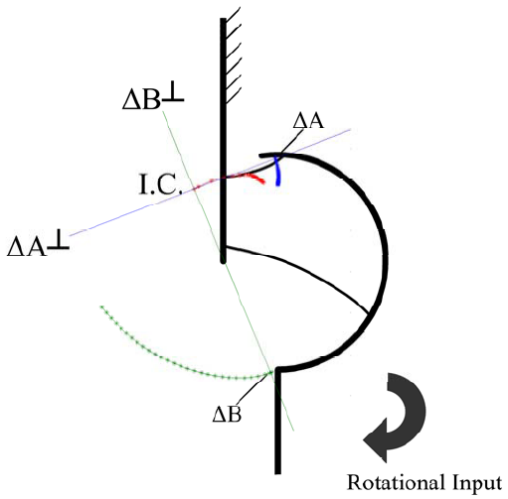

Figure 1-13. Mahler's Knee Instantaneous Center [10]

Mahler explains the four most important design characteristics for a pediatric prosthetic knee: toe clearance, stability, lightweight and adjustability. The toe clearance, and stability were analyzed under the nonlinear FEA, while the lightweight requirement was met with the compliant mechanism design. Adjustability was one of the foremost design challenges met with Mahler's pediatric compliant knee prototype. Adjustability of a prosthesis holds a high level of importance based upon the fact that no two people are exactly alike. Size and shape differences vary the gait pattern slightly from one individual to another, thus requiring the need for prosthesis adjustability. Mahler posed a design which could adjust the required torque necessary to initiate motion of the knee, thus allowing for differences in the child's activity level. The latter goes so far as to allow 'on-site' adjustability allowing the prosthesis to be set for standard walking and to be adjusted immediately for a higher level of activity.

The knee was evaluated at different compliant segment angles, i.e. at different levels of adjustments. The stresses and force data was evaluated for the mechanism at these different points. Stresses appeared to be higher than the materials yield strength and thus a method for removing or redirecting these stresses is needed in future work. These stresses brought about by prescribed compressive loading could be alleviated utilizing one or both of Guèrinot's theories, inversion and isolation, thus improving and perhaps perfecting a pediatric compliant prosthetic knee.

Compliant joint research also evaluated a prosthetic ankle joint with three degrees of freedom (the knee consists of just one degree of freedom). Jason Wiersdorf researched this project under the direction of Dr. Magleby at BYU's CMR [32]. While this project's emphasis is different than this thesis's, it is important to note that prosthesis research has been developed for other applications than the knee joint.

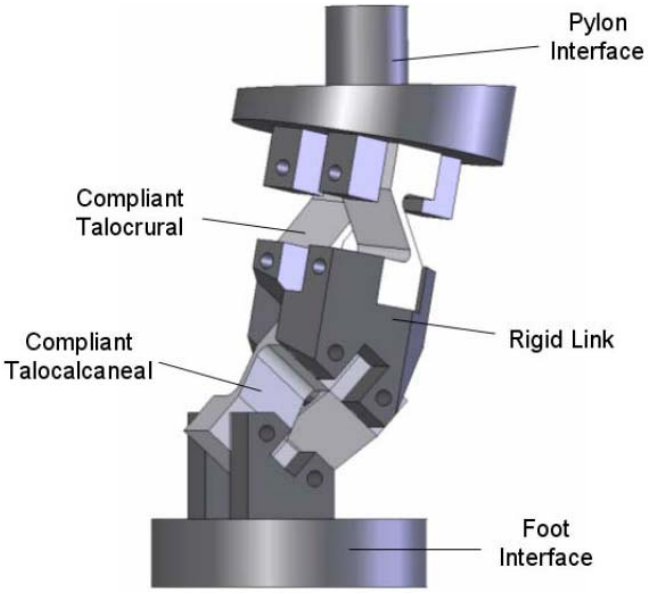

Figure 1-14. Wiersdorf's Modular Experimental Research Ankle (MERA) [32]

1.2 Phases of Gait

Gait, or the means of forward locomotion, has been standardized and broken into two distinct phases, stance and swing. Popular conventions have denoted particular points in the gait cycle by percentages. These percentages follow symmetry with one heel strike of a limb denoted 0% and the heel strike of the same limb as 100%. Each phase of gait can thus be characterized by a percentage of the cycle; stance accounts for the majority of the gait cycle with 60%, and swing owning the remaining 40%. Each phase of gait holds characteristics unique and easily definable. [30]

Stance includes four 'sub-phases': loading, midstance, terminal stance and pre-swing or toe-off. Loading refers to the portion of stance just at and following heel strike when the alignment of the hip, knee and ankle allow loading of the foot. Loading accounts for the first 10% of gait and is also defined as the period from heel strike to contralateral toe-off, depicted in Figure 1-15 (a & b). Some include a separate sub-section just before loading and label it the initial heel strike. Midstance refers to the loading of the full body weight on one leg, the knee is slightly bent and the ankle is in the neutral position, Figure 1-15 (c). Terminal stance is the progression of the weight line through the ball of the foot, anterior to the knee and posterior to the hip. Terminal stance also includes what some have labeled heel-off from observational analysis and is depicted in Figure 1-15 (d). Midstance and terminal stance account for the next 40% of the gait cycle (10%-50% respectively), and overall is characterized by an external rotation of the entire lower limb with respect to the line of progress. Pre-swing, commonly known as toe-off is the portion of stance when the weight line passes from the ball of the foot to the toes, causing the knee to bend and the weight line running closer through the knee and

hip together, Figure 1-15 (e). Toe-off ends at toe-lift and thus begins the next portion of the gait cycle, the swing phase. [19,30]

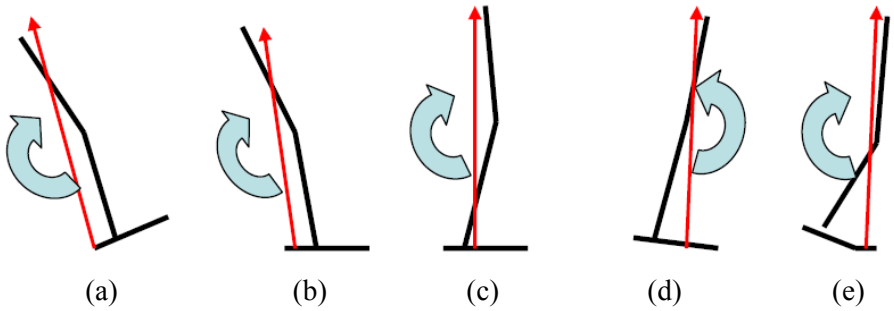

Figure 1-15. Sub-Phases of Stance
Mahler [10]
Red line is the weight line, and the black lines represent upper and lower leg and foot

Just as the stance phase is broken into sub-phases, so is the swing phase. There are three distinct sub-phases during swing: initial swing, mid-swing and terminal swing, shown in Figure 1-16. The swing phase is 40% of the entire cycle and is critical when analyzing the dynamics of gait. The initial swing begins following toe-off of the stance phase and continues until the knee reaches its maximum flexion of 60 degrees. The primary purpose for the initial swing is to clear the foot, meaning that tripping or stubbing of the toe is avoided, and prepare for swing. Clearance is achieved through flexion of the hip, knee and ankle. Following maximum knee flexion and the initial swing phase, mid-swing begins from maximum knee flexion until the tibia is perpendicular to the ground. Finally, terminal swing finishes the swing phase from perpendicular tibia location to initial heel contact with the ground, thus starting the stance phase again.

Figure 1-16. Swing Phase of Gait

Normal gait holds key features which must be mimicked in prosthetic design. To prevent excessive heel rise and to initiate the forward swing of the leg, the quadriceps contract before toe-off. To dampen forward motion of the leg at terminal swing and control where the foot is just prior to heel strike, the hamstring muscles become active. In order to achieve the latter, prostheses have introduced several design features including constant friction, hydraulic and pneumatic dampers as well as other high technological options such as CPU control. Toe clearance during swing is also a challenge; during normal gait, ankle dorsiflexion gives clearance but in the case of an amputee, the muscles are not present and the knee prosthesis or combination of knee and ankle prostheses must provide the necessary clearance to prevent stubbing the toe and tripping. These characteristics of normal gait must be included in the engineering of a prosthesis that is fully suitable to sustain as close to normal gait as possible.

1.3 Knee Disarticulation

A disarticulation is the amputation of a limb through the joint without cutting of the bone. The disarticulation of the knee is a surgery that is done between bone surfaces removing the tibia and fibula while either keeping or removing the knee cap (which is the

judgment of the surgeon). Knee disarticulations are considered somewhat rare and account for only about two percent of major limb loss within North America. The first knee disarticulation in the United States was performed in 1824 and since has received strong support as well as strict skepticism. [27]

1.3.1 Advantages and Disadvantages of Knee Disarticulation

Disadvantages of the knee disarticulation lie within function and cosmetic rationale. Earlier in the development of the knee and ankle disarticulations (1800's) a drop in mortality rates were of utmost importance as the disarticulation decreased infection, bleeding and surgical shock. Modern day healthcare and surgical procedures have decreased the aforementioned mortality rates for all amputations and therefor can no longer be considered the deciding factor in the surgeon's decision. Why then, if the knee disarticulation was so popular when first introduced is there skepticism now? Primarily, complaints have been made based upon the prosthesis fit and the bulbous distal end of the residuum. A particular paper written in 1940 by Dr. S. Perry Rogers, an orthopedic surgeon with a knee disarticulation (from a war injury), highlighted the differing opinions on the amputation. He based the divided opinion on "erroneous conclusions by some physicians and prosthetists" [26], noting the Association of Artificial Limb Manufacturers of America claiming that knee disarticulations were "impeding to successful prosthesis" [26]. Objecting to this statement, Dr. Rogers claimed that it was "no longer grounded in fact" [26]. The claim that the bulbous shape of the distal end of the residual limb was a problem to the patient was also addressed by Dr. Rogers whose

photographic evidence proved that the femoral lower extremity proved to assist in the lifting of the prosthesis as well as increase control over the rotation. Still, many people object to the disarticulation based upon cosmetic reasoning that the bulbous end of the residual limb was unappealing. The bulbous end of the residuum caused issues relating to function as well; creating a socket with the correct fit was challenging, even to the point that some prosthetists were reluctant to make one fearing an unsuccessful fitting. Dr. Rogers commented on this as well stating that the bulbous end essentially makes the socket "self-suspending" [26]. Amongst the cosmetic downside of the knee disarticulation, many people with the amputation note the longer thigh length of the residuum with prosthesis over the sound leg. The residuum, distal padding, socket, connector and knee unit add a few inches to the overall length thus creating a non-symmetric appearance while sitting. Four-bar prosthetic knees (polycentric) reduce the overall length of the amputated limb, but not completely. Figure 1-17 depicts the notable differences in distance from the distal end to the prosthetic knee center (note the right picture is of a polycentric knee). Sitting is cosmetically asymmetric, but standing also has its cosmetic symmetry issues that some dislike. When standing the knee center of the residual limb is a few inches closer to the ground which some say is a problem. As noted by Dr. Smith, "as long as the prosthesis is designed so that the total length of both legs is equal and the hips remain level, the back can be straight, and for many there is no discomfort" [26]. Noting that over sixty years has past since the release of Dr. Rogers' paper, controversy over the drawbacks of the knee disarticulation still remain and are discussed today.

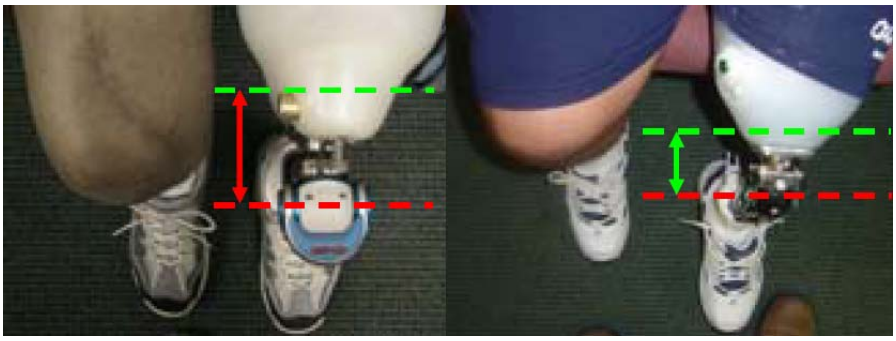

(a) (b)

Figure 1-17. Distances from Distal End to Prosthetic Knee Center
(a) Higher transfemoral (TF) amputation (b) lower TF amputation with polycentric knee
Image by USF College of Medicine School of Physical Therapy and Rehabilitation Sciences
[7]

Advantages of the knee disarticulation over the transfemoral counterpart lie within both functional and surgical rationale. Many individuals unfortunate enough to require lower limb amputation near the knee joint are fortunate enough to hold the option of a transtibial (below-knee) amputation thus leaving the knee intact. For some, there is no choice but to amputate higher up the thigh and through the femur. Though rare in comparison and controversial, the knee disarticulation may be the best option for several groups of individuals:

- Children
- Cancer/Trauma Patients
- Spasticity Patients

Children benefit from the knee disarticulation over transfemoral simply by preserving the growth plates located at the ends of the femur. The bottom growth plate accounts for the majority of femur's growth and with the leg being amputated through the joint the plate is preserved and the femur able to grow through the child's life. If the child undergoes a transfemoral amputation, the residual limb though long when

amputated will result in a shorter residuum as an adult. The growth of the femur without the growth plate would not be able to keep pace with the sound leg and thus result in a short residuum during adulthood. The knee disarticulation also eliminates the childhood condition of painful bone overgrowth, which is a result of new bone growth that forms a spike or bone spur at the amputated end after the bone is transected [26]. Cancer or trauma patients undergo a knee disarticulation if the tibia cannot be saved and the soft tissue that would be located at the distal end is good for "padding" [26]. Patients suffering from problems with spasticity or contractures, which typically are results of spinal cord or brain injuries, can leave their legs in a bent position and are susceptible to being fixed in that position. In these particular cases, "the knee disarticulation can offer some unique advantages over either a transtibial or transfemoral (above-knee) amputation" [26].

One of the most notable advantages of the knee disarticulation over transfemoral is the remaining muscle that is left intact. A full-length femur is left and the thigh muscles tend to be stronger because they are not transected in the middle of the muscle but rather at the end where there is fascia (connecting tissue). Muscles that are dissected mid-length tend to become swollen, need more time to heal, retract and never quite regain the strength. The knee disarticulation is typically an end loading (weightbearing at the distal end) amputation and provides a long mechanical lever-arm with the maximum amount of muscle present to provide necessary moments to control the prosthesis adequately (this is discussed further in section 1-4).

1.4 Prosthetic Knee Inherent Stability

To better understand the required stability needed for a particular patient (over another patient with a different level of transfemoral amputation), the concept of torque must be mastered. In physics, torque, also known as a moment, is the measure of "the tendency of a force to rotate an object about some axis (center)" [7]. Torque can be quantified by the product of a force and the length of the lever arm to which it is applied to the body. In simpler terms, torque is equal to force times distance. The force applied on a residual limb is directed and applied by the remaining muscles of the residuum. The length of the 'lever arm' is the length of the femur (with an above knee amputation). It is interesting to note that the length of the residual femur affects both the force and lever arm because the longer the residuum, the more residual musculature; therefore the length of the femur determines the amount of torque a patient can apply and the more control they will have. USF O&P [7] describes an example which illustrates this idea; a short transfemoral limb will require a larger prosthesis, thus having a higher mass, and is placed at a shorter lever length.

The concept of "inherent stability" [7] is based upon the type of prosthetic knee used and the "alignment or position of the knees COR (Center of Rotation) relative to the TKA (trochanter-knee-ankle) weight line. The type of prosthetic knee determines the ability of the prosthesis to allow or withstand buckling, either during swing or stance. This is a crucial part of the knee classification, but the concept of control versus stability focuses around residuum's torque capabilities and this idea of alignment. With a long transfemoral amputation (e.g. knee disarticulation), the TKA weight line falls posterior to the knees COR and thus is in an unstable position. With this unstable position, the

patient must have the ability to have more control over the prosthesis. With the greater amount of residual musculature, this control is easier than with a shorter transfemoral amputation. Those with the knee disarticulation seem to prefer to have more control over their prosthesis rather than have it heavily stable [7]. A shorter transfemoral amputation requires more stability then a knee disarticulation as the residuum would have less ability to control the prosthesis (less muscle present). The TKA weight line would need to lie anterior to the knee's COR to withstand rotation during loading thus increasing the stability during stance. Figure 1-18, from a presentation put together by Dr. Jason Highsmith and Dr. Jason Kahle [7] depicts the concept of inherent stability versus control and how they relate to residual limb lengths.

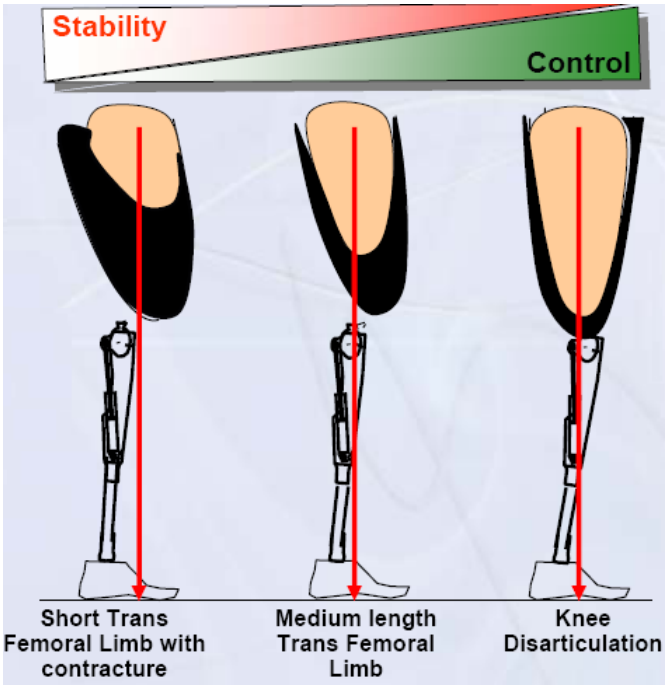

Figure 1-18. Stability vs. Control
Image by USF College of Medicine School of Physical Therapy and Rehabilitation Sciences [7]

Chapter 2 Prosthetic Knee Classifications

The prosthetic knee market is saturated with over 200 different knee joints from dozens of manufacturers and each year that number grows. With the abundance of knee mechanisms it makes it very difficult for the prosthetist to choose the 'correct' knee for the user as there is typically more than one knee which is appropriate for a particular application. The reason behind such large numbers of knee designs can be attributed to two different explanations: designer's choice and contradictory demands made by users. A newly designed prosthetic knee is difficult and expensive to evaluate, typically requiring time-consuming experimentation and clinical trials. Classification of a prosthetic knee is a technical process and is done in several different ways. In this chapter, the following classification schemes are described: function-based schemes, mechanical-design-based schemes, and schemes based on the level of amputation of the user. The tradeoffs between stability and control are also described.

2.1 Classification – Functional

Dr. ir. P.G. van de Veen [29] describes two subcategories under the functional classification of knee prostheses: locking and braking mechanisms. Each of these types has a unique characteristic that makes them more suitable for different environments as

well as different levels of user activity. Table 2-1 summarizes the functional classification of knee mechanisms and gives a few examples of each.

Table 2-1. Functional Classification Examples

Locking:	• Continuously Locking • Automatically Locking • Geometrically Locking
Brake:	• Load-Dependent • Load-Independent

Locking mechanisms mechanically restrict all motion (while in the locked position), regardless of the forces applied (neglecting those which cause mechanical failure). As mentioned, there are three different locking mechanisms which restrict flexion. The first is the continuously locking mechanism which is the simplest form of the locking prosthetic knee. The continuous lock is a manual lock which is enabled or disengaged by a user command alone, such as pushing a button. The second, the automatically-locking mechanism, applies restriction through the knee joint when triggered by either position, load or during a particular input response (flexion of the foot/ankle or other means). The automatically locking knee also includes a point at which the mechanism 'unlocks' and is able to flex. Finally, the geometrically locking knee utilizes the knees center of rotation (COR) to lock the mechanism. The knee is able to lock if the knee's COR lies posterior to the weight line (or load line) during all instances and circumstances. Only when the loading is removed from the knee is it able to flex. Locking knees are worn by those who require the highest level of stability, but many who ambulate with such knees develop gait abnormalities similar to the hiking of

the hip to compensate for the lack of knee flexion (and thus the inability of the leg to shorten through initial swing).

Braking mechanisms provide a "flexion-counteracting moment" [29] to prevent rapid flexion. While this applied moment can be large, it will never be infinite and therefore cannot prevent motion completely (like that of the locking mechanisms above). As listed, two functional braking mechanisms are prominent on the market: load-dependent and independent brake mechanisms. The load-dependent braking mechanism is a friction brake that exerts a counteracting moment that is proportional to the loading on it. Usually, motion is prevented, but is done so by the equilibrium of forces and not a locking mechanism. The load-independent braking mechanism provides counteracting forces that are independent of the applied loading but rather to the speed of rotation (flexion). Load-independent braking knees offer more controlled flexion rather than the strict stability offered by the locking mechanisms. [29]

2.2 Classification – Mechanical

The mechanical classification system focuses primarily on the type of linkage-based mechanism the knee employs. Prosthetic knees can be broken into three mechanical categories: single-axis knee mechanisms, multiple-axis (polycentric) knee mechanisms and 'exotic' knee mechanisms.

Single-axis knee mechanisms tend to be the simplest models, and have a wide range of applicability. There are several types of single-axis knees which incorporate additional features like manual locks or hydraulic cylinders. Single-axis knees tend to

work well with friction, either constant or variable, introduced into the mechanism, which allows for user comfort and safety [29]. The single-axis constant-friction knee is rare in comparison to most prostheses on the market. It is typically designed and limited for pediatric users as it is very durable and light in weight. The design is simple and is ideal for children. Figure 2-1 shows an example of a single-axis constant-friction knee manufactured by Ossur. While constant-friction single-axis knees are limited in number, there are several single-axis knees constructed with variable friction. Microprocessor knees, SNS, pneumatic and other forms of knee designs incorporate the idea of variable friction into the knee mechanism (shown in Figure 2-2).

Figure 2-1. Constant Friction Single Axis Knee by Ossur [13]

OSSUR OTTO BOCK

Figure 2-2. Variable Friction Single Axis Knee [13,14]

Multiple-axis knee mechanisms are characterized by the number of links present in the system. Utilizing multiple links, the engineer can alter the location of the instant

center of rotation and thus the motion of the shank in comparison to the residuum. Manual locks and condylar mechanisms are also incorporated into these types of knees. This thesis focuses on a polycentric four-bar knee manufactured by Otto Bock. Polycentric is a term which refers to the instant center of rotation of the mechanism and is used primarily to allow for the toe to clear the ground during the swing phase (discussed later).

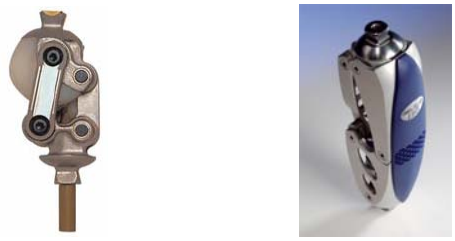

Figure 2-3. Multiple Axial Knee Mechanisms [14]

Exotic knees are a classification which is given to those knees which do not 'neatly' fit into one of the other two mechanical classification systems. These knees can be either single axis, multiple axial or some other type not yet discussed. The exotic approach is new and upcoming and is not widely applied as most have yet to be tested rigorously enough to be applied widely as of yet.

Table 2-2. Mechanical Classification Breakdown

Single Axis Knee:	• Manual Lock • Backward Center of Rotation • Friction Brake • Hydraulic Cylinder
Multiple Axial Knee	• Manual Lock • Condylar Mechanisms • 3 Bar, 4,5,6 and 7 Bar Mechanisms
Exotic Knee	• Single or Multiple Axial Knees

2.3 User Aspects of Swing and Stance

User aspects of prostheses define the necessary attributes of prosthetic knees especially, and sifts knees into finely differentiated categories. These categories enable the prosthetist to confidently fit a patient, knowing that the knee will meet safety and appropriateness criteria during both stance phase and swing phase. The criteria for determining safety and appropriateness for each of the sub-gait categories used by the prosthetist depend on the activity level and abilities of the patient.

The safety of a knee during the stance phase is determined by its stability. Stability refers to the ability of the prosthesis to support its user without buckling, and is one of the first attributes of the prosthesis noticed by its user. If the prosthesis does not feel stable to the user during stance, rejection is common. Typically, more active patients can tolerate lower levels of stability because they are better able to control their residual limb. Also, as mentioned, those with a larger residuum musculature have the ability to apply larger torques and are better suited for less stable knees. The prostheses of more active patients see more use and long-term wear, and the reliability or long term performance becomes a greater concern.

Stability is a necessary part of safe knee performance, but adjustment of the knee's stability is also important. The knee must be able to initiate swing phase without much difficulty. There must also be some flexion under loading, which itself seems counterintuitive to the stability argument. Normal gait includes small knee flexion at heel strike. This flexion serves several purposes: reduce the initial shock brought on by heel strike and reduces the vertical body center oscillation thus reducing energy expended.

The behavior of the knee during swing phase is also very important for user success with the prosthesis. It is important to note that the vast majority of prosthetic knees are passive joints - they do not add any energy to the amputees walking cycle. The swing phase is initiated upon motion of the shank to the posterior. The knee joint must prevent excessive heel rise as this causes delays during the extension phase which can result in the loss of user comfort and confidence as well as increase falling rate when heel strike is not synchronized with shank position. In what is known as mid-swing phase, the shank moves anteriorly under the influence of gravity, inertia and an extension assist device. The motion of the prosthetic shank moves more slowly than the sound limb during extension, thus requiring an extension aid. The introduction of this extension device poses other issues which must be resolved; the extension aid increases terminal impact of the knee's linkage system on the hyperextension stop.

In short the knee joint must meet the following criteria relating to the swing phase:

- Dampen flexion to prevent excessive heel rise.
- Assist extension.
- Dampen terminal impact at end of extension phase.

There are also generalized needs of the users which the knee must also satisfy; the prosthesis is used not only for ambulation but also for everyday activities such as kneeling, sitting and others like driving a car. All of these activities require the knee to bend in a manner that does not impose discomfort or restriction on the user. Cosmetically, during sitting the knee must not protrude far beyond the sound limb. As discussed previously, polycentric 4-bar knees are designed to meet this need. It is

important to note these characteristics of the prosthetic gait in terms of the users needs as this typically determines the success of the amputee with his/her prosthesis (rather than the prosthetic limb's success).

2.4 Medicare Functional Modifier System

The medicare functional modifier system (MFMS) of prosthetic knees (and feet) is unique over the other classification methods/systems discussed in that it evaluates the users' abilities and needs to fit them with the 'most appropriate' prosthesis. Up to now the prosthesis itself and the mechanism have been evaluated in order to classify them for need, but as mentioned, the MFMS evaluates the amputee for their abilities and activity levels, thus creating a prosthesis that would best fit their everyday activities. The MFMS is broken into K-scores ranging from K0 to K4 each having its own designations for activity and ability levels associated with everyday activities.

2.4.1 K-Scores

The K-score is assigned by a prosthetist, and as mentioned, determines the level of activity and the appropriateness of a prosthesis for an amputee. The lowest K-score is the K0 level; the K0 score is indicative of an amputee who does not have the ability or the potential to ambulate safely either with or without assistance, and a prosthesis would not enhance the quality of life. The K0 level patient is not a candidate for either a prosthetic knee or foot and would therefor be limited to mobility via wheelchair. [7] [19]

The K1 level patient shows the ability to ambulate or transfer safely with a prosthesis and has limited (and sometimes unlimited) household use. The amputee can ambulate on level surfaces with a fixed gait speed (cadence). This level is indicative of an amputee who uses their prosthesis for therapeutic purposes and is a candidate for the basic prosthetic knees and feet. [7,19]

An amputee showing the ability to be a community ambulator and is able to negotiate low-level environmental barriers such as curbs, ramps, stairs and small uneven surfaces is designated the K2 score of the MFMS. Those able to perform to this level of activity are candidates for higher levels of prosthetic feet (i.e. multi-axial) and basic prosthetic knees. [7,19]

K3 level individuals show the ability to traverse most environmental barriers and are considered a community ambulator. They are also able to uphold or have the potential to ambulate at a variable cadence, and may have the therapeutic, recreational or exercise activity that demands prosthesis use beyond that of the simple locomotion. In order to perform up to this patient's level of activity, higher end prostheses are used such as dynamic response feet and fluid/pneumatic knees. [7,19]

Finally, the highest level of activity is indicated by the K4 score and is typically assigned to children, bilateral cases, active adults and athletes. These individuals have the ability (or potential) for higher levels of ambulation that possess high impact, stress or energy levels. These amputees are candidates for all the prostheses on the market and are considered to have high levels of control and ability [7,19]. Table 2-3 summarizes the MFMS K-score and the requirements of each.

Table 2-3. MFMS K-Scores [7,19]

K Score	Amputee Activity Level	Prosthetic Knee	Prosthetic Feet
K0	Non-ambulator	NONE	NONE
K1	Limited household use, level surfaces and fixed cadence	Basic	Basic
K2	Community ambulator, able to traverse low-level boundaries	Basic	Multi-axial & alike
K3	Environmental barriers at variable cadence	Fluid/pneumatic	Dynamic response
K4	Children, Bilateral Cases, Active Adults and Athletes	ALL	ALL

Chapter 3 Interface Mechanics Literature Review

The technological advance of lower-limb prostheses has been rapid over the past several years. Recent advances in prostheses have occurred in the materials used to construct the prosthetic limbs, the complex systems of knees with CPU controlled motion, and the interaction between prosthetic foot and ground. Current research that is being applied for the advancement of prostheses, both in manufacturing and patient adaptability, has been primarily done within the "commercial sector: new suspension options, innovative socket configurations, advances in knee mechanisms, and guidelines for prescription and reimbursement of prostheses" [34]. Zahedi [34] reports an "overall amputee satisfaction" varying 70-75% among polled patients, while a 20% reduction in patient care budget was reported.

Computer-aided technology has advanced the manufacturing of the prosthesis tremendously; what took days is now conceived in hours. The prosthetic socket is most affected by the introduction of computer-aided manufacturing. In practice, prosthetists form the residuum geometry via plaster molds (typical), and then create the prosthetic socket around the limb geometry. This practice requires much skill and experience as it is typically a trial and error method. The patient makes a couple of visits for this method of manufacturing, and sometimes even more if the prosthetist's desired fit does not match at first. Engineers have proposed an interactive lab for the prosthetist in which he/she can form the geometry in CAD-Space and from there, a lathe receives geometric inputs from

the CAD-file and carves "a positive of the socket from a plaster composite material" [33]. Finally, the socket is created by vacuum forming a piece of polypropylene over the positive socket cut.

While fit adjustments and design alteration considerations are always present, correct fitting between the prosthetic socket and the patient's residual limb has the following consequences:

- It prevents further injury to the residuum via an inflammatory response (followed by necrosis).
- It allows the patient sufficient control of the prosthetic limb.
- It enhances the patient's comfort.

These are generalized concepts which can lead to a successful prosthetic limb. The socket is the starting point for any prosthesis design phase, primarily because if the patient-prosthesis interface is not created to perfection, problems are inevitable.

This chapter deals with the underlying principles of the interaction between the patient's residual limb and the prosthetic socket (and liner) also referred to as the interface mechanics. Interface mechanics in these terms, reference the interface stresses induced upon the residuum via the prosthesis and loading during ambulation. Shear stresses are felt as friction by the patient, and normal stresses correlate with the pressure caused by stance and ambulation. Stress concentrated around the interface between a residual limb and a prosthetic socket is a crucial piece of information when designing the socket to an individual with an amputation. As mentioned, the prosthesis must be safe to the surrounding tissue, provide some sense of comfort to the individual, and not fall off.

Finite element techniques have posed a possible route to uncovering the stresses on a modeled residual limb. These techniques can facilitate designing a socket which alleviates stresses which cause tissue trauma and/or discomfort to the patient, or designing a prosthesis which can optimize these stresses to better serve user control.

Finite element techniques, in a nut-shell, allow for the small 'finite' division of a complex geometry. This allows for geometries and loads which are very difficult to analyze via analytical methods to be broken into smaller 'elements' which can be analyzed. These techniques have been identified as a tool to enable the in-house lab to create an optimal prosthetic socket, one which ensures the most control over the prosthesis as well as safety to the patient.

This review encapsulates the ideas of interface mechanics, how they relate towards control and their importance within external prosthetics as well as the idealizations of finite element analysis, the assumptions and complications therein, which permit the creation of the 'optimal' prosthesis for each patient.

3.1 Finite Element Analysis Design

The objective of the socket shaping process essentially is to "optimally distribute the *interface stresses* between the residual limb and socket while providing adequate stability and efficient control of the prosthesis" [33]. There are other design criteria besides the geometry of the socket which affect the overall stress distribution; material properties of the inner liner and socket wall also have significant influence.

Finite element analysis (FEA) is an engineering tool which has earned great respect within industry and research institutions and is being incorporated within prosthetics in order to understand the "relevant biomechanical rationale, especially the biomechanical interaction between the stump and the socket" [35]. FEA is widely applied in engineering practice in order to obtain approximate analytical solutions to problems for which no simple closed-form solution exists.

To initialize the model, the geometry which represents the residuum and socket alike, is generated and divided into finite segments (elements) which when put together is referred to as the element mesh. The nodes of the mesh are the points at which there are interface "vertices" [33]. These nodes are crucial in the design phase of modeling as they determine the slip parameters of the interface, which tells the program that the socket and residual limb are not one material and must allow slip as well as no tensile stresses to be induced. The method in which slip is implemented differentiates between research approaches and is described later.

FEA requires distinct knowledge of several overall features of the model itself. Several design characteristics are of critical importance, because of their affect on the accuracy of the model:

- The material properties of the soft tissues which "exhibit nonlinear and non-uniform behavior". [20]
- The way that interface nodes between the socket wall and the residual limb are modeled.
- The accuracy of the residuum geometry: soft tissue, bone, and location.

- The inclusion of pre-stresses within the soft tissue (as a result of wearing the prosthetic socket, 'snug fit'/donning of the socket on the limb).

Each of the above items has been simplified in different ways by different researchers, which allows for variations in results leading to skepticism about the accuracy of FEA of external prosthetic sockets (and interface mechanics). The variations in the research results are discussed later in this chapter.

Finite element analysis, as it applies towards interface mechanics, has progressed tremendously from only accounting for 2-dimensional geometries with linear properties to now integrating 3-dimensional residual limb geometry and incorporating nonlinear tissue properties (bone, epidermis and other soft tissue) as well as pre-stressing of the epidermis due to the donning of the prosthesis. Other newly integrated approaches attempt to find better models by incorporating different distal-end boundary conditions [36]. To summarize the key aspects of the Finite Element techniques, in order to have a working analysis, the inputs into the program are as follows:

- Geometries
- Element Properties
- Boundary Conditions

Each of these inputs allows for the application of different approaches and variations in the design and analysis of the interface stresses, thus creating a need for model validation.

3.2 Finite Element Analysis Techniques

Variations in the three major components of the FE model result in different model predictions. In the next few sections, the different approaches to interface mechanics are reviewed based on their decisions in creating the FE model.

3.2.1 Geometry

The model geometry is one of the more complex areas of focus within any FEA. Within interface mechanics the model geometry varies from researcher to researcher through many facets: interface methods, residuum modeling and interaction with fibula/tibia location within the residual limb. The first two are debated within many papers of the field and are discussed here.

The 'interface methods' describe the type of methodology called upon to describe the interaction of the residuum epidermis and the socket liner and socket itself. Zachariah and Sanders [33] describe three different types of interaction analysis, each of which is analyzed within this section:

- Totally "glued" interface [1], [17], [21]
- Partially "glued" interface [25]
- Slip permitted at the interface [35]

3.2.1.1 Totally-Glued Interface

The totally-glued interface is an assumption that the residual limb and the socket or socket liner (and socket) are modeled as sharing nodes. Sharing these nodes implies that no slip or separation is allowable and thus acts just as a glued interface would. "The interface stress estimated by the FE solution is the nodal stress at the set of common nodes" [33]. Zachariah and Sanders [33] describe the main advantage of the totally-glued interface as its simplicity, both in setup and in computation as well as the low cost of the tools required to perform the computation.

Brennan [1] used a model which employed the method of totally-glued interface between the skin and the socket in an above knee prosthetic socket. The socket was modeled as a rigid structure and no socket liner was employed in the model. The residuum epidermis was not modeled separately and thus shared the common nodes with the rigid socket wall. The Poisson's Ratio and Young's Modulus were standardized (in reference literature), while the material behavior of the soft tissue was based upon other research noted in the paper. Brennan compared the data collected from the FE model to experimental data which was set up to measure the pressure at key points within a modified socket which held piezoresistive pressure transducers in key locations within the socket wall.

Sanders [20] also utilized the totally-glued interface to make early assumptions to simplify analysis. While the method seems common, Sanders did utilize a unique approach in material modeling; both fat, soft tissue and muscle were included in the geometry of the residuum, trying to create a more accurate model of the residuum.

Reynolds [17,18] also employed the assumption of a totally-glued interface in a patellar-tendon-bearing (PTB) below-knee socket "to assess interface pressure sensitivity to socket rectification (socket shape), tissue material properties (modulus), and alignment (force direction at the model boundary)" [33]. The idea behind the assessment of pressure sensitivity to changes in the socket shape is one of the driving forces behind the application of the finite element approach in optimal socket rectification (as mentioned in the introduction). The application of this approach is one way to apply the in-house lab, which could revolutionize the prosthetic industry and become a priceless tool for the prosthetist (beyond what it is currently doing).

3.2.1.2 Partially-Glued Interface

The partially-glued interface is one which was first modeled as totally glued (the socket wall or wall and liner shared a common node with the residuum thus creating the single geometry) but during the post-processing of the FEA a noticeable tensile stress was identified and a modified model was created to eliminate the tension that was present. Different approaches to eliminating the tension are reported; creating separation between pairs (i.e. introducing discontinuities), or defining an extremely low socket modulus at the point of tension are both strategies for the partially-glued interface correction.

Steege [28] reported the existence of the tension and thus utilized the partially-glued interface assumption. Socket information was gathered using CT scans of patients wearing PTB socket with liner (methods of geometric formulation of the residuum is

discussed later in this section). Interestingly, Steege modeled the cartilage as a completely different material than the rest introducing some of the nonlinearities.

This method is generally ignored, as many feel that the simplification of the totally glued interface may work for their application while other researchers tend to model the interface with more of a slip nature – allowing slip between surfaces and eliminating any tensile stresses induced (i.e. allow separation). The latter refers to the final interface method mentioned previously, slip permitted at interface.

3.2.1.3 Slip Permitted at Interface

The method of allowing slip at the interface between the socket and residuum is one which incorporates more complexities in the FE mesh and model. Different tools to incorporate the slip permitted interface are difficult and include slip–elements which are introduced as either springs [16], coulomb frictional elements or by using FE add-ons which allow for the use of slip elements (ABAQUS v6.3, [9].).

The concept of allowing slip is one which is being approached more when modeling interface mechanics; in fact Zhang and Mak [35] were attempting to design a model to test whether the distal-end loading had much of an influence on the overall accuracy of the model. In doing so, they applied the slip-permitted interface method using ABAQUS. They modeled the nodes between the socket and residual limb to be separate which allowed slip and separation. Notice in Figure 3-1 (taken from Zhang and Mak [35]), that the residuum and socket are modeled separately and using ABAQUS are

allowed to separate and slide tangentially past one another while still contacting, creating frictional and normal stresses (interface stresses) that are crucial to the science.

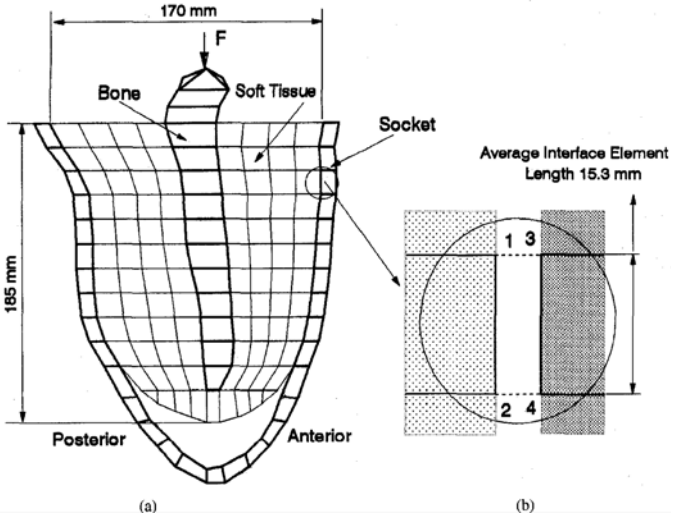

Figure 3-1. Mesh of Above-Knee Stump and Socket (Zhang and Mak)
Zhang and Mak's [35] rendering of (a) "Mesh based on a sagittal plane geometry of an above-knee stump and its socket." And (b) "Interface element consisting of nodes 1 to 4, nodes 1 and 2 on the skin surface and nodes 3 and 4 on the internal surface of the socket".

Figure 3-1 illustrates the entire residuum geometry including: bony tissue, soft tissue, socket as well as the distal-end boundary condition (discussed under *Boundary Conditions*).

Silver-Thorn [23] was mainly interested in determining the importance of the complexity of the residuum geometry to the accuracy of the model. Three different models of varying the complexity (successively increasing the accuracy) were created and tested to determine the point at which simplification to the model is allowable without much tradeoff to the accuracy of the solution. PTB below-knee models were created for this analysis and were also modified to include the joint spacing and cartilage (most considered rigid in the simpler model).

As the demand for the understanding of interface mechanics grows, this method of slip permission at the interface is becoming more appreciated. Determining the route by which one applies this idea is what varies researcher to researcher. Overall the understanding of slip is vital to the success and accuracy of the FE model in general.

3.2.2 Element Properties

Employing the totally-glued interface assumption raises several questions about the material behavior. Fundamentally, knowing that the socket and residuum epidermis have very different material properties, how does the totally-glued interface take this into account? This question led researchers to try to understand the material properties of the different tissues as well as the material properties of the socket.

Noticeably, in most models the material behavior of all the elements – bone, cartilage, soft tissue, liner and socket – were assumed to be homogeneous, isotropic and linearly elastic. It has been shown through extensive modeling that the material properties have an extensive impact on the overall stresses within the prosthetic socket.

The material properties of the socket wall have effects on the overall stress distribution within the socket. Quesada [16] showed that decreasing the overall socket modulus and making the socket 'less stiff' decreased the normal stresses within the socket greatly. Decreasing the stiffness can also be achieved by changing the thickness. Quesada also showed that decreasing the thickness of the socket did affect of stress within the socket greatly and therefore could be applied to situations where the normal stresses were too high. Silver-Thorn [25] reported that the normal and shear stresses

within the socket wall were much more sensitive to the changes in the socket liner stiffness than to the stiffness of the socket itself. These findings seem to be indicative of displacement loading.

The socket liner stiffness also has an effect on the stresses within the prosthesis, but care must be taken not to be too liberal with the softening of the liner as there are tradeoffs. While decreasing the stiffness of the liner eases the stresses within the socket, too the same degree does the patient loose stability in the prosthesis. A certain degree of stress is therefore required to maintain control of the prosthesis, while too much stress causes discomfort and even trauma to the surrounding tissues.

The soft tissue of the residual limb also shows impact on the predicted stresses within the socket. As the tissue grows tougher it exaggerates the stresses within the socket. The shear stresses were shown to be affected more by the increased tissue stiffness than the normal stresses were.

Skin (not to be confused with the soft tissue) was only modeled separately by Sanders [21]. It was shown that the result of the increased stiffness of the skin was opposite to that of the soft tissue with regards to both shear and normal stresses. This may suggest that "membrane elements capable of transferring only tension may play an important role in the FE model" [33].

Bones need to be studied further to determine whether the material properties vary with stress distribution. Currently bones are usually modeled as rigid bodies, but due to some bending of the bones under loading led Steege [18] to use the properties of cortical bone to try and model the phenomena.

3.2.3 Boundary Conditions

The application of boundary conditions has dramatic affects on the overall analysis of the model. One of the most prominent loading assumptions is made based upon the body weight of the person at the hip joint. Typically an assumption (for stance) of one-half of the body weight is loaded directly onto the femur (or is transmitted based upon gait location for below-knee prostheses).

One very interesting analysis was conducted by Zhang and Mak [35] testing whether the distal-end boundary condition had an effect on the interface stresses. Three models were used, one with no distal-end loading (modeled with an air gap between the distal end of the residual limb and the bottom of the gap, Model A), one with full contact between the distal-end and the socket (Model B) and a final model with an air gap simulating a partial loading of the distal end (suction socket with sealed air, Model C). Included here is a Figure which Zhang and Mak [35] used to describe the loading and is depicted here as Figure 3-2 not only for its explanation of the distal-end loading condition.

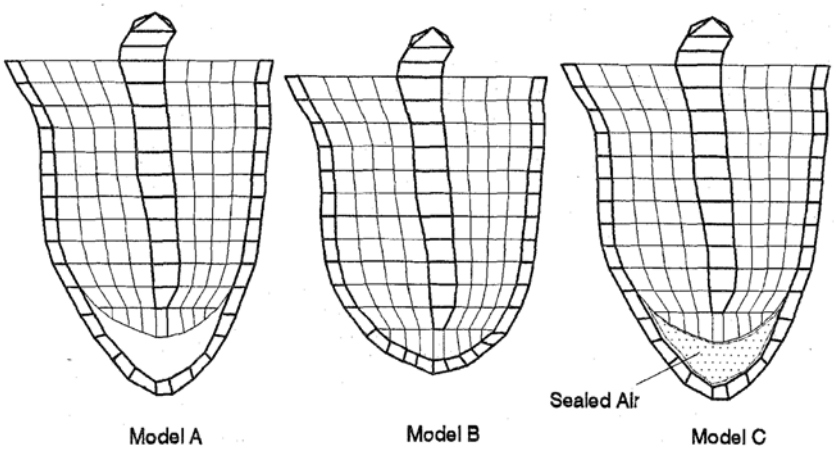

Figure 3-2. Distal-End Boundary Conditions
Image by Zhang and Mak [35]

3.3 Modeling the Residual Limb

Modeling the residual limb in order to input it into the FE model can be costly if done in detail or simple if appropriate assumptions are made. Computed Tomography (CT) is one of the medical approaches attempted to model the internal tissues of the residuum accurately. This is still somewhat difficult and others have approached the more interactive Magnetic Resonance Image (MRI). The main disadvantage of having to use these approaches is their soaring cost. Preliminary research allows such an expense but some assumptions must be made in order to allow simplifications and/or addition of data to model the current patient's residuum accurately, quickly, and inexpensively.

Brennan determined the "shape of the un-deformed residual limb… by digitizing a loose plaster wrap-cast of the subject's residual limb" [33]. The shape and location of the bone structure of the residual limb was constructed using CT scans of a person with similar stature. This applies some of the concepts of complexity management in an inexpensive route via the use of CT scans from another patient with similar stature to that of the current patient.

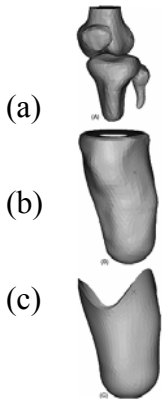

Figure 3-3. FE Modeling
(a) Bone, (b) Soft Tissue and (c) Socket Liner
Image by Faustini et al. [4]

Faustini et al. [4] depicts graphically the FE model used in their estimation of the stresses. The layered geometry allows the bone, soft tissue and socket/liner to all be incorporated into the model in order to create a more realistic model for analysis.

Moreno et al. [12] used MRI as a basis for the reconstruction of the residual geometry. As, mentioned the high costs limit the use of MRI, but not many other methods can match the accuracy of the model generated from such methods. "Magnetic resonance imaging (MRI) was selected as an ideal diagnostic and research tool to study the behavior of hydrogen atoms in the body tissues" [12]. As the hydrogen atoms reflect the frequency emitted by the MRI, a local concentration of the hydrogen atoms allows the differentiation of the tissues within the residuum. This differentiation of the tissues within the limb allows the scientist to model the residuum within 3-dimensional space accurately and efficiently.

In order to perform the MRI without inducing a deformed geometry (from the patient lying down), Moreno et al. [12] fitted the residual limb with a plaster cast which was fit onto the limb slowly and diligently. Care was taken not to alter the anatomically unloaded "topography" of the limb.

It is ideal to use such tools as the MRI and CT that are available to us, but the cost of each of the tests limits the amount of uses that can be applied in a research setting. With a database of such measurements from research, it may be possible to use data from a prior patient to estimate the geometry of a new patient's residuum. These tools, which take cross sectional 'pictures' of the tissues, allow researchers to model the tissues of the residual limb, which differ greatly from the normal limb. It is only through these

techniques that an understanding of the internal tissue orientation can be discovered and modeled for use within finite elements (or other medical purposes).

Future applications of MRI as a research tool include the response of the tissues, bones and epidermis to the mechanical loading applied through the prosthesis. The use of these techniques is limited by costs but there are endless research possibilities.

There are limitations to the use of different imaging techniques: X-ray and CT scans expose the patient to ionizing radiation and X-rays produce a 2-dimensional model (a planar projection of a 3-dimensional image) requiring at least two views in order to extrapolate a 3-dimensional image (resulting in substantial error). As mentioned care must be taken not to influence tissue location based upon the gravitational field; if the patient is lying down, the limb must not distort from that of the limb while in stance.

3.4 Experimental Analysis

Tests have been conducted to define the stresses within the prosthetic socket within laboratory as well as clinical settings by several groups. Both above-knee and below-knee amputations were analyzed and researched for the studies. Pressures were recorded within the socket in order to explore the effects of "prosthetic alignment, relative weight-bearing, muscle contraction, socket liners, and suspension mechanisms on the interface pressure distribution" [25]. Pressure measurements were recorded at discrete points within the socket, which was limited due to the discrete number of locations a transducer could be placed. They were put in locations deemed of 'high interest' within stress analysis ('high interest' termed to describe a point of high stress).

It is difficult to equate the stress measurements from researcher to researcher as the pressures varied as a result of the type of transducer used as well as the method for calibration standard to a particular laboratory.

In most of the completed experimental tests, a special socket was fabricated to house the transducers for measurement. This method is preferred over use of the subject's own prosthesis, as tapped/drilled holes permanently alter the prosthesis. One disadvantage to the experimental techniques is the high cost for transducers and the relatively low area covered in the measurement of stress per transducer. In addition, some transducers have difficulty with quick response and are therefore not suitable for dynamic testing. In laboratory and clinical testing, the finite thickness of the transducer can also play into the role of a stress concentration within the socket and measure stresses higher than what would normally be experienced by the residual limb.

There have been commercial developments within the field of these transducers and are currently being employed as an alternative to the slower less evolved ones in use for earlier testing. "Teksan, Inc. (Boston, MA) markets several biomedical pressure measurement systems… utilizing a grid-based sensor in which the rows and columns are separated by a polymer whose electrical resistance varies with force" [25].

The limiting factors in experimental data collection leave room for the introduction of error, thus preventing of a direct comparison between computational stress methods like FEA, and experimental stress measurements. Further improvements need to be made in experimental approaches as well as to the finite-elements method to get validated stress measurements using interface mechanics.

3.5 Numerical Analysis

One of the primary advantages of using numerical analyses (finite elements) over experimental analyses is the potential to estimate the interface pressures over the entire residuum. In some research, the data collected is not limited to the interface stresses but can also include 'subcutaneous stresses'. The latter can be used to evaluate the overall longevity and success of the prosthesis per the individual, as well as other influential factors within the residuum affecting the prosthesis's success with the patient – thus defining the problem at hand. For the past twenty years, finite elements has been the leading choice when using a numeric methodology; finite elements is chosen primarily based upon the endless boundaries within the software, the analysis is only bounded by the hardware in use (which can be upgraded when needed).

3.6 Validation of the FE Analysis

Currently, validation of the models can only be achieved through experimental means (which possess errors within the test setup as discussed previously). Only discrete points within the socket have been measured leaving holes within the validation of the model. These holes are only filled through theory and/or extrapolation of data (which in itself is theory). Some researchers have quantified data leading to verification of FEA within the range of experimentally recorded data.

Qualitative analytic and experimental stress waveforms were created by Zhang [35] and showed similarities within a double peak. "The predicted resultant shear stresses were less than the experimental values at all measured sites." Zhang [35]

reported a rough 30% difference (lower) in analytic results over experimental. One of the sources of this error is however due to an assumption made within the FE model; the FE model was analyzed under stance where half the body weight is applied through the Femur, while experimentally dynamic analysis was conducted during various stages within the gait cycle [36].

Sanders et al. [20] reported interface shear stresses high enough to cause blisters on the epidermis which fall in the range 4 kPa to 23 kPa (running between 22 and 118 cycles and average coefficient of friction 0.5). The magnitude of the experimental stress varied slightly from the analytical due to the type of socket used in experimental analysis (Berkeley jigs, which are substantially heavier than the typical thermoplastic socket) along with the patients not wearing socks which exaggerates the coefficient of friction (and intuitively causing blisters). [33]

Sanders and Daly [20,21] also reported double-peaked interface stress curves which matched "the general trend in clinical data". They reported a 'best match' between the analytic and experimental data at the postero-distal and antero-proximal sites, while "consistent mismatches were seen in antero-lateral distal normal stress waveforms… and postero-proximal normal stress waveforms" [21]. Much effort was invested into the discussion of the analytical matches with characteristics of waveform shapes [21] and is broken into: loading delays, high frequency events, central stance and toe-off. With collected data, the recurring similarities between the 3-dimensional model (created with MRI technology) and the experimental analysis were proven to be substantial leading to the effective prediction of interface stress with the FE model.

When attempting to quantitatively compare the data it is important to recognize that the technique and methods used to evaluate the stresses varied from study to study. "The type of activity, type of transducer, and location of the transducers on the residual limb surface differed between laboratories" [33], and thus accounts for some of the discrepancies within the data. Clinical data was not always measured within the lab, but was taken from other sources which may have evaluated the stresses at a different period in the gait cycle.

In a general view, the differences in the models are results of the techniques and methods used in the interface model.

3.7 Parametric Analysis

Zachariah et al. explored in detail the idea of *parametric analysis* [33]. Parametric analysis is performed via altering one variable in the system and relating it to a change in a particular quantity output; when "the magnitude of one variable in the model (or one feature of the model) is perturbed about its chosen value and the relative change in the estimated quantity evaluated" [33]. This type of analysis is particularly important now with the technological advance of the finite elements method within interface mechanics in part due to its ability to point out with some level of assuredness that parameter 'X' must be specified to accuracy '%' in order to create a model with as little of error as possible without creating complexities far greater than the level of technology available. In simpler terms, it allows one to conclude just how precise a parameter within the model (material property, geometric measurement/differentiation

etc) must be with the application of simplifications and/or assumptions to the model for ease of calculation or analysis.

Parametric analysis was conducted on geometric properties, element properties and boundary conditions (the three main aspects behind the finite element modeling) in order to determine the 'optimal' model for accuracy and simplicity. All parametric analysis was based upon Silver-Thorn's definition of sensitivity – the ratio of the relative change in the finite element estimate to the parameter disturbed.

Table 3-1. Parametric Analysis
Zachariah et al.'s tabular review of "Experimental Comparisons and Parametric Analyses" [33]

Type of Interface	Investigator (year)	Loading Condition	Experimental, data comparison	Parametric analyses		
				Geometry	Element Properties	Boundary Conditions
Glued	Brennan (1991)	Standing	Std. prosthesis Modified socket	Socket shape	-	-
	Reynolds (1992)	Standing	-	Socket rectification	Soft tissue stiffness	Alignment
	Sanders (1993)	Stance phase	Std. prosthesis Modified alignment	-	Skin stiffness	Force, moment directions
Tension Released	Steege (1988)	Standing	Std. prosthesis Modified alignment	-	-	-
	Steege (1995)	Stance phase	-	-	Bone stiffness	-
	Silver-Thorn (1991)	Standing	Std. prosthesis Modified socket	Socket rectification Absence of fibula Stump length Bone Shape Socket shape	Socket stiffness Liner stiffness Soft tissue stiffness Soft tissue Poisson's Ratio	-
Slip Permitted	Quesada (1991)	Heel strike	-	stump length	Socket stiffness Soft tissue stiffness	No release of tension
	Zhang (1995)	standing	-	-		Coefficient of friction

Table 3-1 – from Zachariah et al. – summarizes the work of several researchers in the area and the area on which they focused their work within interface mechanics. It is included here as a well defined summary of the work in the area up to the year 1996. The parametric analyses conducted by each researcher tend to form the overall picture of the importance of elements within the main sections of finite element modeling.

The geometric parametric analysis ranged from the socket (shaping and rectification therein) to the very distinct realities of the residuum biological tissue differentiation.

Zachariah et al. report that Silver-Thorn's analysis of a short socket with PTB rectification experienced small deviations in normal stresses but noticeable variations within shear with the absence of the fibula in the model.

The residuum length had an affect on the normal stresses within the socket; the shorter the residuum the higher the normal stresses recorded (Quesada's model of heel strike). In theory, the variations in normal stresses are a result of the change in the lever arm acting with the bending moment of the limb as well as the area which is exposed to the loading of the person (dynamic or static).

As noticed in Zachariah et al.'s table summarizing the parametric analyses (Table 3-1), the element properties were believed to have just as much impact on the accuracy of the models as that of the geometry. First and foremost, the modeling of the socket itself requires insight into the material behavior and its properties to model the stresses stored within the thermoplastic. Studies varying the thickness of the socket (stiffness) achieved by Silver-Thorn reflects the latter theory of element property importance, in that as the thickness of the socket wall decreased so did that of the normal stresses within. Even

with these stress alleviations, Silver-Thorn reported that the sensitivity of stress relief was not as great for the introduction of compliance into the socket as it was when the socket liner was analyzed.

Silver-Thorn's model also varied the socket liner stiffness and recorded the changes in stresses within the socket. As the socket liner stiffness increased the normal stress increased greatly. There is a trade-off involved in liner stiffness decrease though, as a relief in stress is seen with a less-stiff socket a reduction of socket stability is also noticeable. [23]

When modeling the geometry of the system the location of the tissues were of great importance (which is why more elaborate methods of tissue differentiation are being utilized more often), and were thus exposed to the parametric analysis as well. The stiffness of the soft tissues were increased and reports by Quesada, Reynolds and Silver-Thorn all showed an increase in the stress. This is parallel to the medical knowledge of tissues which have been injured and have healed to a permanently hardened state (which reflects that of scar tissue). These tissues have less ability to flex under loading and as such experience much higher stresses than those which can yield to the applied loading.

Steege's [28] test of transtibial prosthetic gait showed significant "bone bending" which led to the use of the material properties of cortical bone as opposed to cancellous (1.5 GPa as opposed to 10 MPa). Zachariah et al. report that the parametric analyses of these preliminary results are essential to the full understanding of bone properties within the finite element model.

The final aspect of the FE modeling – Boundary Conditions – is also reviewed parametrically and touches upon the interface, external loading and alignment issues.

Modeling of the interface is the key within the finite element model and the conditions for slip/stick are of utmost importance. The three methodologies used were analyzed including the totally-glued interface, which revealed that tensile interface stresses reduce the peak compressive stresses (60-85%) [33].

External loading is fairly intuitive as the model is most susceptible to variations in stress magnitudes through axial and bending moments in the sagittal plane. Sanders reported parametric analyses of these conditions and noted that the normal stresses and shear stresses were most susceptible to the axial force and sagittal bending moment while the normal stresses were also sensitive to alterations in the sagittal shear force while the shear stresses were more sensitive to the torsional moments applied.

As a general research investment, parametric analyses are highly informative towards the future direction of the computational analysis of the interface stresses (or estimation thereof). It allows the scientist to model complex residuum geometry with appropriate assumptions which are not detrimental to the success of the model itself and are able to provide the necessary information to differentiate the simplifications made in the model.

3.8 Conclusions on Interface Mechanics Review

Through extensive research it has been shown that the finite elements method has the possibility to be an extremely powerful computational tool for the estimation of interface stresses within external prosthetics studies. As technology advances and computers become more powerful, the bounds upon which finite elements can be applied

are approaching limitless. There is a strong possibility that finite elements can contribute greatly towards efficiency in prosthesis care as a tool for the estimation of stress as well as that of parametric analysis.

While many of the experimental techniques are not suitable for routine clinical settings, it is clear that with the incorporation of the thin pressure membranes into a smaller transducer-like function, it is possible to enhance the clinical measurement of each patient as prostheses are manufactured. It is one of the main goals of the further understanding of interface mechanics to enhance patient care and prosthetic efficiency.

It is clear that the interface is of great importance within prostheses, and as the research has shown, the experimental grounds behind measurement yield limitations in the discrete number of locations force measurements can be taken without inducing higher errors in the form of stress concentrators. Numerical finite element analysis is becoming useful in its ability to evaluate over the entire surface and even subcutaneously.

Chapter 4 Bistable Compliant Extension Aid

A Bistable Compliant Extension Aid (BCEA), designed to be added to an existing polycentric prosthetic knee, was developed and analyzed using a finite elements software package (ANSYS). Design criteria for the BCEA were based on swing control requirements that are not inherently satisfied by the geometry of the polycentric knee's four-bar frame. The requirements of the prevention of excessive heel rise and a stable sitting position, were achieved by optimizing the BCEA's geometry. The optimization procedure was based on knee flexions ranging between 0 and 90 degrees and the resulting reaction moments experienced by the compliant segment.

4.1 Design by Specialization

The majority of commercially available prosthetic knee joints are designed to meet the user's level of performance, whether it is being fitted to a limited household ambulator or an Olympic athlete, the prosthetic knee must perform optimally. There is no one-size-fits-all prosthetic knee; therefore, performance is 'designed' on a case-by-case user-defined basis, meaning that there is a spectrum of knee prostheses which meet high-stability needs while others meet the maximum user-control preference and all those between.

The tradeoff between control and stability is among the first attributes the user notices when getting acquainted with a new prosthesis. Typically the higher the level of amputation, the more stability is required of the knee mechanism, as there is less residual musculature the amputee has at their disposal; conversely the lower the level of amputation, leading to the knee disarticulation, leaves much more thigh muscle intact along with a longer lever-arm, thus leaving a higher ability to apply control over the prosthetic limb [7].

Achieving necessary tradeoffs, while meeting basic functional requirements is accomplished by *design by specialization*. In a prosthetic knee, many basic functional requirements are achieved by the polycentric (four-bar) knee design, while important functional tradeoffs can be accomplished by design specializations. As examples, Figure 4-1 depicts two different specializations of the same polycentric knee mechanism: the Otto Bock (a) 3R32 and (b) 3R55. The Otto Bock 3R32 specialization consists of a manual lock and facilitates a K1 level amputee ("poor voluntary control" and "transfer only" [14]), while the 3R55 specialization is designed to meet the K3-K4 level amputee ("good voluntary control" and "community ambulators who can walk with variable cadence and for patients who participate in high impact activities such as running" [14]).

(a) (b)

Figure 4-1. 3R32 with Manual Lock (a) and 3R55 with Pneumatic Cylinder (b) [14]

The purpose of this chapter is to introduce a compliant link add-on as a specialization of the Otto Bock 3R32 and 3R55 frame, acting as an extension aid which prevents excessive heel rise and provides a stable sitting position.

4.2 Background

Traditionally, prosthetic knees are designed as rigid frames with pin joints accommodating motion (if appropriate). They are typically analyzed using force loading and failure is determined by stance criteria and buckling. Compliant mechanisms, on the other hand, gain some or all of their motion from the deflection of flexible segments, thus producing a form of directed buckling of the linkage. Because of the buckling effects, compliant mechanisms are more effectively analyzed under displacement loading rather than applied force.

Why then would compliant mechanisms be a good fit for prostheses? The general advantages of compliant mechanisms within the prosthetics area include relative lighter-weights, lower costs both in a reduction of part count as well as manufacturing (most are polymers), they hold high reliability and can be designed for high-precision applications [8]. This chapter will also introduce a specialized design advantage the compliant mechanism add-on can offer – the introduction and transfer of moments that vary over a given displacement, needed for proper swing control.

Compliant mechanisms have been studied as a feasible alternative to rigid-body mechanisms within prosthetic joint design. Prominently, work done by Guérinot et al. [5] introduced methods of using compliant mechanisms – which are predominantly used with

tensile loading – under high compression situations similar to those seen by a prosthetic knee joint, known as High Compression Compliant Mechanisms (HCCM). These methods have proven to be the foundation for the introduction of compliant mechanisms to prosthetic knee and ankle design. The two methods, inversion and isolation, either transform a compressive load to tensile via geometric alterations (inversion) or transfer the compressive loads through rigid links and away from the compliant links, similar to traditional prosthetic knee mechanisms (isolation).

More recently a project undertaken by Mahler [10] also combined compliant mechanisms and prostheses by designing an adjustable pediatric compliant prosthetic knee mechanism to better suit the needs of a growing child who would be subjected to harsher, more active environments. His research focused on the kinematic instant center of rotation of the mechanism in order to understand motion (extension and flexion) relative to 'knee adjustment'.

Both projects along with several others including a prosthetic ankle [32] have proven the validity of compliant mechanisms technology within prosthetic joint research. This chapter further introduces compliant mechanism technology and its inherent advantages to the field of prosthetics via a design specialization of the Otto Bock 3R55 and 3R32 knee frame.

4.3 Functional Criteria

The compliant extension aid was designed to meet functional criteria for efficient prosthetic swing control, which have been standardized by the prosthetics industry over

years of practice. The standards of stance control are also of importance in prosthetics, however for this project, stance was not evaluated since a prosthetic knee mechanism – the Otto Bock 3R55 and 3R32 – which has been tested and validated, was used as a base and therefore does not require further scrutiny (only to the extent that the BCEA does not interfere with its function). The functional criteria which were pre-defined are those of: sufficient ground clearance, prevention of excessive heel rise at the end of knee flexion, a fast extension phase and in some cases a terminal impact stop just before heel strike. Table 4-1 summarizes these functional criteria.

Table 4-1. Summary of Swing Phase Requirements

Swing Phase Requirements	**Purpose**
- Ground Clearance	Prevents stubbing of the toe.
- Prevent Excessive Heel Rise	Allows the shank to be in position for stance phase.
- Fast Extension Phase	Ensures the shank moves into position.
- Terminal Impact Hyperextension Stop	Provides a signal that shank is in position for load bearing (although not a strict requirement).

With the exception of recent advanced prosthetic knees on the market (i.e. bionic technology by Ossur – Power Knee), prosthetic knees are passive knee joints; they do not add energy to the amputee's gait. Since these prostheses do not add energy to the swing phase they must conform to certain principles in order to function properly to maintain a proper gait pattern. Normal prosthetic swing is initiated by movement of the shank posteriorly under the influence of inertia. It is imperative that excessive heel rise is

prevented since it slows the extension phase (thus causing falling). During mid-swing, the shank moves anteriorly under the influences of inertia (providing there is an extension aid present) and gravitational forces.

The rotational speed of the prosthetic limb (knee) is slower than that of the sound limb not only due to the lack of input energy via musculature, but also due to differing mass distribution. The result is a slower-abnormal gait. This gait abnormality is addressed and alleviated by an extension assist device built within the prosthetic knee. With most extension aids, a terminal impact results at the end of the swing phase (caused by the contact of the knee's mechanism and the hyperextension stop), however flawed this may seem to the designer concerned about impact loads, many amputees prefer a noticeable signal that the limb is in position for loading.

Ground clearance is the fundamental design goal of prosthetic knees when considering the swing phase of prosthetic gait. Polycentric four-bar knees, like that of the Otto Bock 3R55, were designed to 'shorten' the limb in order to achieve clearance between the toe and ground during mid-swing, preventing the stubbing of the toe (leading to falls). Beyond ground clearance, prevention of excessive heel rise is paramount; during flexion, if the heel rises too far (knee angle exceeding 60 degrees), the rotational speed of the prosthetic shank is too slow under the action of gravity to ready the prosthesis for heel strike, thus resulting in 'excessive' knee flexion leading to buckling under stance loading. The prosthesis thus requires a fast extension phase, and the extension assist device must provide the necessary moments to perform to these optimal swing characteristics.

Figure 4-2 illustrates the dynamics of the knee angle over the gait cycle and the importance of the knee angle between the flexion and extension phase. As shown, if the knee does not resist motion beyond 60 degrees during mid-swing, the swing phase ends at a knee flexion exceeding what it should during the beginning of stance, which will inevitably lead to buckling and falling.

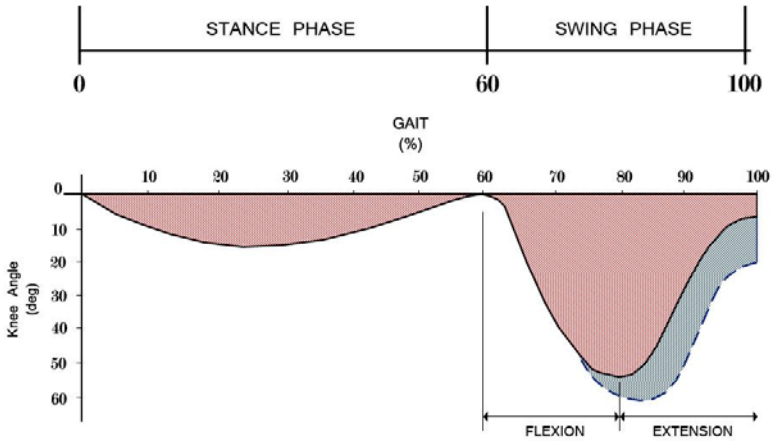

Figure 4-2. Knee Angle vs. Gait – Shown with and without Excessive Heel Rise With excessive heel rise is shown as gray, without, in red.

Under these conditions it seems as though a simple elastic strap would suffice to meet these extension characteristics, however, though the moments exerted by the strap *do* meet the necessary criteria of eliminating excessive heel rise, it *does not* meet the behavior necessary for the amputee to sit (a common position of everyday life). When seated, the prosthetic knee and extension assist device must not exert extension moments causing the prosthetic limb to 'kick-out' to full extension; they must be designed in such a way that their influences (applied extension moments) are at a maximum near 60 degrees of knee flexion (to account for proper swing) and then begin to decrease afterwards to zero near 90 degrees to account for the seated position.

Figure 4-3 depicts the optimal influence of an extension aid on a prosthetic knee. Notice the gradual increase of the applied extension moment to a maximum at a knee flexion nearest 60 degrees to account for normal gait, and a sharp decrease following to minimum near 80-90 degrees in order to prepare the knee for the seated position. [29]

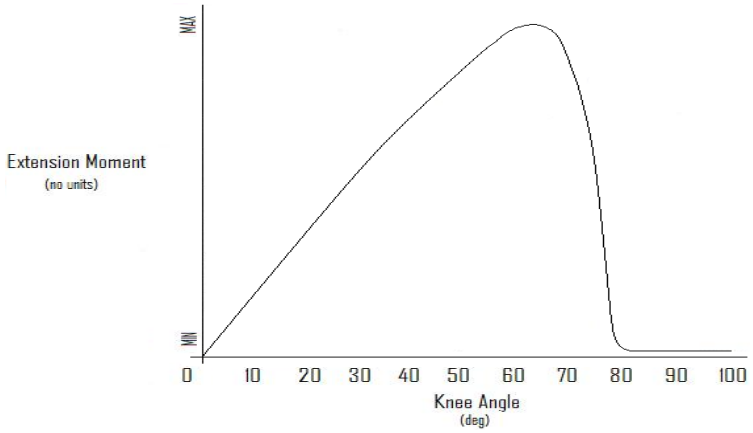

Figure 4-3. Optimal Influence of Prosthetic Knee Extension Assist

4.4 Concept of Bistability

Bistability is easily associated with the well-known ball and hill analogy shown in Figure 4-4. Bistability occurs when an object has two points where its' potential energy is at a minimum. These points are known as stable equilibrium points, labeled (A) and (B) in Figure 4-4. In order for the particle to deviate from either of these positions, an external energy must act in a way to force the particle from its resting state. If the ball is resting in position (A) and is pushed to the right to point (C), the ball has the ability to balance itself at this point and be in equilibrium also; point (C) is known as the unstable equilibrium. If any external energy is added to the ball at the unstable equilibrium point,

it will always assume one of its stable equilibrium points (A) or (B). Stability refers to the ability to resist or recover from small displacements.

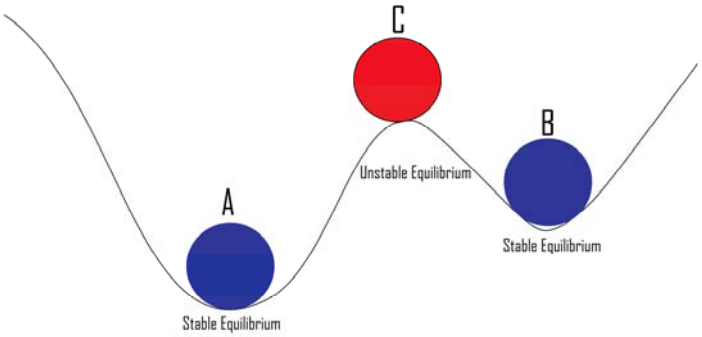

Figure 4-4. Bistability Analogy with a Ball and Hill

The bistable compliant extension aid addressed in this paper must perform as the ball would on the hill. Point (A), when the ball is at its first equilibrium point coincides to the prosthetic knee during stance. When energy is added to the knee, via inertia during swing, it will tend to return back to its original position accommodating stance at heel strike. When enough energy is added to the knee, like when crouching to sit down, it transitions to a second equilibrium point, just as the ball does at point (B).

4.5 Bistable Compliant Extension Aid (BCEA) Design

The BCEA was designed on the existing polycentric frame of the Otto Bock 3R55. A simplified four-bar schematic was used by converting the top link of the mechanism to ground, shown in Figure 4-5. The BCEA was pre-assembled as a straight, unstressed polypropylene copolymer beam measuring 1mm x 5mm x L_{BCEA}, where L_{BCEA} is the length parameter whose optimal length was determined and added to the four-bar frame via pinning it to the existing anterior-bottom pin (pin 2 in Figure 4-6(a)).

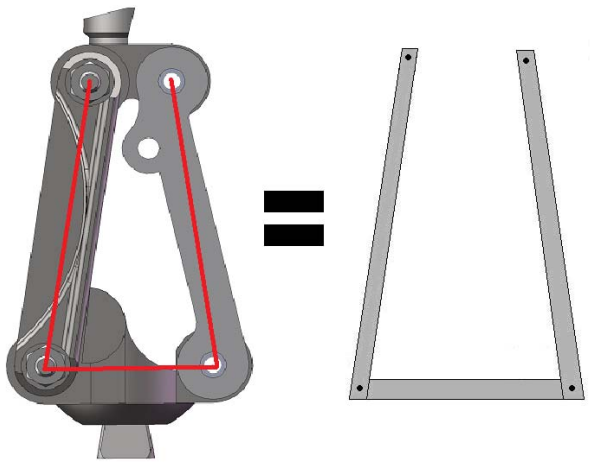

Figure 4-5. Knee Mechanism Simplification Model

After the BCEA was inserted into the model as a straight unstressed beam, displacement loading was applied to the top of the BCEA link and it was moved in the manner shown in Figure 4-6(b). Once the top of the BCEA was aligned with Pin 1, it was fixed to the top link of the mechanism (shown as ground) as seen in Figure 4-6(c).

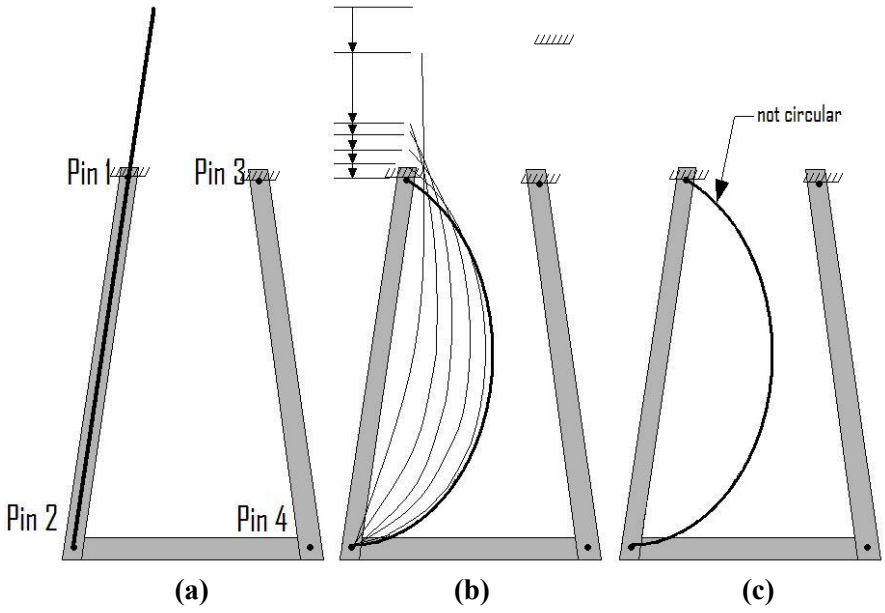

Figure 4-6. Otto Bock Knee Mechanism with BCEA Assembly
(a) pre-assembly, (b) mid-assembly showing pre-stress stepping motion of top pin, (c) final assembly.

Pre-stressing the BCEA into position (as opposed to creating an un-stressed curved beam) was a critical step ensuring that bistability was achieved. Bistability allows the knee mechanism to reach a stable equilibrium point, like those needed when standing and sitting (0 and 90 degrees of flexion). By pre-stressing the BCEA, we were able to achieve a 'snap-phenomena' resulting in the desired bistability and extension moments at the appropriate degree of knee flexion (discussed in more detail in results section).

The length of the BCEA was optimized by evaluating the lengths which produced an arc-angle, Φ, ranging from 0 to $\pi/2$, shown in Figure 4-6. Note that the arc-angle is defined after pre-stressing the assembly into the position shown in Figure 4-6(c). For simplified design purposes, the final shape of the BCEA (shown in Figure 4-6(c)) was assumed to be circular. Arc-angles which produced BCEA curvatures exceeding a quarter-circle were also evaluated but produced results outside of the set criteria and thus were not included here.

Optimization of the geometry was conducted by looping an FEA model to run a knee flexion simulation from 0 to 90 degrees, over a series of BCEA lengths (L_{BCEA}), and the resulting extension moment characteristics were compared with the optimal influence shown in Figure 4-3. The overall arc-length, L_{BCEA}, was evaluated using geometry parameters shown in Figure 4-7. The max arc-angle, Φ_{max}, was defined and used to alter L_{BCEA} incrementally in order to better understand how the length of the BCEA affected its function.

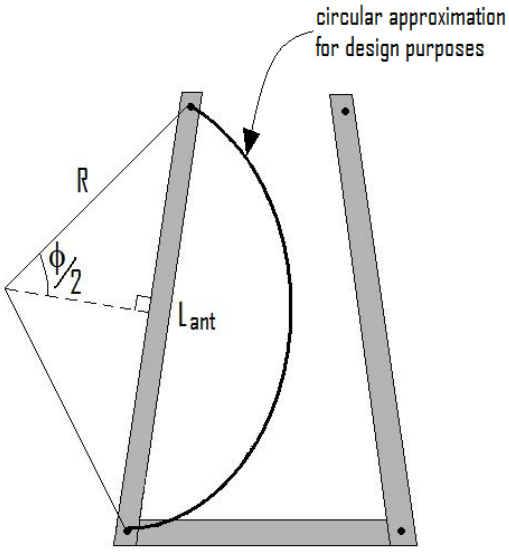

Figure 4-7. Design Approximation of the BCEA Geometry

The geometric input Φ_{max}, was broken into a prescribed number, δ, of segments, yielding the step arc-length (3) of the BCEA which was then used to create the overall length, L_{BCEA}.

$$0 \le \phi \le \frac{\pi}{2} \tag{1}$$

$$\phi_{\max} = \frac{\pi}{2} = \max angle \tag{2}$$

$$\phi_{increment} = \frac{\phi_{\max}}{\delta} \tag{3}$$

$$\phi = j\phi_{increment} \quad , j=1,2,3\ldots(1-\delta) \tag{4}$$

From Figure 4-6, L_{BCEA} can be equated to the arc-angle Φ by equations (5) and (6) as a function of the length of the anterior link, L_{ANT}, of the 3R55 knee mechanism.

$$R = \left(\frac{L_{ANT}}{2\sin\left(\frac{\phi}{2}\right)} \right) \tag{5}$$

$$L_{BCEA} = R\Phi \quad , \quad 0 < \Phi < {}^{\pi}/_{2} \tag{6}$$

For the extreme conditions, $\Phi=0$ and $\pi/2$, L_{BCEA} was calculated using equations (7) and (8).

$$L_{BCEA} = L_{ANT} \quad , \Phi=0 \tag{7}$$

$$L_{BCEA} = \left(\frac{L_{ANT}\pi}{4\sin\left(\frac{\pi}{4}\right)} \right) \quad , \Phi=\pi/2 \tag{8}$$

Once the desired L_{BCEA} was calculated, it was inserted into the model as described previously, and was then pre-stressed into the analysis-ready position.

4.6 Analysis and Results

Figure 4-8 depicts the free-body-diagram of the knee model used for analysis. Reaction forces at pin joints 1 and 2 were calculated over a knee flexion from 0 to 90 degrees, as well as the reaction moment applied at pin 1 as a result of the BCEA.

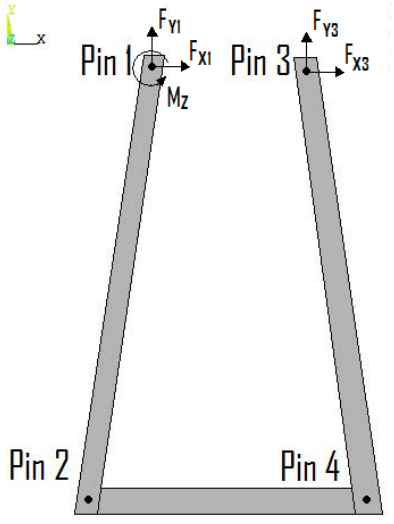

Figure 4-8. Free-Body Diagram of Knee and BCEA

Successful geometry optimization was determined by the criteria of maximum reaction moment closest to 60 degrees of flexion followed by a sharp decrease in the reaction moment closest to 0 N-m on, or before 90 degrees of flexion (as shown in Figure 4-3).

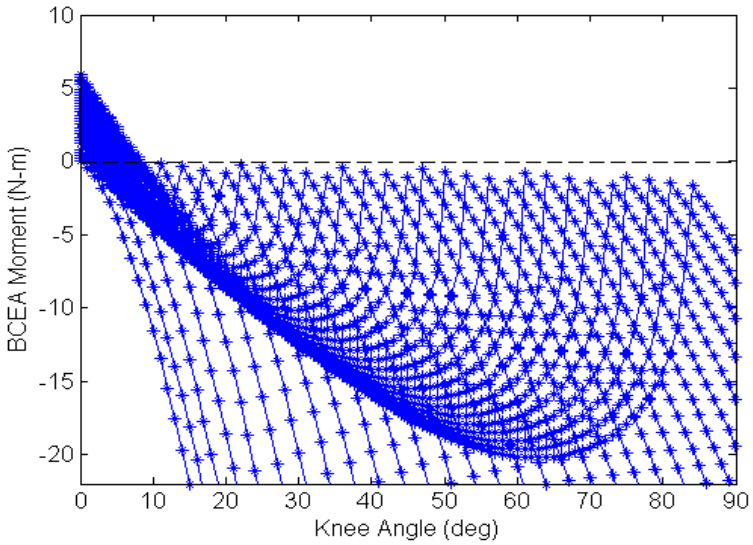

Figure 4-9. BCEA Extension Moment vs. Knee Flexion

The extension moment and knee flexion data, when graphed over 0-90 degrees of knee flexion yield results that model closely to that of the pre-design criteria depicted in Figure 4-3. Figure 4-9 graphs the entirety of the extension moment results defined by equations (1)-(3), with $\delta = 30$, and also shows the variation of the extension moment magnitude with respect to L_{BCEA}. Each curve represents a different value for L_{BCEA}, with $L_{BCEA}(\Phi=0)$ furthest to the left, and $L_{BCEA}(\Phi=\pi/2)$ furthest to the right.

Using Figure 4-9, it can be said that L_{BCEA} would be the most functional, with regards to prevention of excessive heel rise and correct extension characteristics during 90 degrees flexion, at an arc-angle closest to $\pi/2$ ($\Phi=\pi/2$). As shown in Figure 4-9, the moment increases over flexion, then 'snaps' to zero (or nearly zero); this 'zero'-moment

point is a stable-equilibrium point, and defines when the knee is in the sitting position and will not return back to stance unless acted upon. It seems as though the data smoothly returns to zero, but in fact the data points jump from a high magnitude to relative zero in one step, which is a result of the 'snap phenomena'.

The snap phenomena is brought upon the BCEA when the flexion of the knee has reached a point of instability, and is then pushed passed that point until the BCEA snaps into its second equilibrium position. The end-conditions of the BCEA allow it to rotate freely at its bottom while the top remains fixed to the knee's top link, which causes the segment to rotate uniquely. Figure 4-10 illustrates the snap phenomena by showing the BCEA in its initial point (a), its maximum-extension-moment point, (b), pre-snap position (c) and the seated position (d). Between 60-85 degrees of flexion, the BCEA snaps through as a result of the extension moments being relieved by a rotation in pin 2. Figure 4-11 highlights the extension moment key-points: maximum extension, snap phenomena and stable equilibrium.

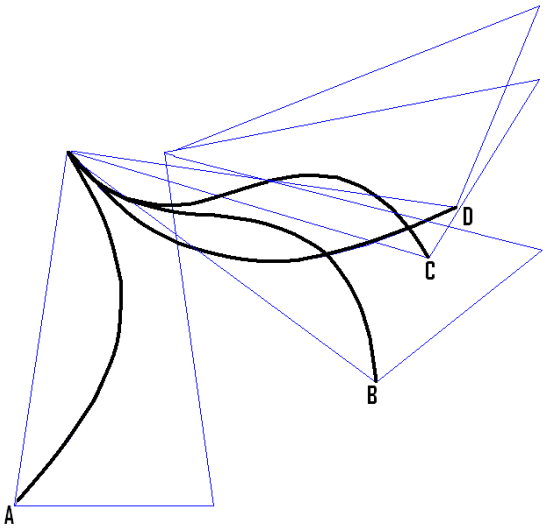

Figure 4-10. BCEA Snap Phenomena
Knee flexions corresponding to: (a) initial position, (b) maximum extension moment, (c) pre-snap, (d) seated position

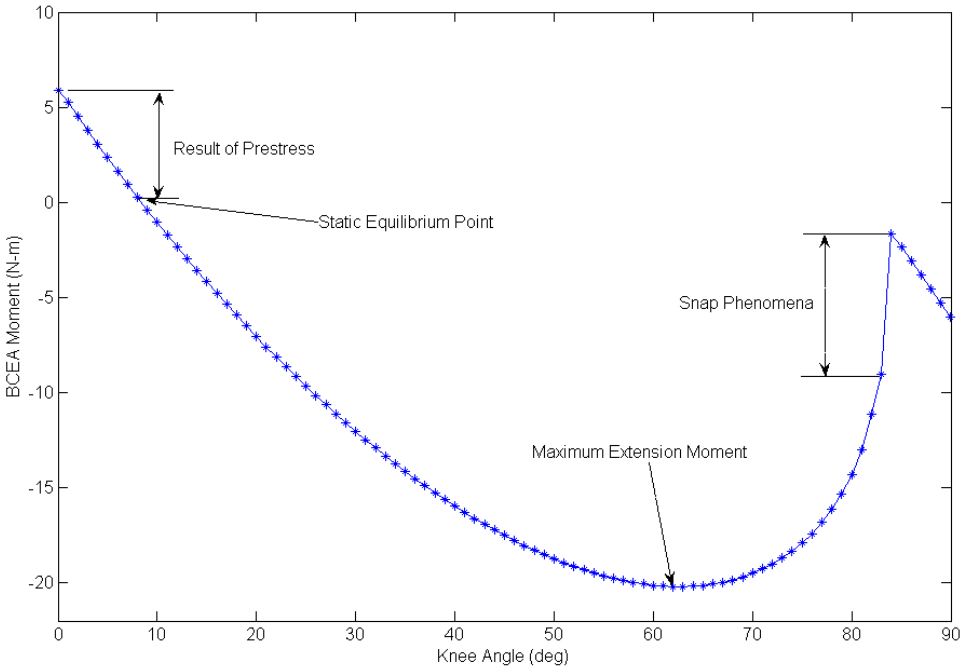

Figure 4-11. BCEA Extension Moment Graph with Labeled Key-points

The data for the curves nearest an arc-angle of $\pi/2$ ($\Phi=\pi/2$) is tabulated in Table 4-2. As L_{BCEA} increases in length, the maximum applied extension moment increases as well. With that, the angle of knee flexion corresponding to the maximum extension moment increases. The increase in maximum extension moment with respect to the length of the BCEA corresponds to the compliant member storing more of the strain-energy during rotation. The longer the compliant link, the more strain-energy can be stored, which will then be released at the point of snap.

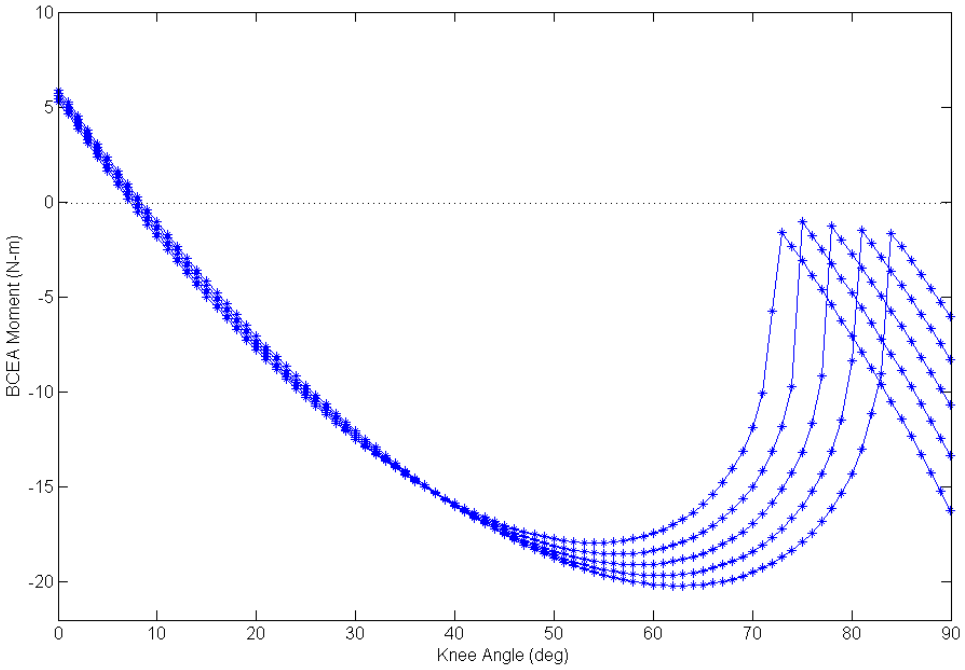

Figure 4-12. BCEA Extension Moment vs. Knee Flexion – Optimal Geometry Sets

Table 4-2. Extension Moment Data for Optimized L_{BCEA}

L_{BCEA}	Extension Moment		
(mm)	Maximum	Knee Angle at maximum	Knee Angle at snap
	(N-m)	(Degrees)	(Degrees)
93.584	17.942	54	72
94.172	18.525	56	75
94.787	19.096	58	78
95.430	19.654	60	80
96.103	20.201	62	83

Optimally, the maximum extension moment should correspond to a knee flexion of 60 degrees, along with a snap angle between 80 and 90 degrees. The particular data sets listed in Table 4-2 and Figure 4-12 depict the L_{BCEA} values necessary to optimize the geometry to meet the design requirements.

4.7 Knee and BCEA Unloading After Snap

The data depicted in Figures 4-9, 4-11 and 4-12 all have not definitively shown the second stable equilibrium position (which would naturally follow BCEA snap, and is defined by the resulting BCEA moments to be 0 N-m). The resulting loads which were continually placed on the mechanism during analysis in ANSYS, in order to force the mechanism through 90 degrees of flexion, prohibit the BCEA from being unloaded completely. In order to define this second point of stable equilibrium, unloading of the knee and the consequent results were analyzed.

Figure 4-13 depicts the unloading characteristics of the mechanism from 90 degrees of flexion (post-snap) to zero degrees of flexion (stance). It can be shown that the unloading curve has many of the same characteristics of the loading curve (shown in Figure 4-11), with a resultant maximum flexion moment as well as a snap-phenomena resulting in the release of strain-energy via a rotation in Pin 2.

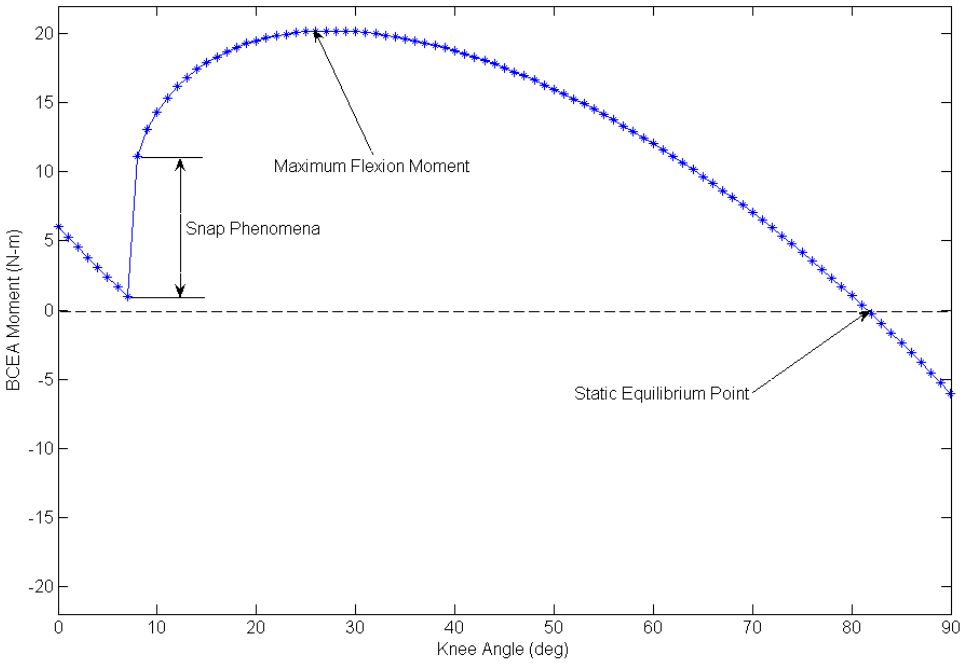

Figure 4-13. BCEA Unloading Curve

The characteristics of the unloading curve distinctly define the second stable equilibrium point (seated position). This point was unable to be correctly shown in previous 'loading' curves due to the fact that displacement loading was continuously being applied following snap. Physically speaking, if the mechanism were loaded beyond the snap point of knee flexion and the load released, the knee would assume a stable equilibrium point at a slight decrease in knee flexion all due to the presence of a small knee extension moment following snap.

Figure 4-14 overlays the unloading curve on the loading curve and labels the inherent key-points during both situations. The snap-phenomena of flexion and the snap phenomena of extension result in each of the positions 'second'-equilibrium points; the flexion-snap phenomena's second equilibrium point being the seated position, while the

extension-snap phenomena results in the knee's stance position. All stable equilibrium points are also defined and labeled on the graph.

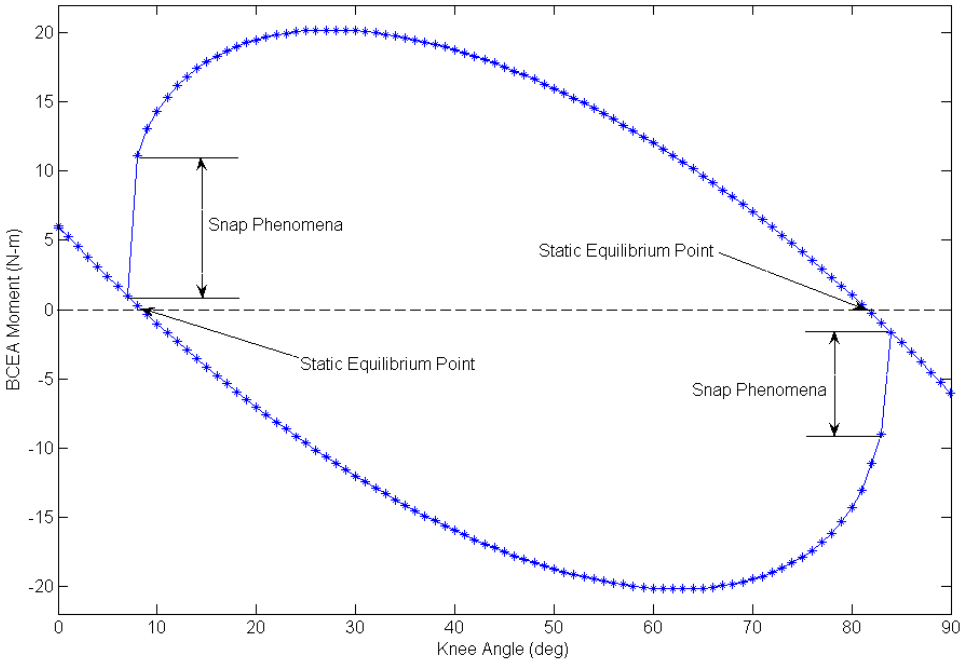

Figure 4-14. Complete BCEA Cycle: 90 Degrees of Flexion and Extension

4.8 BCEA Stress Analysis and Factor of Safety

Stresses which were induced within the BCEA during flexion were calculated using ANSYS. A static stress analysis was conducted at each degree of knee flexion and the maximum stress state analyzed (i.e. the position of the knee and BCEA for which the maximum stress was discovered). Geometrically and analytically, the maximum stress state was found to be the position just before snap, 82 degrees of flexion. The stresses ranged from 6.1252 MPa to 28.047 MPa, and the stress magnitudes over the length (L_{BCEA}) are shown in Figure 4-15.

Fully reversed stress cycles occur over the knee flexions/extensions shown in Figure 4-15 (90 degrees of flexion and subsequent extension) as a result of similar force/moment reactions over flexion and extension. The BCEA stress analysis and the corresponding factor of safety for the optimized BCEA geometry ($\Phi=\pi/2$) are summarized in Table 4-3. These values are based off the yield strength of polypropylene S_y = 34 MPa [8].

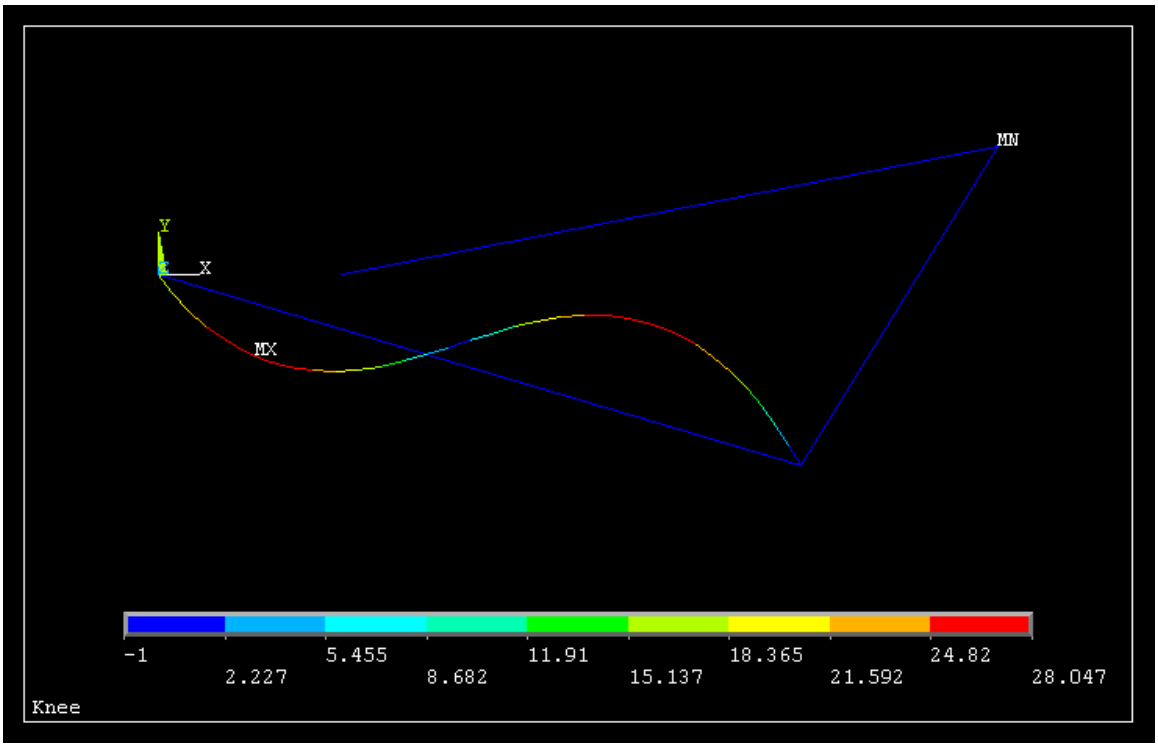

Figure 4-15. BCEA Stress Magnitude and Distribution at Maximum Stress State

Table 4-3. BCEA Stress Summary

Max. Stress (MPa)	Min. Stress (MPa)	Factor of Safety
28.047	6.1252	1.2123

4.9 BCEA Design Conclusion

The bistable compliant extension aid developed within this CAD structure shows promise in its ability to conform to the principles of prosthetic swing needed for normal gait. While the data shows the selection of geometric variations to be of a wide-range, the corresponding data shown in Figure 4-12 develops itself well into those criteria outlined in its design and allows for further geometric refinement based on amputee needs.

The data collected from the design of the BCEA contributes to the validation of compliant mechanisms even further into the prosthetics industry. This chapter has introduced a compliant prosthetic knee extension aid design that has the ability to apply the necessary extension moments in order for a prosthetic knee to function properly during the swing phase and while seated.

Chapter 5 Proprioception via Variable Internal Socket Stress Patterns

A finite element model was constructed to simulate a below-knee prosthesis during the swing phase of gait in order to show the stress variations on the inner surface of a prosthetic socket and to pose the hypothesis of increased proprioception based on these variable stress patterns. The hypothesis is that the changing loads caused by the bending of the BCEA will be felt by the amputee and will give him/her a sense (proprioception) of the amount of flexion in the prosthetic knee. The external forces applied to the system were based on the Bistable Compliant Extension Aid design and were applied via direct loading of the finite element model. The criterion adopted for the proprioception hypothesis was variable stress patterns on the prosthetic socket over different degrees of knee flexion without failure of the polypropylene socket. The interface stresses varied in magnitude and location over knee flexion angles and can be used to develop the hypothesis of proprioceptive feedback via variable stress patterns on the inner surface of the prosthetic socket.

5.1 Interface Mechanics and Proprioception

The biomechanical interaction between the residuum and socket, also known as interface mechanics, has evolved into discrete numerical stress analyses with the use of modern finite elements software packages. Finite element analysis is able to produce

approximate analytical solutions in the prosthetics field (as well as many other engineering fields) to problems in which no simple closed-form solution exists.

The advantages that finite elements and interface mechanics bring to the prosthetics industry are inherent in the functional design of each prosthesis: the ability to discretely analyze the stresses and their subsequent capacity to affect the functional design of the prosthesis. Research centered on interface shear and compressive stresses have consistently been focussed on their ability to apply on-hand data to form-fit a better prosthetic socket allowing for an 'optimal prosthesis' both in comfort and control.

Control over lower-limb prostheses during swing has been an issue addressed heavily as of late through means of developing prosthetic knees which are able to apply active moments at key points during swing. The Power Knee by Ossur is an example of such a knee which can adapt to swing phase characteristics in order for the amputee to hold better control over their gait cycle. These knees hold state-of-the-art technology and also own a price-tag to match, thus restricting its commonality within the lower-limb amputee population.

Proprioception, the sense of the orientation of one's limbs, is the 'natural' method of offering complete control over biological gait. Prosthesis control via proprioceptive feedback could offer potential advantages even over the active prosthetic knee(s) on the market by providing a more natural/biological control as opposed to motor driven control. Even better, by enhancing proprioception via inexpensive mechanical means, the greater majority of the lower-limb amputation population would be offered the ability to share these control advantages.

The BCEA, developed in the last chapter, offers 'optimized' extension moments applied to the knee mechanism and thus the prosthetic socket over a range of knee flexion angles. This chapter proposes a method of providing and analyzing proprioceptive feedback via variable stress patterns imposed on the inner part of a prosthetic socket as a result of forces and moments induced by the BCEA.

5.2 Finite Element Design Characteristics

Geometry, element properties and boundary conditions develop the accuracy, complexity and computational intensity of the finite element model, each being developed and enhanced by continuing research. While simplifications of each design characteristic can offer the foundation for state-of-the-art research, increasing the complexity allows for the accuracy of the analytical solution to mirror itself closer to physical results (that may be experimentally determined).

The input geometry emphasizes the importance of stress concentrations and the correct loading of differing materials over their boundaries (i.e. over solid-contact points). Variations of geometries are common when modeling the residual-limb; these differentiations from one researcher to another associate themselves with those complexities of biology: bone, soft-tissue, epidermis, cartilage etc. In order to increase the complexity of the residuum geometry, more complex methods of modeling must be used: X-ray, computed-tomography (CT) scan and MRI as examples [33].

The increasing complexities of the model geometries bring with it the need for the introduction of new materials and their properties; when the bones, muscles and skin are

introduced into the model, these properties must also accompany them in order to justify their interactions. The material properties of biological tissues bring complexities that can only be solved for by clinical testing. Many of these properties are approximations to better serve the models to which they are applied, but the clinical-data is becoming readily available and can be used to run statistical measurement and approximation determination.

Finally, the boundary conditions within the finite element model tell the program how to treat two nodes in contact from two different bodies, i.e. the residual limb and the prosthetic socket. Heavy approximations have been made relating to the boundary conditions in interface mechanics due to: (1) the complexities of the materials undergoing loads, and (2) the computational intensity increases and in some cases a solution is indeterminate. Three cases of socket-residuum contact have been employed by researchers: the fixed interface, partially fixed interface and free [33]. The completely fixed interface is the least computationally intensive, however this boundary condition allows for the residual tissue to undergo tensile loading (which is not the case with prosthetic limbs, unless suction is present). Partially fixed allows the researcher to remove these tensile loads through a post-processing command, and the free interaction removes these loads completely before the analysis is run. The approximation of the boundary condition must be analyzed in order to determine the validity of the analysis and can in turn lead to false results if not done carefully.

5.3 Modeling

The CAD model of the lower-limb prosthesis used in this analysis was constructed in a SolidWorks environment and included a simplified residual limb, prosthetic socket, the Otto Bock 3R21 knee frame, and simplified shank and foot (shown in Figure 5-1). In order to introduce the BCEA to the model shown, the reaction forces and moments that were calculated using ANSYS were directly applied to the knee frame; this was done due to the inefficiencies and nonlinearities in the model and the errors induced by solving the FEA with large deflection as well as rigid body motion (quite simply, large errors were experienced when the BCEA was directly modeled in the system).

Figure 5-1. Complete Model of Lower-Limb Prosthesis

The prosthetic socket and residuum were modeled with a bonded global contact; the program bonds the source and target entities, which may be touching or within small distances from each other. As mentioned, this is the simplest approximation in the boundary conditions listed previously, and will affect tensile stresses on the residual limb (which were not being analyzed here). The socket was constructed out of polypropylene copolymer (Elastic Modulus = 8.96e08 $^{N}/_{m^2}$, Poisson's Ratio = 0.4103, Shear Modulus = 3.16e08 $^{N}/_{m^2}$ and Density = 2.77e-05 $^{kg}/_{m^3}$), and the residuum was simplified and modeled as rubber (Elastic Modulus = 6.099e06 $^{N}/_{m^2}$, Poisson's Ratio = 0.49, Shear Modulus = 2.899e06 $^{N}/_{m^2}$). Each of these elements' geometries were simplified and approximated as cylinders in order to ease the computational intensity (high-end modeling techniques as described in Chapter 3 could propose further advancements to this simplification). The purpose of this chapter is to develop a finite element analysis simulation of the introduction of the BCEA to the model and the resulting stresses between these two surfaces (residuum and socket) analyzed.

The knee mechanism was constructed from titanium and steel (as built) with very few design simplifications only associated with the pinning of the mechanism together. The shank and foot were also constructed of metal and were assigned the properties of steel.

The simplifications imposed on this model (i.e. residuum geometry) are such that the work here should only be used for analytical approximations and further refinement of the model should be considered in order to closely mirror real-world situations.

5.4 Applied Loads

In order to introduce the BCEA to the model shown in Figure 5-1, the reaction loads as calculated from the BCEA were applied to the top bracket of the knee mechanism (as determined by the ANSYS FEA) and were introduced to the model using direct transfer loading in the finite element programming. Figure 5-2 depicts the resultant extension moments induced by the BCEA which was applied to the model, summarized in Table 5-1.

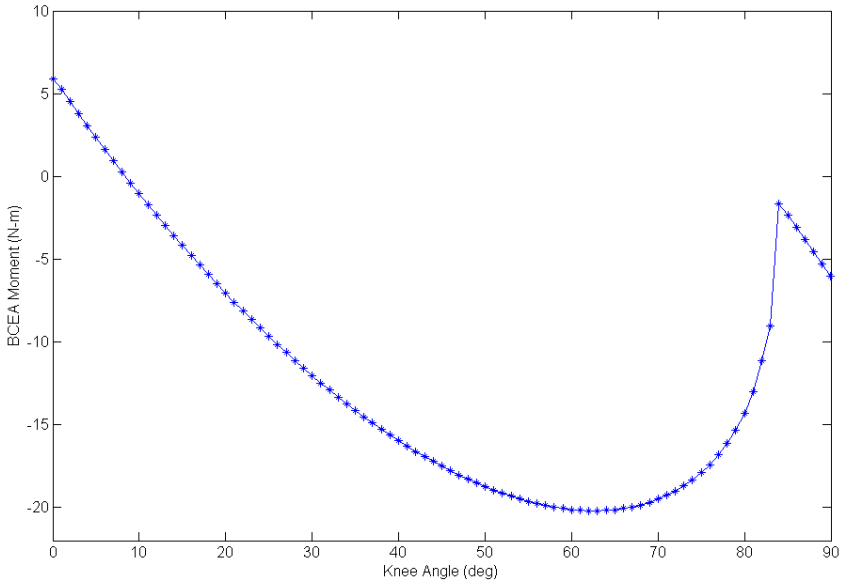

Figure 5-2. Applied BCEA Moments

Table 5-1. Summary of BCEA Applied Extension Moments

Extension Moment		
Maximum	Knee Angle at maximum	Knee Angle at snap
(N-m)	(Degrees)	(Degrees)
20.201	62	83

The reaction forces at the top anterior and posterior pins of the prosthetic knee were also developed in the BCEA design and are shown graphically in Figure 5-3. Figure 5-3 depicts the magnitude of the anterior and posterior pin reaction forces versus the knee flexion angle. The reaction forces of the posterior pin were very small and are shown near zero, while the anterior pin forces were more prominent. These reaction forces were separated into the x and y directions and applied to their respective pin locations labeled in Figure 5-4 along with the extension moments discussed.

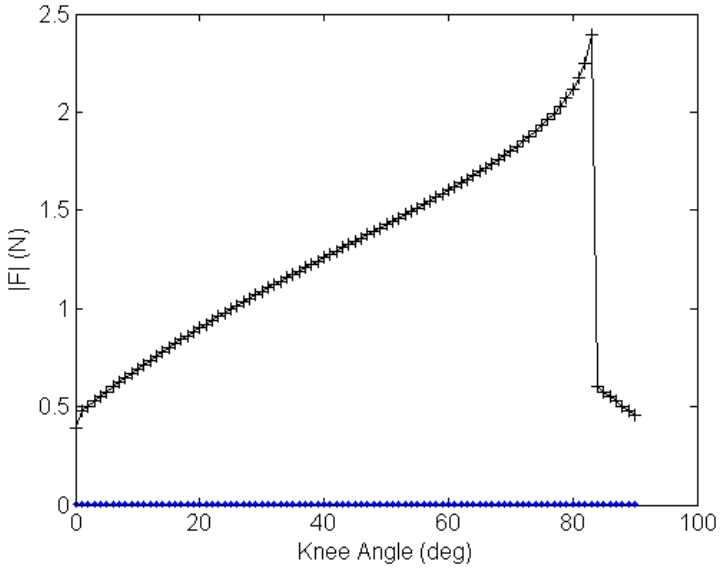

Figure 5-3. BCEA Reaction Forces vs. Knee Flexion Anterior (black) and Posterior (Blue)

Table 5-2. Summary of BCEA Applied Reaction Forces

Reaction Force				
Pin	Maximum		Min	
	$\|F_X\|$	$\|F_Y\|$	$\|F_X\|$	$\|F_Y\|$
	(N)		(N)	
Top-Anterior	2.287	1.199	0.00116	0.135
Top-Posterior	4.74e-5	1.929e-5	2.11e-10	2.12e-10

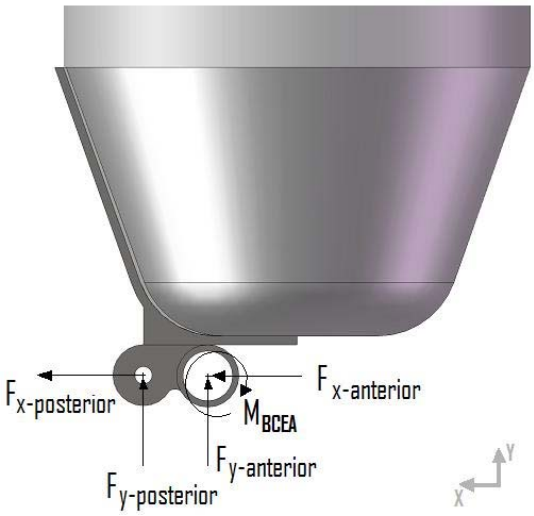

Figure 5-4. Free Body Diagram of the Prosthetic Knee's Top Bracket and Socket

These variable external loads were the driving forces behind stress variations within the prosthesis and were analytically calculated using ANSYS. Based on magnitudes of the forces and moments calculated, the moments applied as a result of the BCEA will have more impact on the stresses induced within the prosthetic socket than those of the reactions forces (which were induced as good measure).

5.5 Analysis and Results

Stresses induced on the inner part of the prosthetic socket were evaluated for each degree of knee flexion and stress magnitude photos were created using SolidWorks (COSMOSWorks). The external loads (as discussed previously) varied from small knee flexions to large and induced varying stress magnitudes. The criterion we adopted for analyzing proprioception was that the stresses applied to the inner part of the prosthetic

socket showed distinct variation over knee flexions and did not cause failure of the polypropylene socket.

When conducting interface mechanics research it is crucial to determine whether the stresses exposed to the residuum cause tissue damage, which could lead to necrosis and further injury to the residual limb and surrounding tissues. This chapter evaluates stresses at the inner socket interface and were analyzed as opposed to the interface stresses on the residual limb due to higher amounts of error present as a result/lack of residual sock (which was unaccounted for in the present model), soft-tissue, epidermis and bone. The simplifications imposed on the model to make it less computationally intensive also lend themselves to higher error and less justification when crossing material interfaces, therefore only the stresses on the inner socket wall were analyzed. For this reason, ensuring that the stresses induced on the residual tissue would not cause further tissue damage, was not adopted for this thesis, but should be analyzed with further expansion of the geometry and before any clinical testing.

Stress 'pictures' of the inner cone of the prosthetic socket were developed for each degree of knee flexion ranging 0-90 degrees as a result of static failure analysis by the von Mises principle. These results are summarized in Figure 5-5, which shows the stresses from 15-90 degrees for every 15 degree step. As shown, the stresses increase over flexions from 0 degrees to 60 degrees and then begin to decrease. This is characteristic of the moments shown in Figure 5-2; Figure 5-5 (F) occurs post-snap, which is a result of the knee and BCEA ready for the seated position. These stress patterns offer initial validation that the BCEA will offer variable stress patterns on the inner part of the prosthetic socket.

Figure 5-6 emphasizes the stress variations over the results. Figure 5-6 (A) and (D) depicts the lowest stress states, resulting near each of the knee's stable equilibrium points (stance and sitting). Figure 5-6 (C) is a result of the maximum extension moments which occur at 62 degrees of flexion, while (D) is an intermediate point between (A) and (C). These stress variations are a direct result of the BCEA and pose the hypothesis of increased proprioception via stress variations over the swing phase. Table 5-3 summarizes the stress results at maximum knee flexion (62 degrees), shown in Figure 5-6 (C).

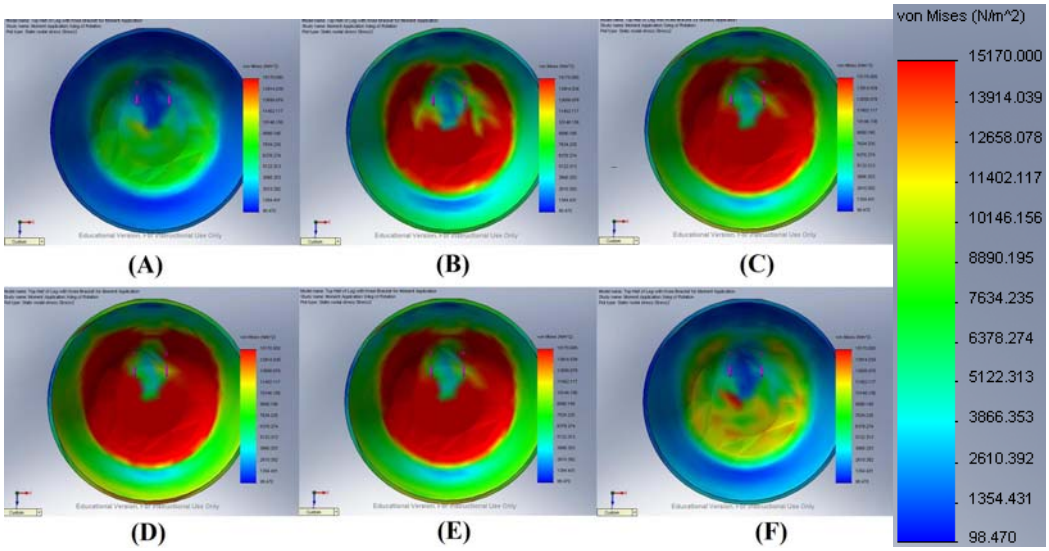

Figure 5-5. Stress Patterns on Inner Part of Prosthetic Socket by Knee Flexion (A) 15 degrees, (B) 30 degrees, (C) 45 degrees, (D) 60 degrees, (E) 75 degrees, (F) 90 degrees

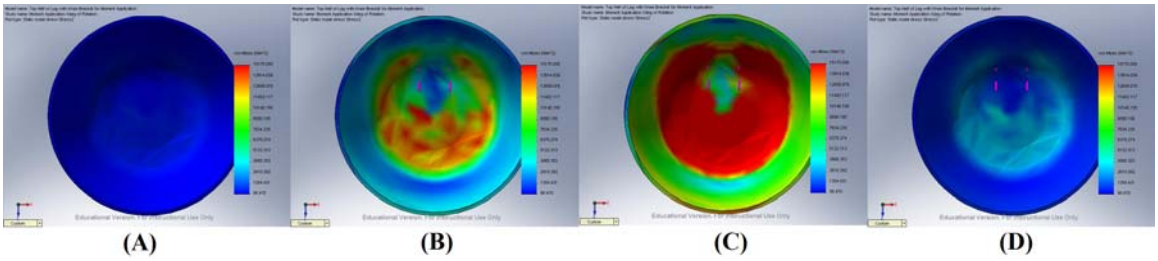

Figure 5-6. Stress Pattern Summary Over Key Knee Flexions (A) 8 degrees, (B) 20 degrees, (C) Max Extension Moment (62 degrees), (D) 83 degrees

Table 5-3. Surface Stress Summary at 62 Degrees of Flexion

Surface Stress Summary at 62 Degrees		
	Value	
Sum	10.613	MPa
Average	14.719	kPa
Maximum	51.705	kPa
Minimum	0.98013	kPa
RMS	18.103	kPa
Safety Factor	657.64	

These results correspond to the BCEA designed previously; the magnitude of the forces applied by the compliant segment (BCEA) can be increased or decreased with the geometry (its width). The safety factor above is large and can be decreased with increasing the applied forces. The resulting strains caused at maximum knee flexion were also analyzed and are shown in Figure 5-7, and summarized in Table 5-4.

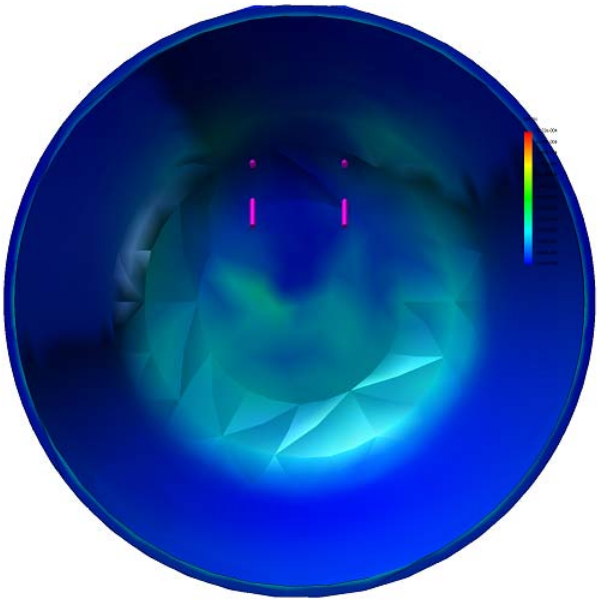

Figure 5-7. Strain at Maximum Knee Flexion

Table 5-4. Surface Strain Summary at 62 Degrees of Flexion

Surface Strain Summary at Max Knee Flexion	
	Value
Sum	0.059192
Average	8.2097e-005
Maximum	0.00028839
Minimum	5.4667e-006
RMS	0.00010097

In each of the stress photos, a noticeable stress variation is located near the top of the illustration, as shown in Figure 5-8. This stress 'anomaly' is not an anomaly, but a result of the fixation applied to the prosthetic knee's top bracket and the socket. The model is constructed in a way that the polypropylene socket at the surface of contact between the knee's top bracket is fixed at each node (as mentioned previously in boundary conditions), and restricts stresses, strains and deflections at the contact pairs. Figure 5-9 shows the area of contact and the pairs that are bonded together which form this stress diagram anomaly. In reality, the fixation methods of the prosthetic socket to the knee will cause stress concentrators via screws, pins or bolts, and will result in higher stresses in the area highlighted as opposed to the lower stresses calculated here.

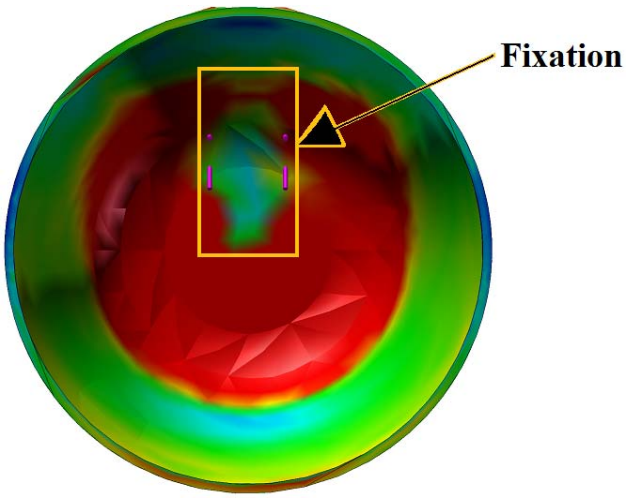

Figure 5-8. Stress Anomaly Due to Knee Fixation

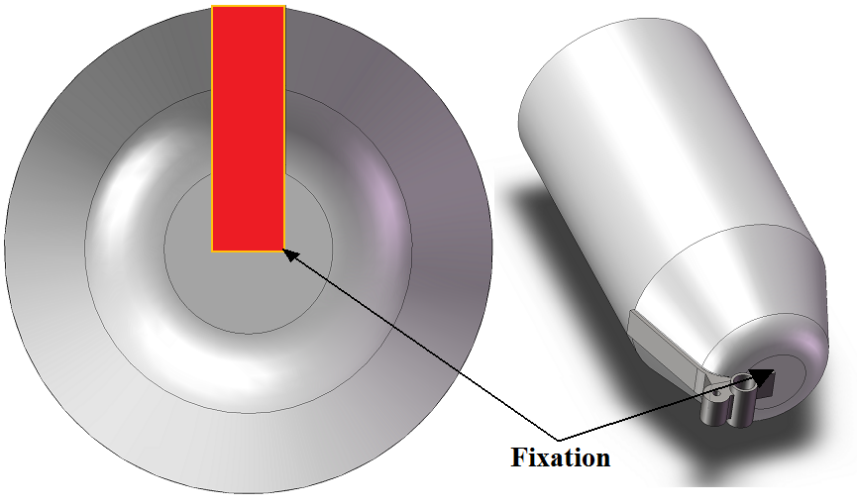

Figure 5-9. Socket and Knee Fixation/Contact Area

5.6 Proprioception and Variable Stress Conclusions and Future Work

The stresses and strains induced over 90 degrees of flexion varied over the results as shown, and can be used to develop the hypothesis of increased proprioception based off variable stress patterns in a prosthetic socket as a result of a bistable compliant extension aid. The strains calculated at the maximum flexion moment knee angle were also analyzed in order to develop the concept of socket deflection under flexion, and showed that the moments caused by the BCEA were sufficient to cause small strains which can be 'optimized' further by altering the reaction forces brought on by the BCEA (via altering its geometry).

These analytical results form the foundation for the measurement/increase of proprioceptive feedback in lower-limb prostheses by analyzing stress variations within the prosthetic socket. These surface stresses and strains can be used to justify further complexity to the FEA model and calculation of the surface stresses induced on a modeled residual limb. Stresses on the modeled residual limb, when calculated efficiently, can produce pre-clinical testing results and the basis for experimentation of stress patterns versus proprioception.

Chapter 6 Conclusions

This chapter focuses on the conclusions of this thesis, the contributions made to the mechanical engineering field and recommendations for future work are provided.

A bistable compliant extension aid (BCEA) which has the ability to conform to the necessary functional requirements of prosthetic swing of an above-knee prosthesis has been developed and optimized. The resulting BCEA extension moments were analytically calculated using ANSYS and were shown to provide the necessary moment characteristics of a prosthetic knee extension aid. A method for evaluating prosthetic proprioception over the swing phase by interface stresses between the prosthetic socket and residual limb, as a result of the bistable compliant extension aid, has been introduced. These stresses on the inner cone of the prosthetic socket were calculated using COSMOSWorks. The results were plotted as stress magnitude photos and were visually analyzed over knee flexions from 0 to 90 degrees, and showed the necessary magnitude variations for validation of the proprioception-via-stress-variation hypothesis.

6.1 Contributions

As discussed in Chapter 3, interface mechanics have been researched in depth and have shown promise in future research and application. Interface mechanics, as shown in this thesis as well as other research, have the ability to provide ground-breaking

advancements in the field of prosthetics in the form of proprioceptive feedback. Compliant mechanism technology has also shown promise in their applications in prosthetic joint research. The primary contributions made by this research are as follows:

- A compliant link (BCEA) has been developed that can act efficiently as a prosthetic extension aid by providing the necessary extension moments during key knee flexions. The geometry of the BCEA was optimized in order to meet these functional swing-moment requirements, and the resulting forces on the knee mechanism were analytically calculated in order to analyze the stresses induced on the prosthetic socket by the compliant add-on. The BCEA design specialization also offers a way of optimizing a prosthetic knee during swing (applied extension moments) to any particular patient by altering the geometry of the compliant segment.

- The external forces and moments induced by the bistable compliant extension aid were applied to a finite element model of an above-knee prosthesis. The interface stresses on the inner-surface of the prosthetic socket were analyzed in order to lay the foundation for the measurement of proprioceptive feedback by means of induced variable stress patterns. This hypothesis was analytically validated by a simplified finite element model and laid the groundwork for further model refinement.

6.2 Suggestions for Future Work

Future work should be directed at the refinement and advancement of the finite element model geometries and material properties used in order to better estimate the interface mechanics developed in this thesis. Residuum tissues such as the epidermis, bone and cartilage should be added to the residual geometry. A residual sock should be included, and the material properties should be verified. Once the model closely reflects actual geometries, the analysis should focus on the stresses on the residual limb rather than the prosthetic socket's inner surface. Analytical results should verify that the induced stresses do not cause tissue trauma to the residual limb.

The use of compliant mechanism technology offers several design advantages: if the stresses induced on the residual limb are too high, the BCEA extension moments could be optimized by optimizing the width of the BCEA geometry; while if the stresses on the BCEA are too high, the thickness of the link could be optimized thinner to reduce these stresses. These design advantages allow for further modification and research of the BCEA and how it affects the interface-stress proprioception theory.

List of References

[1] Brennan, J.M. and Childress, D.S., "*Finite element and experimental investigation of above-knee amputee limb/prosthesis systems: A comparative study*", Advances in Bioengineering, ASME, Vol. 20 pp. 547-550, 1991.

[2] Britt, M. and Ellen, L. and Thomas, H., "*Prosthetic Devices*", Retrieved June 15, 2008 from http://www.unc.edu/~mbritt/

[3] Childress, D.S. and Steege, J.W. and Wu, Y. et al., "*Finite element methods for below-knee socket design",* Rehabilitation Res. Development Prog. Reports, Vol. 29, pp. 22-23, 1992.

[4] Faustini, M. and Neptune, R. and Crawford, R., "*The quasi-static response of compliant prosthetic sockets for transtibial amputees using finite element methods*", Medical Engineering & Physics, Vol. 18, pp. 114-121, 2006.

[5] Guérinot, A.E., Magleby, S.P., and Howell, L. L., "*Preliminary Design Concepts for Compliant Mechanism Prosthetic Knee Joints"*, ASME Design Engineering Technical Conference, Salt Lake City, Utah, 2004.

[6] Guérinot, A. E., Magleby, S. P., Howell, L. L., and Todd, R, H, "*Compliant Joint Design Principles for High Compressive Load Situations*", Journal of Mechanical Design, in press, 2004.

[7] Highsmith, J.M., Kahle, J.T., "*Prosthetic Knees: Classification & Overview*", Retrieved May 10, 2008 from http://oandp.health.usf.edu/prosthetics_main.html

[8] Howell, L. L., "*Compliant Mechanisms"*, Wiley, New York, 2001.

[9] Jia, X. and Zhang, M. and Li, X. and Lee, W., "*A quasi-dynamic nonlinear finite element model to investigate prosthetic interface stresses during walking for trans-tibial amputees*", Clinical Biomechanics Vol. 20 Num. 6, pp. 630-635.

[10] Mahler, S., "*Compliant Pediatric Prosthetic Knee",* M.S. Thesis, University of South Florida, Tampa, Florida, 2007.

[11] Advameg, Inc., 2007, "*Medical Discoveries*", Retrieved May 17, 2008 from http://www.discoveriesinmedicine.com/index.html

[12] Moreno, R. and Jones, D. and Solomonidis, S. and Mackie, H., "*Magnetic Resonance Imaging of Residual Soft Tissues for Computer-Aided Technology Applications in Prosthetics – A Case Study*", JPO, Vol. 11 Num. 1 p. 6, 1999.

[13] Ossur®, (n.d.), Retrieved December 2007 from http://www.ossur.com/

[14] Otto Bock®, (n.d.), Retrieved December 2007 from http://www.ottobockus.com/

[15] Pitkin, M., "*Effects of Design Variants in Lower-Limb Prostheses on Gait Synergy*", Journal of Prosthetics and Orthotics, Vol. 9 Num. 3, pp. 113-122, 1997.

[16] Quesada, P. and Skinner, H.B., "*Analysis of a below-knee patellar tendon-bearing prosthesis: A Finite element study*", J. Rahab. Res. Develop., Vol. 28, Num. 3, pp. 1-12, 1991.

[17] Reynolds, D.P., "*Shape design and interface load analysis of below-knee prosthetic sockets*", Ph.D. dissertation, University of London, 1988.

[18] Reynolds, D.P. and Lord, M., "*Interface load analysis for computer-aided design of below-knee prosthetic sockets*", Med. Biol. Eng. Comput., Vol. 30, pp. 419-426, 1992.

[19] Rosenberger, B., "*Medicare O & P Reimbursement: Part 3 of 3: Can I Have a Cadillac?*", inMotion, Vol. 10 Issue 5, 2000.

[20] Sanders, J. and Daly, C., "*Normal and shear stresses on a residual limb in a prosthetic socket during ambulation: Comparison of finite element results with experimental measurements*", Journal of Rehabilitation Research and Development Vol. 30 Num. 2, pp. 191-204, 1993.

[21] Sanders, J. and Daly, C. and Burgess, E., "*Interface shear stresses during ambulation with a below-knee prosthetic limb*", Journal of Rehabilitation Research and Development Vol. 29 Num. 4, pp. 1-8, 1992.

[22] Serway, R. A. and Jewett, Jr. J. W., "*Physics for Scientists and Engineers*", 6th Ed., Brooks Cole, 2003.

[23] Silver-Thorn, M.B., "*Estimation and experimental verification of residual limb/prosthetic socket interface pressures for below-knee amputees*", Ph.D. dissertation, Northwestern University, 1991.

[24] Silver-Thorn, M.B. and Childress, D.S., "*Parametric analysis using the finite element method to investigate prosthetic interface stresses for persons with trans-tibial amputation*", Journal of Rehabilitation Research and Development, Vol. 33 Issue 3, pp. 227-238, 1996.

[25] Silver-Thorne, B. and Steege, J., "*A review of prosthetic interface stress investigations*", Journal of Rehabilitation Research & Development, Vol. 33 Issue 3, pp. 253-266, 1996.

[26] Smith, D., "*The Knee Disarticulation: It's Better When It's Better and It's Not When It's Not*", inMotion, Vol. 14 Issue 1, 2004.

[27] Stark, G., "*Overview of Knee Disarticulation,*" Journal of Prosthetics and Orthotics, Vol. 16 Issue 4, pp.130-137, 2004.

[28] Steege, J.W. and Childress, D.S., "*Analysis of trans-tibial prosthetic gait using the finite element technique*", American Academy of Orthotists and Prosthetists, New Orleans, LA, pp. 13-14, 1995.

[29] van de Veen, P.G., "*Above-knee Prosthesis Technology*", P.G. van de Veen Consultancy, The Netherlands, 2001.

[30] Wheeless, C., "*Wheeless' Texbook of Orthopaedics*," Duke University, 2000, retrieved June 29, 2008 from http://www.wheelessonline.com/ortho/gait

[31] Winter, D.A., *Biomechanics and Motor Control of Human Movement*, Wiley, New Jersey, 2005.

[32] Wiersdorf, J., "*Preliminary Design Apporoach for Prosthetic Ankle Joints Using Compliant Mechanisms*", M.S. Thesis, Brigham Young University, Provo, Utah, 2005.

[33] Zachariah, S. and Sanders, J., "*Interface Mechanics in Lower-Limb External Prosthetics: A Review of Finite Element Models*", IEEE Transactions on Rehabilitation Engineering, Vol. 4 Num. 4, December 1996.

[34] Zahedi, S., "*Lower Limb Prosthetic Research in the 21st Century*", ATLAS of Prosthetics, (n.d.).

[35] Zhang, M. and Mak, A., "*A Finite Element Analysis of the Load Transfer Between an Above-Knee Residual Limb and Its Prosthetic Socket – Roles of Interface Friction and Distal-End Boundary Conditions*", IEEE Transactions of Rehabilitation Engineering, Vol. 4, Num. 4, pp. 337-346, December 1996.

[36] Zhang, M. and Mak, A. and Roberts, V.V., "*Finite element modeling of a residual lower-limb in a prosthetic socket: a survey of the development in the first decade*", Medical Engineering & Physics, Vol. 20, pp. 360-373, 1998.

Appendices

Appendix I: ANSYS Knee Code

```
!*****************************************************************
!/INPUT,C:\DOCUME~1\aroetter\Desktop\KneeCode2,txt,,1
!/CWD,'C:\Documents and Settings\amunoz4\'
!*****************************************************************

FINISH
/CLEAR

/FILENAME, Knee
/title,Knee

/PREP7                  ! Enter the pre-processor


!*****************************************************************
!************** Model Parameters ***********************************
!*****************************************************************

WRITE=1                 ! 1= Write output files, Else= Don't Write

PI=acos(-1.)

hp=6                    ! Posterior Thickness (mm)
bp=17                   ! Posterior Width (mm)

ha=2                    ! Anterior Thickness (mm)
ba=12                   ! Anterior Width (mm)

hb=26                   ! Bottom Width (mm) (approx.)
bb=5                    ! Bottom Width (mm) (approx.)


hc=5                    ! Compliant Geometry
bc=1


K1=1e6                  ! Joint Stiffness


!*****************************************************************
```

Appendix I (Continued)

```
!*************** Define Area ***********************************************
!*******************************************************************************

Ap = hp*bp                          ! Cross sectional area of posterior
Izp= 1/12*bp*hp*hp*hp               ! Second Moment of Area (aka Area Moment of
Inertia)
Ixp= 1/12*hp*bp*bp*bp

Aa = ha*ba                          ! Cross sectional area of anterior links
Iza= 1/12*ba*ha*ha*ha               ! Second Moment of Area (aka Area Moment of
Inertia)
Ixa= 1/12*ha*ba*ba*ba

Ab = hb*bb                          ! Cross sectional area of bottom link (approx.)
Izb= 1/12*bb*hb*hb*hb               ! Second Moment of Area (aka Area Moment of
Inertia)
Ixb= 1/12*hb*bb*bb*bb

Ac = hc*bc                          ! Cross sectional area of compliant link
Izc= 1/12*bc*hc*hc*hc               ! Second Moment of Area (aka Area Moment of
Inertia)
Ixc= 1/12*hc*bc*bc*bc


!*******************************************************************************
!*************** Define Keypoints ******************************************
!*******************************************************************************

! Create Keypoints: K(Point #, X-Coord, Y-Coord, Z-Coord)

K,1,0,0,0,          !(mm)
K,2,23.62,0,0,      !(mm)
K,3,35.52,-85.58,0, !(mm)
K,4,35.52,-85.58,0, !(mm)
K,5,-12.74,-85.58,0,!(mm)
K,6,-12.74,-85.58,0,!(mm)
K,7,35.52,-85.58,1, !(mm)
K,8,-12.74,-85.58,1,!(mm)
K,9,-12.74,-85.58,0,!(mm)
```

Appendix I (Continued)

```
!*****************************************************************************
!*************** Create Links ************************************************
!*****************************************************************************

L,2,3                       ! Anterior link
L,4,5                       ! bottom link
L,1,6                       ! Posterior link
L,6,8                       ! Pin Joint Direction Line
L,4,7                       ! Pin Joint Direction Line


!*****************************************************************************
!************ Declare Element Type  ******************************************
!*****************************************************************************

SECTYPE,   1, BEAM, RECT, , 0    ! Defines BEAM188 Properties
SECOFFSET, CENT
SECDATA,1,5,1,1,0,0,0,0,0,0      ! Defines BEAM188 Geometry


ET,1,BEAM4                       ! Element Type 1 - Rigid Links
!KEYOPT,1,2,1
!KEYOPT,1,6,1

ET,2,COMBIN7,,1                  ! Element Type 2 - Pin Joints

ET,3,BEAM188                     ! Element Type 3 - Compliant Link(BEAM188)
!KEYOPT,3,2,1
!KEYOPT,3,6,1

!*****************************************************************************
!************ Define Real Constants ******************************************
!*****************************************************************************

R,1,Ap,Ixp,Izp,hp,bp,        ! Properties of Posterior Links
R,2,K1,K1,K1,0,0,0           ! Properties of the  pin joints
R,3,Aa,Ixa,Iza,ha,ba,        ! Properties of Anterior Links
R,4,Ab,Ixb,Izb,hb,bb,        ! Properties of Bottom Link
!R,5,Ac,Ixc,Izc,hc,bc,       ! Properties of compliant Link
```

Appendix I (Continued)

```
!*****************************************************************
!********** Define Material Properties ***************************************
!*****************************************************************

MP,EX,1,207000          ! Young's Modulus of Elasticity Steel (MPa)
MP,PRXY,1,0.29          ! Poisson's ratio

MP,EX,2, 1400           ! Young's Modulus of Elasticity Polypropylene (MPa)
MP,PRXY,2,0.4103        ! Poisson's ratio

!*****************************************************************
!******************** Mesh ***************************************************
!*****************************************************************

type,1                  ! Use element type 1 (Beam4)
mat,1                   ! use material property set 1
real,1                  ! Use real constant set 1

LESIZE,ALL,,,2
LMESH,3,3               ! Mesh Posterior Link

real,3                  ! Use real constant set 3

LMESH,1,1               ! Mesh Anterior Link

real,4                  ! Use real constant set 4

LMESH,2,2               ! Mesh Bottom Link


nx = 12.74              ! Initial x position for prestressed link (xdirections)
ny = 85.58              ! Initial y position for prestressed link (ydir)

n_abs = SQRT(12.74*12.74+85.58*85.58)


Delta = 2               ! NUMBER OF INCREMENTAL CHANGES IN
COMPLIANT LINK


phi_max = PI/2                  ! deleted /2
```

Appendix I (Continued)

```
phi_incr = phi_max/Delta
*DO,j,0,Delta,1                    ! Begin the Compliant Link Creation Loop
!*********************************************************************
!************** DEFINE COMPLIANT ***************************************
!*********************************************************************

phi = j*phi_incr                   ! Defines the "Arc Angle"

*IF,j,EQ,0,THEN                    ! First iteration: Arc Length=link length
R = 1000
L = n_abs
*ELSE
R = n_abs/(2*sin(phi/2))
L = R*phi
*ENDIF


DX = (L-n_abs)*nx/n_abs            ! Defines Steps in x direction
DY = (L-n_abs)*ny/n_abs            ! Defines steps in y direction


K,10,DX,DY,0                       ! Defines keypoint (top of compliant link)
L,9,10,                            ! Line #6 = Compliant Link


type,3                             ! Use element type 3 (Beam188)
mat,2
!real,5
secnum,1                           ! Makes BEAM188 active for Meshing
LESIZE,6,,,32
LMESH,6,6                          ! Mesh Compliant Link

!*********************************************************************
!***************** GET NODES ***************************************
!*********************************************************************

ksel,s,kp,,1
nslk,s
*get,nkp1,node,0,num,max      ! Retrieves and stores a value as a scalar or part of an array


ksel,s,kp,,2
nslk,s
```

Appendix I (Continued)

```
*get,nkp2,node,0,num,max      ! Retrieves and stores a value as a scalar or part of an array

ksel,s,kp,,3
nslk,s
*get,nkp3,node,0,num,max
ksel,s,kp,,4
nslk,s
*get,nkp4,node,0,num,max      ! Retrieves and stores a value as a scalar or part of an array


ksel,s,kp,,5
nslk,s
*get,nkp5,node,0,num,max      ! Retrieves and stores a value as a scalar or part of an array

ksel,s,kp,,6
nslk,s
*get,nkp6,node,0,num,max

ksel,s,kp,,7
nslk,s
*get,nkp7,node,0,num,max      ! Retrieves and stores a value as a scalar or part of an array

ksel,s,kp,,8
nslk,s
*get,nkp8,node,0,num,max

ksel,s,kp,,9
nslk,s
*get,nkp9,node,0,num,max      ! Retrieves and stores a value as a scalar or part of an array

ksel,s,kp,,10
nslk,s
*get,nkp10,node,0,num,max

ALLSEL


TYPE,2
mat,1                         ! use material property set 1
REAL,2
E,nkp3,nkp4,nkp7              ! Defines an element by node connectivity.
E,nkp5,nkp6,nkp8
E,nkp5,nkp9,nkp8
```

Appendix I (Continued)

```
FINISH                          ! Finish pre-processing



!*****************************************************************************
!***************** SOLUTION ***************************************************
!*****************************************************************************
*get,date,active,,dbase,ldate
*get,time,active,,dbase,ltime

year=nint(date/10000)
month=nint(nint(date-year*10000)/100)
day=date-(nint(date/100))*100
hour=nint(time/10000-.5)
minute=nint((time-hour*10000)/100-.5)


KEYW,PR_SGUI,1                  ! Suppresses "Solution is Done" text box
/SOL                            ! Enter the solution processor

/gst,off                        ! Turn off graphical convergence monitor
ANTYPE,0                        ! Analysis type, static
NLGEOM,1          ! Includes large-deflection effects in a static or full transient analysis
LNSRCH,AUTO                     ! ANSYS automatically switches line search on/off
NEQIT,50                        ! Set max # of iterations
DELTIM,,0.0001                  ! Set minimum time step increment


!*****************************************************************************
!*********** Define Displacement Constraints ******************************
!*****************************************************************************

DK,1,,0,,,UX,UY,UZ,ROTX,ROTY  ! Pin Joint at Keypoint 1
DK,2,,0,,,UX,UY,UZ,ROTX,ROTY  ! Pin Joint at Keypoint 2

!*****************************************************************************
!********** Pre-Stress Compliant Member ***************************************
!*****************************************************************************

DK,10,,0,,,UZ,ROTX,ROTY,        ! Constrains the top pin before prestressing
preload_steps = 10              ! Applies Prestress to Compliant Link in steps
DK,1,ROTZ,0                     ! Constrains KP1 while Prestressing
```

Appendix I (Continued)

```
*DO,step, 1,preload_steps,1

DK,10,UX,-DX/preload_steps*step
DK,10,UY,-DY/preload_steps*step
FK,10,MZ,4              ! Apply a moment to direct the Compliant Link during "assembly"
LSWRITE, step
*ENDDO
!*********************************************************************
!************ Displacement Load ***************************************
!*********************************************************************

FKDELE,10,MZ
DK,10,ROTZ,phi/2
Maxrot = 191                                    ! Maximum rotation
STABILIZE,CONSTANT,ENERGY,1e-5  ! Applies a stabilization damping action during snap phenomena
*DO,step,1,90,1

theta=step*PI/180

DK,1,ROTZ,theta

LSWRITE,step+preload_steps
*ENDDO

*DO,step,90,0,-1

theta=step*PI/180

DK,1,ROTZ,theta

LSWRITE,191-step
*ENDDO


LSSOLVE,1,Maxrot
STABILIZE                       ! De-activates the Stabilize command
FINISH                          ! Finish the solution processor

!*********************************************************************
!************** Postprocessor *****************************************
!*********************************************************************
```

Appendix I (Continued)

```
/POST1                    ! Enter the postprocessor

PLDISP,1                  ! Displays deformed & undeformed shape

SET,LAST
/REPLOT

*DIM,ANTERIOR,TABLE,Maxrot,3
*DIM,POSTERIOR,TABLE,Maxrot,3
*DIM,COMPLIANT,TABLE,Maxrot,3

*Do,i,1,Maxrot
SET,i                             ! Read data for step "i"
*GET,rotz1,Node,nkp1,ROT,Z        ! Assign ANTERIOR data to ANTERIOR table
*SET,ANTERIOR(i,1),rotz1
*GET,fx1,Node,nkp1,RF,FX
*SET,ANTERIOR(i,2),fx1
*GET,fy1,Node,nkp1,RF,FY
*SET,ANTERIOR(i,3),fy1


*GET,rotz1,Node,nkp2,ROT,Z        ! Assign POSTERIOR data to POSTERIOR table
*SET,POSTERIOR(i,1),rotz1
*GET,fx1,Node,nkp2,RF,FX
*SET,POSTERIOR(i,2),fx1
*GET,fy1,Node,nkp2,RF,FY
*SET,POSTERIOR(i,3),fy1

*GET,mz,Node,nkp10,RF,MZ          ! Assign COMPLIANT data to COMPLIANT table
*SET,COMPLIANT(i,1),mz
*GET,fx1,Node,nkp10,RF,FX
*SET,COMPLIANT(i,2),fx1
*GET,fy1,Node,nkp10,RF,FY
*SET,COMPLIANT(i,3),fy1

*ENDDO

*IF,WRITE,EQ,1,THEN
*cfopen,C:\DOCUME~1\aroetter\ANSYS_Results\index%j%,txt

*vwrite,month,'-',day,'-',year,hour,':',minute
%I %C %I %C %I %4.2I %C %2.2I
```

Appendix I (Continued)

```
*vwrite,'ANTERIOR LINK'
%C

*vwrite,'ROTX (rad)','FX','FY'
%-17C %-17C %-17C


*vwrite,ANTERIOR(1,1),ANTERIOR(1,2),ANTERIOR(1,3)
%16.8G %16.8G %16.8G
*vwrite,'POSTERIOR LINK'
%C

*vwrite,'ROTX (rad)','FX','FY'
%-17C %-17C %-17C


*vwrite,POSTERIOR(1,1),POSTERIOR(1,2),POSTERIOR(1,3)
%16.8G %16.8G %16.8G

*vwrite,'COMPLIANT LINK, L = ',L
%C %16.8G

*vwrite,'MZ','FX','FY'
%-17C %-17C %-17C


*vwrite,COMPLIANT(1,1),COMPLIANT(1,2),COMPLIANT(1,3)
%16.8G %16.8G %16.8G

*cfclose
*ENDIF
FINISH


!*********************************************************************
!********** DELETE COMPLIANT LINK **********************************
!*********************************************************************

/PREP7
LCLEAR,6,6
LDELE,6,6
KCLEAR,11
```

Appendix I (Continued)

```
*ENDDO

!ANTIME,45,0.1, ,1,1,0,0       ! Animate


!*****************************************************************************
!****************** FINISH ***************************************************
!*****************************************************************************
```

Appendix II: ANSYS Results File ($\Phi=\pi/2$)

ANTERIOR LINK

ROTX (rad)	FX	FY
0.0000000	-0.12275462	-0.25355748
0.0000000	-8.25826006E-02	2.21055171E-02
0.0000000	-6.57499172E-02	0.14110606
0.0000000	-5.61195668E-02	0.21184787
0.0000000	-4.97955059E-02	0.26050694
0.0000000	-4.53107617E-02	0.29694249
0.0000000	-4.19729793E-02	0.32580702
0.0000000	-3.94107317E-02	0.34960197
0.0000000	-3.74030535E-02	0.36981594
0.0000000	-3.58098291E-02	0.38739485
1.74532925E-02	1.16364284E-03	0.47859500
3.49065850E-02	4.37110341E-03	0.50367282
5.23598776E-02	6.51178243E-03	0.52845713
6.98131701E-02	7.60999646E-03	0.55293795
8.72664626E-02	7.68930672E-03	0.57710563
0.10471976	6.77245016E-03	0.60095079
0.12217305	4.88137068E-03	0.62446422
0.13962634	2.03725745E-03	0.64763689
0.15707963	-1.73942494E-03	0.67045996
0.17453293	-6.42890129E-03	0.69292461
0.19198622	-1.20120547E-02	0.71502223
0.20943951	-1.84703932E-02	0.73674423
0.22689280	-2.57860222E-02	0.75808212
0.24434610	-3.39416081E-02	0.77902742
0.26179939	-4.29203595E-02	0.79957175
0.27925268	-5.27059897E-02	0.81970670
0.29670597	-6.32826936E-02	0.83942389
0.31415927	-7.46351245E-02	0.85871497
0.33161256	-8.67483681E-02	0.87757156
0.34906585	-9.96079145E-02	0.89598528
0.36651914	-0.11319965	0.91394775
0.38397244	-0.12750980	0.93145053
0.40142573	-0.14252498	0.94848518
0.41887902	-0.15823210	0.96504324
0.43633231	-0.17461838	0.98111617
0.45378561	-0.19167134	0.99669543

Appendix II (Continued)

0.47123890	-0.20937879	1.0117724
0.48869219	-0.22772881	1.0263385
0.50614548	-0.24670970	1.0403851
0.52359878	-0.26631004	1.0539033
0.54105207	-0.28651862	1.0668844
0.55850536	-0.30732449	1.0793196
0.57595865	-0.32871688	1.0912000
0.59341195	-0.35068528	1.1025166
0.61086524	-0.37321935	1.1132605
0.62831853	-0.39630901	1.1234226
0.64577182	-0.41994434	1.1329938
0.66322512	-0.44411570	1.1419649
0.68067841	-0.46881362	1.1503267
0.69813170	-0.49402889	1.1580699
0.71558499	-0.51975255	1.1651851
0.73303829	-0.54597587	1.1716629
0.75049158	-0.57269040	1.1774937
0.76794487	-0.59988800	1.1826681
0.78539816	-0.62756082	1.1871762
0.80285146	-0.65570139	1.1910082
0.82030475	-0.68430260	1.1941544
0.83775804	-0.71335777	1.1966047
0.85521133	-0.74286068	1.1983490
0.87266463	-0.77280566	1.1993769
0.89011792	-0.80318759	1.1996782
0.90757121	-0.83400206	1.1992421
0.92502450	-0.86524539	1.1980580
0.94247780	-0.89691477	1.1961148
0.95993109	-0.92900836	1.1934013
0.97738438	-0.96152545	1.1899058
0.99483767	-0.99446662	1.1856167
1.0122910	-1.0278339	1.1805216
1.0297443	-1.0616312	1.1746080
1.0471975	-1.0958643	1.1678627
1.0646508	-1.1305413	1.1602720
1.0821041	-1.1656733	1.1518216
1.0995574	-1.2012746	1.1424963
1.1170107	-1.2373633	1.1322803
1.1344640	-1.2739624	1.1211564
1.1519173	-1.3111007	1.1091064
1.1693706	-1.3488138	1.0961105
1.1868239	-1.3871462	1.0821472
1.2042772	-1.4261532	1.0671926
1.2217305	-1.4659037	1.0512205

Appendix II (Continued)

1.2391838	-1.5064846	1.0342012
1.2566371	-1.5480058	1.0161009
1.2740903	-1.5906085	0.99688061
1.2915436	-1.6344765	0.97649452
1.3089969	-1.6798542	0.95488767
1.3264502	-1.7270747	0.93199262
1.3439035	-1.7766082	0.90772408
1.3613568	-1.8291483	0.88196996
1.3788101	-1.8857852	0.85457508
1.3962634	-1.9483987	0.82530731
1.4137167	-2.0207494	0.79377348
1.4311700	-2.1132177	0.75909882
1.4486233	-2.2875178	0.71674734
1.4660766	-0.57671990	0.16870011
1.4835299	-0.55434973	0.16075208
1.5009832	-0.53120905	0.15378854
1.5184364	-0.50747209	0.14770845
1.5358897	-0.48314117	0.14253714
1.5533430	-0.45821857	0.13830084
1.5707963	-0.43270667	0.13502674
1.5707963	-0.43266698	0.13501719
1.5533430	-0.45821527	0.13830003
1.5358897	-0.48313831	0.14253639
1.5184364	-0.50746965	0.14770776
1.5009832	-0.53120696	0.15378792
1.4835299	-0.55434796	0.16075152
1.4660766	-0.57689025	0.16857409
1.4486233	-0.59883148	0.17723195
1.4311700	-0.62016917	0.18670221
1.4137167	-0.64090084	0.19696273
1.3962634	-0.66102384	0.20799202
1.3788101	-0.68053548	0.21976931
1.3613568	-0.69943296	0.23227440
1.3439035	-0.71771337	0.24548772
1.3264502	-0.73537363	0.25939020
1.3089969	-0.75241062	0.27396335
1.2915436	-0.76882104	0.28918914
1.2740903	-0.78460149	0.30505004
1.2566371	-0.79974843	0.32152891
1.2391838	-0.81425819	0.33860906
1.2217305	-0.82812698	0.35627416
1.2042772	-0.84135089	0.37450828
1.1868239	-0.85392584	0.39329578
1.1693706	-0.86584766	0.41262139

Appendix II (Continued)

1.1519173	-0.87711207	0.43247013
1.1344640	-0.88771462	0.45282730
1.1170107	-0.89765076	0.47367846
1.0995574	-0.90691582	0.49500944
1.0821041	-0.91550501	0.51680633
1.0646508	-0.92341343	0.53905542
1.0471975	-0.93063604	0.56174321
1.0297443	-0.93716769	0.58485644
1.0122910	-0.94300316	0.60838206
0.99483767	-0.94813705	0.63230718
0.97738438	-0.95256388	0.65661912
0.95993109	-0.95627804	0.68130539
0.94247780	-0.95927383	0.70635370
0.92502450	-0.96154541	0.73175192
0.90757121	-0.96308681	0.75748813
0.89011792	-0.96389196	0.78355061
0.87266463	-0.96395464	0.80992782
0.85521133	-0.96326849	0.83660845
0.83775804	-0.96182703	0.86358142
0.82030475	-0.95962362	0.89083586
0.80285146	-0.95665143	0.91836119
0.78539816	-0.95290348	0.94614708
0.76794487	-0.94837259	0.97418352
0.75049158	-0.94305137	1.0024608
0.73303829	-0.93693221	1.0309697
0.71558499	-0.93000720	1.0597013
0.69813170	-0.92226821	1.0886471
0.68067841	-0.91370674	1.1177992
0.66322512	-0.90431396	1.1471504
0.64577182	-0.89408060	1.1766939
0.62831853	-0.88299697	1.2064238
0.61086524	-0.87105285	1.2363352
0.59341195	-0.85823740	1.2664240
0.57595865	-0.84453913	1.2966872
0.55850536	-0.82994574	1.3271233
0.54105207	-0.81444403	1.3577323
0.52359878	-0.79801975	1.3885159
0.50614548	-0.78065744	1.4194780
0.48869219	-0.76234016	1.4506248
0.47123890	-0.74304932	1.4819657
0.45378561	-0.72276431	1.5135134
0.43633231	-0.70146215	1.5452849
0.41887902	-0.67911698	1.5773024
0.40142573	-0.65569946	1.6095942

Appendix II (Continued)

0.38397244	-0.63117606	1.6421966
0.36651914	-0.60550797	1.6751555
0.34906585	-0.57864987	1.7085292
0.33161256	-0.55054811	1.7423922
0.31415927	-0.52113837	1.7768399
0.29670597	-0.49034223	1.8119958
0.27925268	-0.45806227	1.8480225
0.26179939	-0.42417476	1.8851377
0.24434610	-0.38851814	1.9236406
0.22689280	-0.35087392	1.9639559
0.20943951	-0.31093284	2.0067146
0.19198622	-0.26822884	2.0529145
0.17453293	-0.22199235	2.1042863
0.15707963	-0.17073312	2.1643744
0.13962634	-0.11064601	2.2427072
0.12217305	4.73122866E-03	0.62439373
0.10471976	6.77244703E-03	0.60095073
8.72664626E-02	7.68930383E-03	0.57710559
6.98131701E-02	7.60999253E-03	0.55293791
5.23598776E-02	6.51177769E-03	0.52845709
3.49065850E-02	4.37109710E-03	0.50367276
1.74532925E-02	1.16352861E-03	0.47859481
0.0000000	-3.13624507E-03	0.45323340

POSTERIOR LINK

ROTX (rad)	FX	FY
4.14762417E-07	-1.03590297E-10	8.31092147E-10
4.16918034E-07	-1.06284760E-10	7.88110742E-10
4.20321322E-07	1.16419659E-10	-8.43510450E-10
4.24171207E-07	1.05138429E-10	-8.45079124E-10
4.28276799E-07	-2.36527072E-10	1.64390138E-09
4.32568497E-07	1.26457928E-12	1.75841798E-13
4.37012983E-07	1.11480755E-10	-8.29994968E-10
4.41596322E-07	-1.48313694E-11	2.63421695E-11
4.46310565E-07	1.09795665E-10	-8.16027036E-10
4.51152099E-07	-2.11737686E-10	1.63314613E-09
1.74750786E-02	-5.08725134E-09	3.18856876E-08
3.49929066E-02	-5.94695857E-09	3.34431501E-08
5.25540019E-02	-6.90012012E-09	3.51042395E-08
7.01585608E-02	-8.22974336E-09	3.82613477E-08
8.78067967E-02	-9.03186141E-09	3.84402078E-08
0.10549894	-1.05264652E-08	4.15939279E-08
0.12323525	-1.17756891E-08	4.32158845E-08
0.14101598	-1.33242437E-08	4.58023841E-08
0.15884142	-1.47434502E-08	4.73178646E-08

Appendix II (Continued)

0.17671189	-1.67372681E-08	5.05309114E-08
0.19462770	-1.83293541E-08	5.21717638E-08
0.21258921	-2.00185711E-08	5.37786626E-08
0.23059678	-2.27204650E-08	5.77588800E-08
0.24865079	-2.48944730E-08	6.01429103E-08
0.26675165	-2.81434577E-08	6.45700814E-08
0.28489980	-3.09190516E-08	6.76934251E-08
0.30309566	-3.46401040E-08	7.21830625E-08
0.32133973	-3.75724014E-08	7.45728286E-08
0.33963248	-4.07827653E-08	7.74493924E-08
0.35797443	-4.58312915E-08	8.33032594E-08
0.37636611	-5.10724535E-08	8.88296990E-08
0.39480808	-5.67189356E-08	9.46764176E-08
0.41330092	-6.27278000E-08	1.00366837E-07
0.43184523	-6.84125974E-08	1.05024158E-07
0.45044163	-7.65807111E-08	1.12908459E-07
0.46909077	-8.38427106E-08	1.18664615E-07
0.48779331	-9.21669777E-08	1.25360335E-07
0.50654995	-1.01732241E-07	1.33078322E-07
0.52536140	-1.12851553E-07	1.41960354E-07
0.54422840	-1.24736479E-07	1.50877541E-07
0.56315170	-1.38005818E-07	1.60473966E-07
0.58213209	-1.52153354E-07	1.70360813E-07
0.60117037	-1.69568438E-07	1.82744179E-07
0.62026736	-1.88162362E-07	1.95151794E-07
0.63942391	-2.06965971E-07	2.06511679E-07
0.65864090	-2.30071205E-07	2.20924511E-07
0.67791920	-2.56260256E-07	2.36718966E-07
0.69725973	-2.84561125E-07	2.52804581E-07
0.71666341	-3.16024578E-07	2.69900963E-07
0.73613120	-3.52218503E-07	2.89117421E-07
0.75566405	-3.90943761E-07	3.08205395E-07
0.77526296	-4.35214506E-07	3.29522251E-07
0.79492892	-4.85301318E-07	3.52727662E-07
0.81466294	-5.40763760E-07	3.76864436E-07
0.83446606	-6.02798595E-07	4.02458208E-07
0.85433931	-6.74050314E-07	4.30962778E-07
0.87428374	-7.51247862E-07	4.59474432E-07
0.89430042	-8.39558802E-07	4.90497508E-07
0.91439041	-9.37366354E-07	5.22637162E-07
0.93455477	-1.04974239E-06	5.57767411E-07
0.95479459	-1.17195401E-06	5.92723721E-07
0.97511094	-1.31261858E-06	6.30685831E-07
0.99550489	-1.46921558E-06	6.69328522E-07

Appendix II (Continued)

1.0159775	-1.64448127E-06	7.08878688E-07
1.0365298	-1.84096817E-06	7.49113707E-07
1.0571629	-2.06205856E-06	7.89723539E-07
1.0778778	-2.30911789E-06	8.30126251E-07
1.0986754	-2.58627865E-06	8.69414058E-07
1.1195569	-2.89800145E-06	9.07272204E-07
1.1405230	-3.24163069E-06	9.40879881E-07
1.1615748	-3.62923346E-06	9.71189915E-07
1.1827132	-4.05938368E-06	9.94932782E-07
1.2039388	-4.54150554E-06	1.01146057E-06
1.2252527	-5.07357900E-06	1.01726875E-06
1.2466554	-5.66598723E-06	1.01060704E-06
1.2681476	-6.32192634E-06	9.88028431E-07
1.2897300	-7.04716257E-06	9.46420623E-07
1.3114030	-7.84815566E-06	8.81513754E-07
1.3331672	-8.72976617E-06	7.88983039E-07
1.3550228	-9.70260304E-06	6.63999172E-07
1.3769701	-1.07625402E-05	5.00105303E-07
1.3990092	-1.19201500E-05	2.91386339E-07
1.4211403	-1.31827123E-05	3.10895031E-08
1.4433632	-1.45493575E-05	-2.88168021E-07
1.4656777	-1.60298310E-05	-6.74683821E-07
1.4880835	-1.76191819E-05	-1.13636846E-06
1.5105800	-1.93263039E-05	-1.68256701E-06
1.5331667	-2.11479135E-05	-2.32219033E-06
1.5558428	-2.30912406E-05	-3.06545070E-06
1.5786073	-2.51643888E-05	-3.92373613E-06
1.6014591	-2.73952180E-05	-4.91285048E-06
1.6243969	-7.36181232E-10	-2.12467544E-10
1.6474193	-2.38266363E-09	-5.18788189E-10
1.6705246	-3.56291520E-05	-8.78645618E-06
1.6937103	-3.61645686E-05	-9.98972057E-06
1.7169750	-3.85147803E-05	-1.16072207E-05
1.7403162	-4.08468308E-05	-1.33549578E-05
1.7637314	-4.31349029E-05	-1.52269867E-05
1.7872181	-4.53493010E-05	-1.72135802E-05
1.8107733	-4.74532170E-05	-1.92996512E-05
1.8107733	8.06359272E-10	4.35563040E-10
1.7872181	-4.13113288E-05	-1.56931109E-05
1.7637314	-3.96171975E-05	-1.39969930E-05
1.7403162	-3.78015765E-05	-1.23707171E-05
1.7169750	-3.58945854E-05	-1.08284464E-05
1.6937103	-3.39233111E-05	-9.38111152E-06
1.6705246	-3.19185494E-05	-8.03730769E-06

Appendix II (Continued)

1.6474197	-2.99024403E-05	-6.80120927E-06
1.6243976	-2.78977847E-05	-5.67517681E-06
1.6014600	-2.59281419E-05	-4.65983709E-06
1.5786084	-2.40092611E-05	-3.75255196E-06
1.5558440	-2.21540199E-05	-2.94924520E-06
1.5331681	-2.03691295E-05	-2.24448743E-06
1.5105814	-1.86741586E-05	-1.63305484E-06
1.4880850	-1.70642763E-05	-1.10742278E-06
1.4656793	-1.55485035E-05	-6.60769804E-07
1.4433649	-1.41326189E-05	-2.85874870E-07
1.4211420	-1.28125947E-05	2.46985831E-08
1.3990110	-1.15884815E-05	2.78039676E-07
1.3769719	-1.04562528E-05	4.80854611E-07
1.3550247	-9.41597270E-06	6.39660385E-07
1.3331691	-8.46602003E-06	7.60778542E-07
1.3114050	-7.59502068E-06	8.48916227E-07
1.2897320	-6.80384664E-06	9.09744676E-07
1.2681497	-6.08599727E-06	9.47538841E-07
1.2466574	-5.43497185E-06	9.65918119E-07
1.2252548	-4.84837587E-06	9.68791726E-07
1.2039410	-4.31952076E-06	9.59052325E-07
1.1827153	-3.84463431E-06	9.39207348E-07
1.1615770	-3.41781742E-06	9.11804718E-07
1.1405252	-3.03687751E-06	8.78885842E-07
1.1195591	-2.69870864E-06	8.42481836E-07
1.0986777	-2.39213995E-06	8.01872019E-07
1.0778800	-2.11967658E-06	7.59929844E-07
1.0571651	-1.87988102E-06	7.18141619E-07
1.0365321	-1.66523889E-06	6.75705605E-07
1.0159798	-1.47449070E-06	6.33786165E-07
0.99550716	-1.30471062E-06	5.92689893E-07
0.97511322	-1.15333609E-06	5.52550978E-07
0.95479687	-1.02223384E-06	5.15471285E-07
0.93455705	-9.04038768E-07	4.78989811E-07
0.91439268	-7.99182246E-07	4.44363846E-07
0.89430270	-7.07212862E-07	4.12018162E-07
0.87428602	-6.25885454E-07	3.81589592E-07
0.85434158	-5.52546181E-07	3.52150264E-07
0.83446832	-4.88168474E-07	3.24774024E-07
0.81466519	-4.31993646E-07	3.00117864E-07
0.79493116	-3.83363621E-07	2.77572497E-07
0.77526519	-3.38215503E-07	2.55271020E-07
0.75566627	-2.99778880E-07	2.35657561E-07
0.73613340	-2.65747348E-07	2.17453732E-07

Appendix II (Continued)

```
  0.71666560      -2.34464185E-07   1.99459978E-07
  0.69726190      -2.08466835E-07   1.84370744E-07
  0.67792135      -1.83952469E-07   1.69303695E-07
  0.65864303      -1.62206827E-07   1.55195387E-07
  0.63942602      -1.43645950E-07   1.42767620E-07
  0.62026945      -1.26662156E-07   1.30808351E-07
  0.60117243      -1.12970323E-07   1.21289210E-07
  0.58213413      -9.93648212E-08   1.10788646E-07
  0.56315371      -8.71907857E-08   1.00957420E-07
  0.54423038      -7.79921793E-08   9.38192826E-08
  0.52536335      -7.01087904E-08   8.77331245E-08
  0.50655187      -6.10875305E-08   7.96067981E-08
  0.48779519      -5.38099820E-08   7.27375902E-08
  0.46909261      -4.73315328E-08   6.64753522E-08
  0.45044344      -4.15701943E-08   6.08042163E-08
  0.43184699      -3.74674202E-08   5.70107299E-08
  0.41330264      -3.32544575E-08   5.27598843E-08
  0.39480976      -2.91313036E-08   4.81349651E-08
  0.37636774      -2.59132607E-08   4.48412096E-08
  0.35797601      -2.24924221E-08   4.06213356E-08
  0.33963401      -2.05984129E-08   3.89202621E-08
  0.32134121      -1.76991231E-08   3.48676539E-08
  0.30309709      -1.45921288E-08   3.00940068E-08
  0.28490116      -1.32133675E-08   2.85352336E-08
  0.26675295      -1.17851906E-08   2.68157833E-08
  0.24865202      -9.97614384E-09   2.37924154E-08
  0.23059794      -9.02836419E-09   2.27840445E-08
  0.21259029      -8.14118153E-09   2.18481453E-08
  0.19462869      -6.14660881E-09   1.71525668E-08
  0.17671278      -4.66600838E-09   1.38345413E-08
  0.15884220      -2.36450556E-10   7.44723913E-10
  0.14101660       1.53403203E-11   4.39759000E-12
  0.12323525      -2.32018913E-10   8.09669424E-10
  0.10549894      -3.56419321E-09   1.38678047E-08
  8.78067967E-02  -2.94076450E-09   1.23316964E-08
  7.01585608E-02  -2.81346042E-09   1.30400919E-08
  5.25540019E-02  -1.97318858E-09   9.77909261E-09
  3.49929066E-02  -2.03928196E-09   1.14398919E-08
  1.74750786E-02  -1.20443953E-09   7.32510239E-09
  3.39573733E-07  -1.06427490E-09   7.37626628E-09
COMPLIANT LINK, L =    96.102983
MZ                FX                FY
   5.8959368       0.12273181        0.25367429
   5.8959368       8.25794175E-02  -2.20957357E-02
```

Appendix II (Continued)

5.8959368	6.57280172E-02	-0.14105002
5.8959368	5.61188787E-02	-0.21184645
5.8959368	4.97954614E-02	-0.26050689
5.8959368	4.50273356E-02	-0.29645170
5.8959368	4.18012981E-02	-0.32553479
5.8959368	3.92950865E-02	-0.34943282
5.8959368	3.73187904E-02	-0.36970157
5.8959368	3.57448207E-02	-0.38731258
5.2817123	-1.16360698E-03	-0.47859513
4.5327583	-4.37110328E-03	-0.50367275
3.7955388	-6.51178398E-03	-0.52845708
3.0699153	-7.60999905E-03	-0.55293789
2.3557480	-7.68931040E-03	-0.57710557
1.6529045	-6.77245435E-03	-0.60095072
0.96125970	-4.88137600E-03	-0.62446415
0.28069578	-2.03726381E-03	-0.64763683
-0.38889782	1.73941754E-03	-0.67045988
-1.0476242	6.42889270E-03	-0.69292453
-1.6955793	1.20120449E-02	-0.71502215
-2.3328517	1.84703822E-02	-0.73674415
-2.9595227	2.57860092E-02	-0.75808203
-3.5756664	3.39415943E-02	-0.77902733
-4.1813498	4.29203439E-02	-0.79957165
-4.7766324	5.27059715E-02	-0.81970659
-5.3615668	6.32826742E-02	-0.83942379
-5.9361982	7.46351034E-02	-0.85871486
-6.5005648	8.67483445E-02	-0.87757145
-7.0546973	9.96078891E-02	-0.89598517
-7.5986197	0.11319962	-0.91394763
-8.1323482	0.12750977	-0.93145040
-8.6558922	0.14252495	-0.94848505
-9.1692536	0.15823206	-0.96504310
-9.6724268	0.17461833	-0.98111602
-10.165399	0.19167129	-0.99669528
-10.648150	0.20937874	-1.0117723
-11.120651	0.22772875	-1.0263384
-11.582867	0.24670963	-1.0403849
-12.034753	0.26630997	-1.0539031
-12.476258	0.28651855	-1.0668842
-12.907322	0.30732441	-1.0793194
-13.327875	0.32871679	-1.0911997
-13.737840	0.35068518	-1.1025163
-14.137130	0.37321924	-1.1132602
-14.525649	0.39630887	-1.1234223

Appendix II (Continued)

-14.903290	0.41994420	-1.1329934
-15.269938	0.44411553	-1.1419645
-15.625464	0.46881344	-1.1503263
-15.969731	0.49402869	-1.1580695
-16.302587	0.51975232	-1.1651847
-16.623868	0.54597561	-1.1716624
-16.933399	0.57269011	-1.1774933
-17.230987	0.59988767	-1.1826675
-17.516426	0.62756046	-1.1871756
-17.789492	0.65570099	-1.1910076
-18.049944	0.68430214	-1.1941537
-18.297521	0.71335725	-1.1966040
-18.531943	0.74286010	-1.1983482
-18.752903	0.77280500	-1.1993761
-18.960072	0.80318685	-1.1996772
-19.153094	0.83400123	-1.1992411
-19.331579	0.86524446	-1.1980569
-19.495107	0.89691372	-1.1961136
-19.643217	0.92900717	-1.1933999
-19.775409	0.96152411	-1.1899044
-19.891133	0.99446511	-1.1856151
-19.989787	1.0278322	-1.1805199
-20.070707	1.0616293	-1.1746061
-20.133160	1.0958621	-1.1678606
-20.176332	1.1305389	-1.1602698
-20.199319	1.1656706	-1.1518191
-20.201106	1.2012715	-1.1424937
-20.180552	1.2373598	-1.1322774
-20.136365	1.2739585	-1.1211533
-20.067077	1.3110963	-1.1091030
-19.970997	1.3488088	-1.0961068
-19.846175	1.3871406	-1.0821430
-19.690329	1.4261469	-1.0671881
-19.500769	1.4658966	-1.0512155
-19.274279	1.5064766	-1.0341957
-19.006965	1.5479967	-1.0160947
-18.694029	1.5905980	-0.99687366
-18.329444	1.6344644	-0.97648644
-17.905460	1.6798399	-0.95487793
-17.411809	1.7270574	-0.93198018
-16.834386	1.7765859	-0.90770680
-16.152846	1.8291169	-0.88194284
-15.335871	1.8857339	-0.85452485
-14.330426	1.9482930	-0.82519101

Appendix II (Continued)

-13.032101	2.0204384	-0.79340264
-11.155889	2.1132167	-0.75909681
-9.0192968	2.2874484	-0.71665331
-1.6532915	0.57681237	-0.16853089
-2.3557479	0.55432110	-0.16074229
-3.0699154	0.53117826	-0.15377864
-3.7955388	0.50743909	-0.14769851
-4.5327582	0.48310592	-0.14252724
-5.2817206	0.45818110	-0.13829107
-6.0425807	0.43266697	-0.13501718
-6.0425808	0.43266698	-0.13501719
-5.2817206	0.45818110	-0.13829107
-4.5327582	0.48310592	-0.14252724
-3.7955388	0.50743909	-0.14769851
-3.0699154	0.53117826	-0.15377864
-2.3557478	0.55432111	-0.16074229
-1.6529045	0.57686523	-0.16856495
-0.96125978	0.59880825	-0.17722298
-0.28069594	0.62014769	-0.18669345
0.38889793	0.64088104	-0.19695423
1.0476242	0.66100565	-0.20798382
1.6955792	0.68051883	-0.21976143
2.3328515	0.69941776	-0.23226686
2.9595228	0.71769952	-0.24548053
3.5756665	0.73536106	-0.25938338
4.1813497	0.75239923	-0.27395691
4.7766323	0.76881075	-0.28918308
5.3615669	0.78459221	-0.30504435
5.9361982	0.79974008	-0.32152359
6.5005647	0.81425070	-0.33860408
7.0546972	0.82812026	-0.35626953
7.5986198	0.84134488	-0.37450398
8.1323483	0.85392047	-0.39329179
8.6558922	0.86584288	-0.41261770
9.1692535	0.87710780	-0.43246672
9.6724269	0.88771082	-0.45282416
10.165399	0.89764739	-0.47367557
10.648150	0.90691283	-0.49500679
11.120651	0.91550236	-0.51680389
11.582867	0.92341108	-0.53905318
12.034753	0.93063396	-0.56174117
12.476258	0.93716586	-0.58485458
12.907321	0.94300154	-0.60838035
13.327875	0.94813562	-0.63230562

Appendix II (Continued)

13.737840	0.95256262	-0.65661771
14.137130	0.95627695	-0.68130411
14.525649	0.95927287	-0.70635253
14.903290	0.96154457	-0.73175086
15.269938	0.96308608	-0.75748717
15.625464	0.96389132	-0.78354974
15.969731	0.96395408	-0.80992704
16.302587	0.96326801	-0.83660775
16.623868	0.96182662	-0.86358078
16.933399	0.95962326	-0.89083529
17.230987	0.95665113	-0.91836068
17.516426	0.95290322	-0.94614663
17.789492	0.94837238	-0.97418312
18.049944	0.94305120	-1.0024605
18.297521	0.93693206	-1.0309694
18.531943	0.93000710	-1.0597010
18.752903	0.92226813	-1.0886469
18.960072	0.91370668	-1.1177990
19.153094	0.90431392	-1.1471502
19.331579	0.89408058	-1.1766938
19.495107	0.88299697	-1.2064237
19.643217	0.87105286	-1.2363352
19.775409	0.85823743	-1.2664239
19.891133	0.84453917	-1.2966872
19.989787	0.82994579	-1.3271233
20.070707	0.81444409	-1.3577324
20.133160	0.79801982	-1.3885160
20.176332	0.78065751	-1.4194781
20.199319	0.76234023	-1.4506249
20.201106	0.74304939	-1.4819658
20.180552	0.72276439	-1.5135135
20.136365	0.70146221	-1.5452850
20.067077	0.67911702	-1.5773024
19.970997	0.65569948	-1.6095942
19.846175	0.63117604	-1.6421965
19.690329	0.60550789	-1.6751554
19.500769	0.57864970	-1.7085290
19.274279	0.55054781	-1.7423918
19.006965	0.52113786	-1.7768392
18.694029	0.49034138	-1.8119946
18.329445	0.45806087	-1.8480205
17.905460	0.42417244	-1.8851343
17.411809	0.38851414	-1.9236348
16.834386	0.35086669	-1.9639453

Appendix II (Continued)

```
   16.152847       0.31091875       -2.0066940
   15.335871       0.26819827       -2.0528696
   14.330426       0.22191417       -2.1041715
   13.030323       0.17073315       -2.1643746
   11.155582       0.11064468       -2.2427060
  0.96163888      -4.89963670E-03  -0.62440516
   1.6529045      -6.77245572E-03  -0.60095072
   2.3557480      -7.68931150E-03  -0.57710557
   3.0699153      -7.60999988E-03  -0.55293789
   3.7955388      -6.51178452E-03  -0.52845707
   4.5327583      -4.37110352E-03  -0.50367275
   5.2817208      -1.16353473E-03  -0.47859479
   6.0425805       3.13623875E-03  -0.45323340
Max Stress
   6.1251658
   7.7995846
   9.1967479
   10.386807
   11.462996
   12.454655
   13.371542
   14.229913
   15.029086
   15.803786
   14.017332
   14.037438
   14.093132
   14.144231
   14.239578
   14.331166
   14.428180
   14.556667
   14.681731
   14.803323
   14.949454
   15.105262
   15.258134
   15.408012
   15.559058
   15.739972
   15.918394
   16.094262
   16.267512
   16.438081
```

Appendix II (Continued)

16.606119
16.804978
17.001622
17.195985
17.388001
17.577605
17.764731
17.949315
18.131290
18.330078
18.538316
18.744389
18.948229
19.149772
19.348948
19.545689
19.739925
19.931585
20.120597
20.306885
20.490374
20.700464
20.909066
21.115349
21.319241
21.520667
21.719550
21.915809
22.109361
22.300120
22.487994
22.672890
22.854705
23.033336
23.208669
23.380586
23.579214
23.796170
23.995157
24.175361
24.342269
24.529522
24.713642
24.894495

Appendix II (Continued)

```
25.071937
25.245810
25.415938
25.582126
25.744154
25.925583
26.098868
26.244099
26.357657
26.549890
26.756104
26.927398
27.073487
27.255062
27.435807
27.617228
27.803307
28.046970
```

Appendix III: Matlab Code for Plotting Flexion and Extension Moments

```
clf
for index = 0:30
   filename = ['index',num2str(index),'.txt']
   string1  = 'C:\DOCUME~1\aroetter\ANSYS_~1\';   % Directory
   fid1     = fopen([string1,filename]);         % opens the file
   ABT      = fread(fid1);                       % reads the file into variable ABT in machine
code
   fclose(fid1);                                 % closes the data file
   GBT      = native2unicode(ABT)';              % changes data from machine code to text
and writes it to GBT
   header_begin = findstr('FY', GBT);            % finds end of first header
   anterior_end = findstr('POSTERIOR', GBT);
   posterior_end = findstr('COMPLIANT', GBT);
   compliant_end = length(GBT);
   ANTERIOR       = str2num(GBT(header_begin(1)+3:anterior_end-1));    % turns the
data into a numerical matrix
   POSTERIOR    = str2num(GBT(header_begin(2)+3:posterior_end-1));
   COMPLIANT    = str2num(GBT(header_begin(3)+3:compliant_end));



   h=figure(1)
   h1=plot(ANTERIOR(:,1)*180/pi,COMPLIANT(:,1),'*-')
   hold on
   h4 =gca
   set(h4,'FontSize',12)
   axis([0 90 -15 15]) % low x high x, low y high y
   %grid on
   h2=xlabel('Knee Angle (deg)')
   set(h2,'FontSize',12)
   h3=ylabel('BCEA Moment (N-m)')
```

Appendix III (Continued)

```
set(h3,'FontSize',12)


    h=figure(2)
   h1=plot(ANTERIOR(101:191,1)*180/pi,COMPLIANT(101:191,1),'*-')
   hold on
   h4 =gca
   set(h4,'FontSize',12)
   axis([0 90 -15 15]) % low x high x, low y high y
   %grid on
   h2=xlabel('Knee Angle (deg)')
   set(h2,'FontSize',12)
   h3=ylabel('BCEA Moment (N-m)')
   set(h3,'FontSize',12)
end
 %print BCEAMomentall -dtiff -r600

% MATLAB Code for Extension Data Graphing

clf
for index = 25:30
   filename = ['index',num2str(index),'.txt']
   string1  = 'C:\DOCUME~1\aroetter\ANSYS_~1\Loadin~1\';   % Directory
   fid1     = fopen([string1,filename]);         % opens the file
   ABT      = fread(fid1);                       % reads the file into variable ABT in machine
code
   fclose(fid1);                          % closes the data file
   GBT      = native2unicode(ABT)';              % changes data from machine code to text
and writes it to GBT
   header_begin = findstr('FY', GBT);             % finds end of first header
   anterior_end = findstr('POSTERIOR', GBT);
   posterior_end = findstr('COMPLIANT', GBT);
   compliant_end = length(GBT);
```

Appendix III (Continued)

```
 ANTERIOR     = str2num(GBT(header_begin(1)+3:anterior_end-1));   % turns the data
into a numerical matrix
   POSTERIOR    = str2num(GBT(header_begin(2)+3:posterior_end-1));
   COMPLIANT    = str2num(GBT(header_begin(3)+3:compliant_end));

   h=figure(1)
   h1=plot(ANTERIOR(:,1)*180/pi,COMPLIANT(:,1),'*-')
   hold on
   h4 =gca
   set(h4,'FontSize',12)
   axis([0 90 -15 5]) % low x high x, low y high y
   h2=xlabel('Knee Angle (deg)')
   set(h2,'FontSize',12)
   h3=ylabel('BCEA Moment (N-m)')
   set(h3,'FontSize',12)
end
 %print BCEAMomentall -dtiff -r600
```

Appendix IV: Matlab Code for Plotting Reaction Forces

```
clf
index = 30
   filename = ['index',num2str(index),'.txt']
   string1  = 'C:\DOCUME~1\aroetter\ANSYS_~1\';   % Directory
   fid1     = fopen([string1,filename]);         % opens the file
   ABT      = fread(fid1);                       % reads the file into variable ABT in machine
code
   fclose(fid1);                                 % closes the data file
   GBT      = native2unicode(ABT)';              % changes data from machine code to text
and writes it to GBT
   header_begin = findstr('FY', GBT);            % finds end of first header
   anterior_end = findstr('POSTERIOR', GBT);
   posterior_end = findstr('COMPLIANT', GBT);
   compliant_end = length(GBT);
   ANTERIOR      = str2num(GBT(header_begin(1)+3:anterior_end-1));   % turns the

data into a numerical matrix
   %ANTERIORFX    = str2num(GBT(header_begin(1)+19:anterior_end-1));
   %ANTERIORFY    = str2num(GBT(header_begin(1)+36:anterior_end-1));
   POSTERIOR   = str2num(GBT(header_begin(2)+3:posterior_end-1));
   %POSTERIORFY   = str2num(GBT(header_begin(2)+36:posterior_end-1));

   ANTERIOR_MAG = (ANTERIOR(10:100,2).^2+ANTERIOR(10:100,3).^2).^0.5;
   ANTERIOR_ANG = atan2(ANTERIOR(10:100,3),ANTERIOR(10:100,2))*180/pi;

   POSTERIOR_MAG = (POSTERIOR(10:100,2).^2+POSTERIOR(10:100,3).^2).^0.5;
   POSTERIOR_ANG = atan2(POSTERIOR(10:100,3),POSTERIOR(10:100,2))*180/pi;


   h=figure(1)
   h1=plot(ANTERIOR(10:100,1)*180/pi,ANTERIOR(10:100,2),'*-')
   hold on
   h4 =gca
   set(h4,'FontSize',12)
   %axis([0 90 -15 15]) % low x high x, low y high y
   %grid on
   h2=xlabel('Knee Angle (deg)')
   set(h2,'FontSize',12)
   h3=ylabel('Fx-Anterior (N)')
   set(h3,'FontSize',12)
```

Appendix IV (Continued)

```
h=figure(2)
h1=plot(ANTERIOR(10:100,1)*180/pi,ANTERIOR(10:100,3),'*-')
hold on
h4 =gca
set(h4,'FontSize',12)
%axis([0 90 -15 15]) % low x high x, low y high y
%grid on
h2=xlabel('Knee Angle (deg)')
set(h2,'FontSize',12)
h3=ylabel('Fy-Anterior (N)')
set(h3,'FontSize',12)

h=figure(3)
h1=plot(ANTERIOR_ANG,ANTERIOR_MAG,'*-')
hold on
h4 =gca
set(h4,'FontSize',12)
%axis([0 90 -15 15]) % low x high x, low y high y
%grid on
h2=xlabel('Direction (deg)')
set(h2,'FontSize',12)
h3=ylabel('|F|-Anterior (N)')
set(h3,'FontSize',12)

h=figure(4)
h1=plot(ANTERIOR(10:100,1)*180/pi,ANTERIOR_MAG,'*-')
hold on
h4 =gca
set(h4,'FontSize',12)
%axis([0 90 -15 15]) % low x high x, low y high y
%grid on
h2=xlabel('Knee Angle (deg)')
set(h2,'FontSize',12)
h3=ylabel('|F|-Anterior (N)')
set(h3,'FontSize',12)




h=figure(5)
h1=plot(ANTERIOR(10:100,1)*180/pi,POSTERIOR(10:100,2),'*-')
hold on
h4 =gca
```

Appendix IV (Continued)

```
set(h4,'FontSize',12)
 %axis([0 90 -15 15]) % low x high x, low y high y
 %grid on
 h2=xlabel('Knee Angle (deg)')
 set(h2,'FontSize',12)
 h3=ylabel('Fx-Posterior (N)')
 set(h3,'FontSize',12)

 h=figure(6)
 h1=plot(ANTERIOR(10:100,1)*180/pi,POSTERIOR(10:100,3),'*-')
 hold on
 h4 =gca
 set(h4,'FontSize',12)
 %axis([0 90 -15 15]) % low x high x, low y high y
 %grid on
 h2=xlabel('Knee Angle (deg)')
 set(h2,'FontSize',12)
 h3=ylabel('Fy-Posterior (N)')
 set(h3,'FontSize',12)

 h=figure(7)
 h1=plot(POSTERIOR_ANG,POSTERIOR_MAG,'*-')
 hold on
 h4 =gca
 set(h4,'FontSize',12)
 %axis([0 90 -15 15]) % low x high x, low y high y
 %grid on
 h2=xlabel('Direction (deg)')
 set(h2,'FontSize',12)
 h3=ylabel('|F|-Posterior (N)')
 set(h3,'FontSize',12)

 h=figure(8)
 h1=plot(ANTERIOR(10:100,1)*180/pi,POSTERIOR_MAG,'*-')
 hold on
 h4 =gca
 set(h4,'FontSize',12)
 %axis([0 90 -15 15]) % low x high x, low y high y
 %grid on
 h2=xlabel('Knee Angle (deg)')
 set(h2,'FontSize',12)
 h3=ylabel('|F|-Posterior (N)')
 set(h3,'FontSize',12)
```

Appendix IV (Continued)

```
h=figure(9)
h1=plot(ANTERIOR(10:100,1)*180/pi,POSTERIOR_MAG,'.-')
hold on
h4 =gca
set(h4,'FontSize',12)
%axis([0 90 -15 15]) % low x high x, low y high y
%grid on
h2=xlabel('Knee Angle (deg)')
set(h2,'FontSize',12)
h3=ylabel('|F| (N)')
set(h3,'FontSize',12)
h5=plot(ANTERIOR(10:100,1)*180/pi,ANTERIOR_MAG,'k+-')


%print BCEAMomentall -dtiff -r600
```

Appendix V: Reaction Force Plots

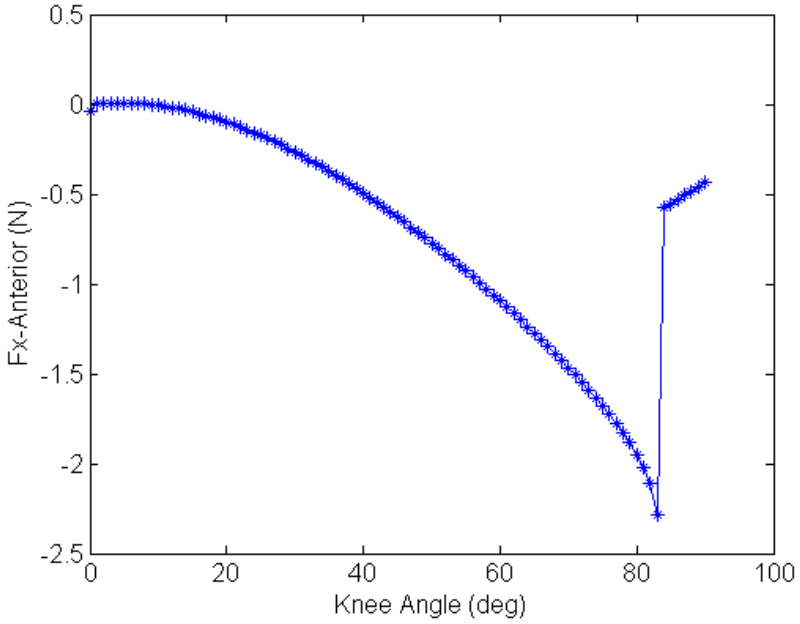

Figure A-1. Anterior Force in x-Direction vs. Knee Angle

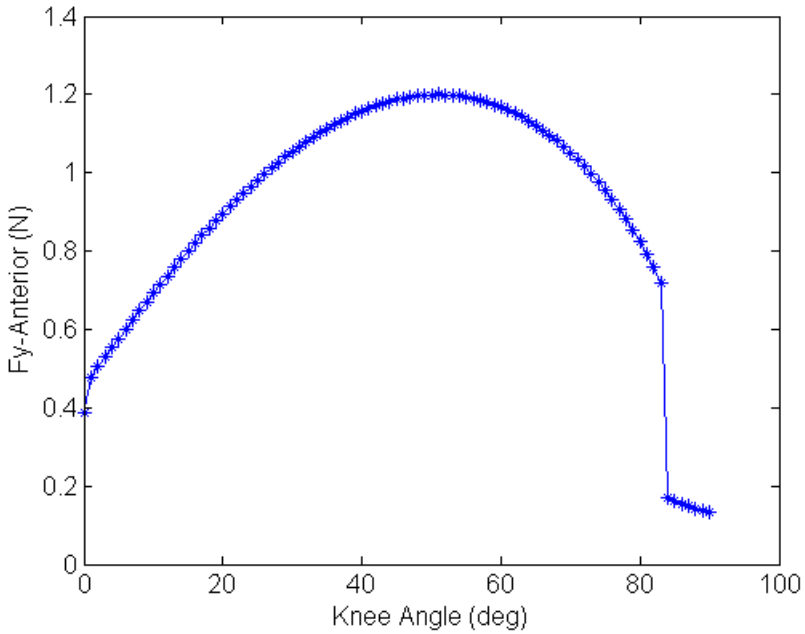

Figure A-2. Anterior Force in y-Direction vs. Knee Angle

Appendix V (Continued)

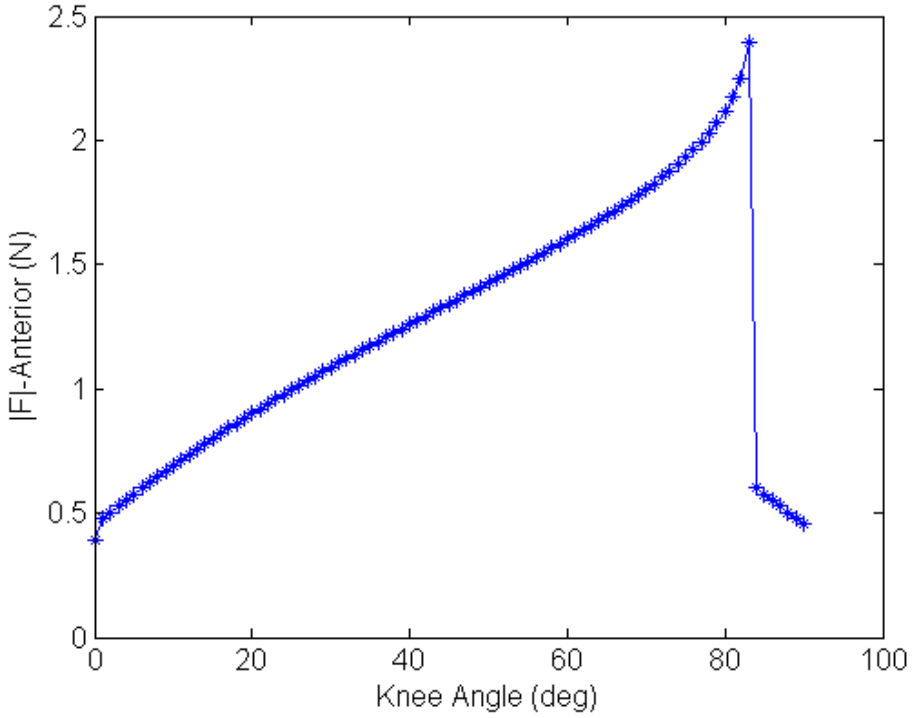

Figure A-3. Magnitude of Anterior Force vs. Knee Angle

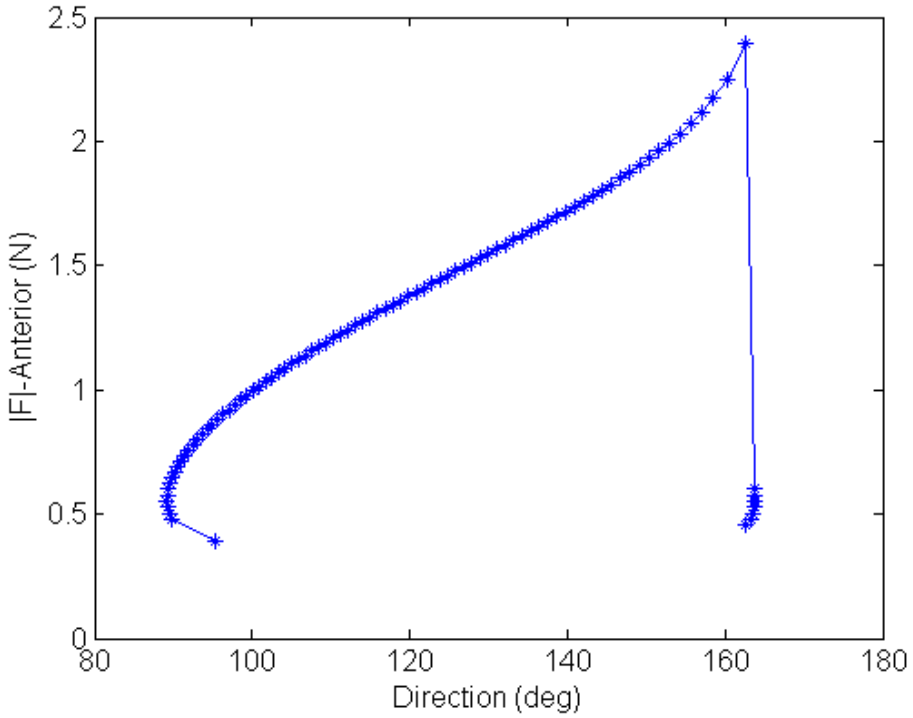

Figure A-4. Magnitude of Anterior Force vs. Direction

Appendix V (Continued)

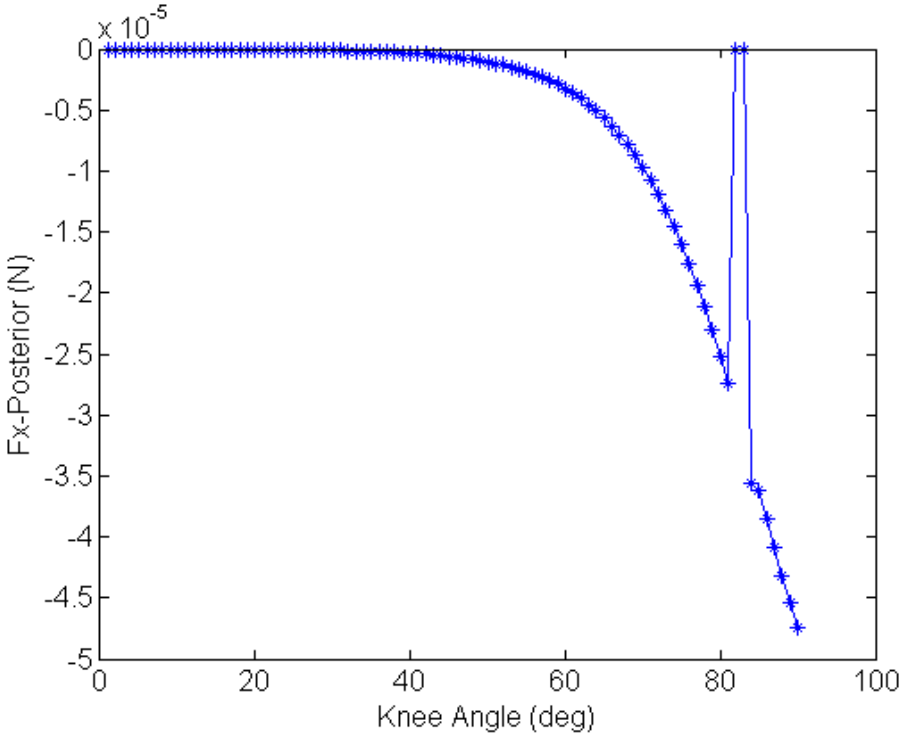

Figure A-5. Posterior Force in x-Direction vs. Knee Angle

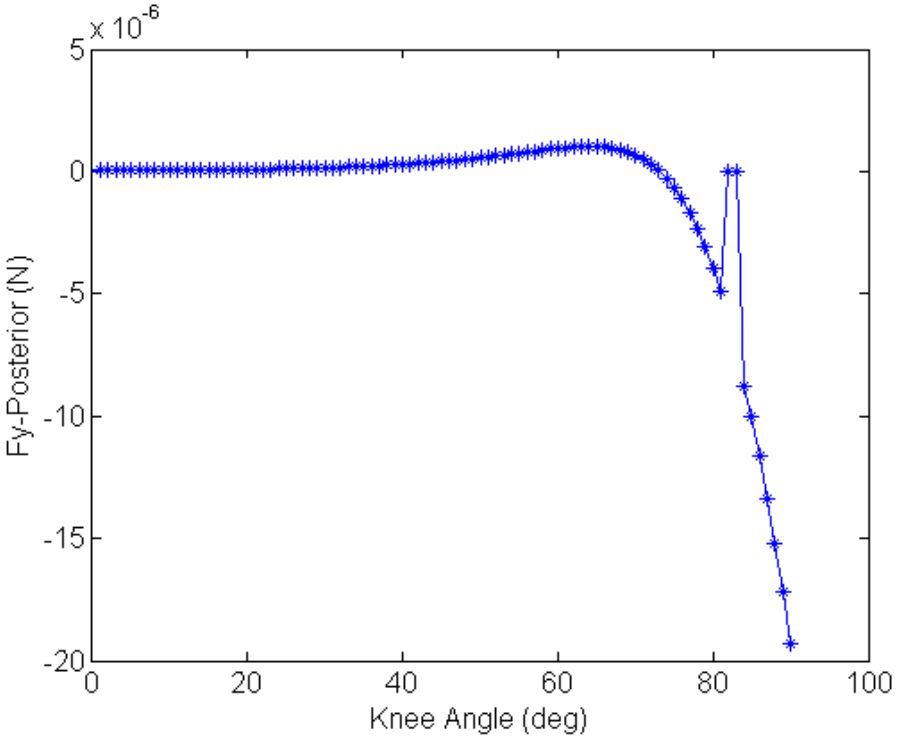

Figure A-6. Posterior Force in y-Direction vs. Knee Angle

Appendix V (Continued)

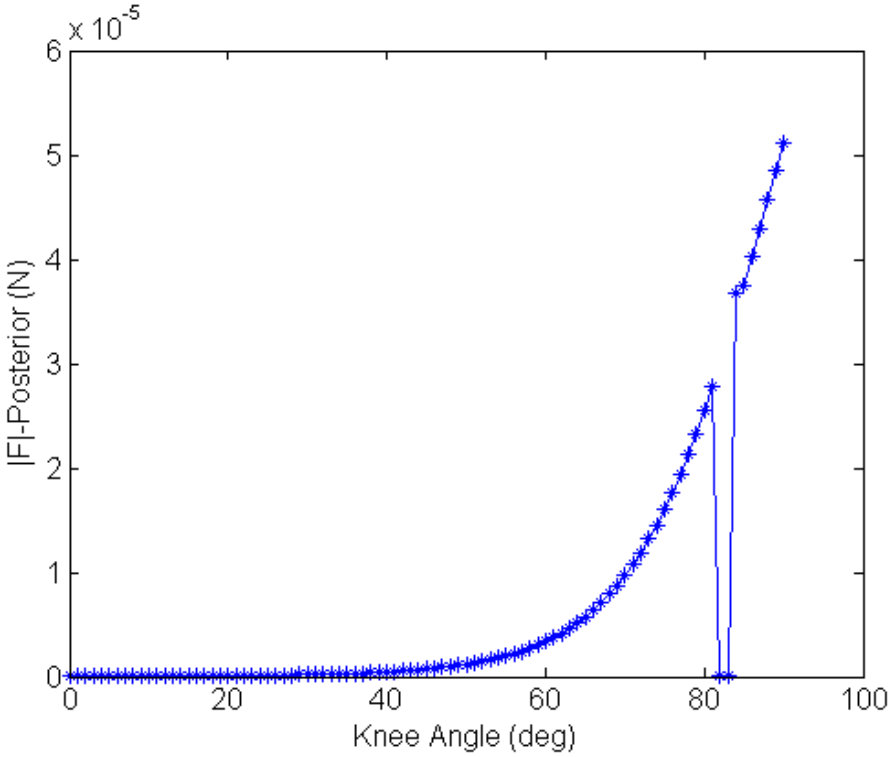

Figure A-7. Magnitude of Posterior Force vs. Knee Angle

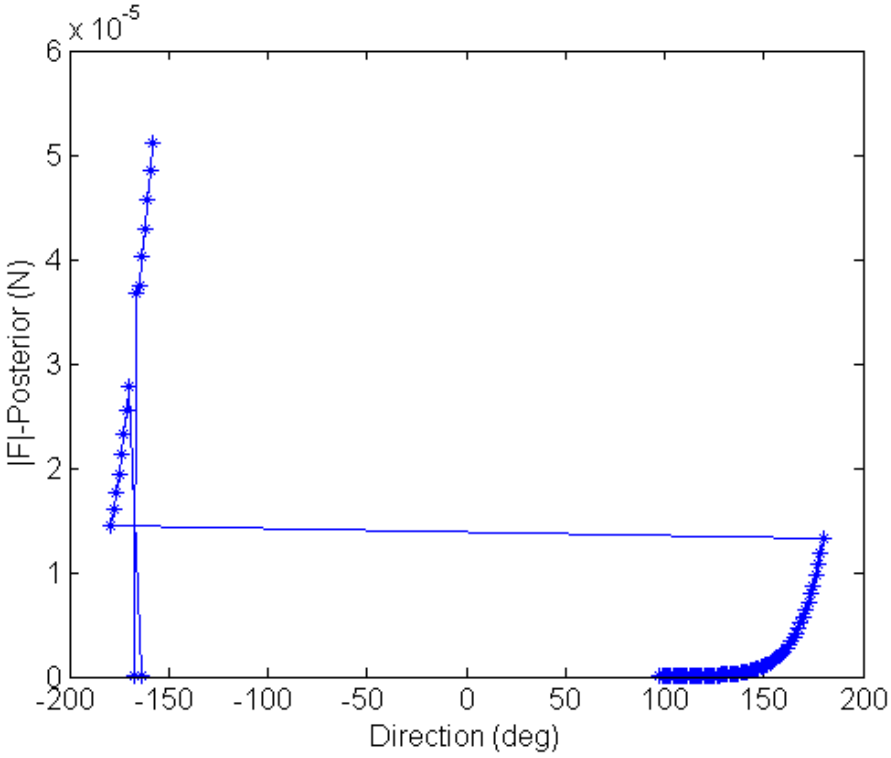

Figure A-8. Magnitude of Posterior Force vs. Direction

Appendix VI: COSMOSWorks Report File – Socket and Knee

Stress analysis of Residuum and Knee with BCEA Loads during Flexion
Author: Adam D. Roetter

---

1. Introduction

Summarize the FEM analysis on Top Half of Leg with Knee Bracket for Moment Application
Note:
Do not base your design decisions solely on the data presented in this report. Use this information in conjunction with experimental data and practical experience. Field testing is mandatory to validate your final design. COSMOSWorks helps you reduce your time-to-market by reducing but not eliminating field tests.

Appendix VI (Continued)

2. File Information

Model name:	Top Half of Leg with Knee Bracket for Moment Application
Model location:	C:\Users\Adam\Documents\SolidWorks Thesis\Top half of System (Residuum Stresses)\Top Half of Leg with Knee Bracket for Moment Application.SLDASM
Results location:	c:\users\adam\appdata\local\temp
Study name:	Moment Application Xdeg of Rotation (-Default-)

---

3. Materials

No.	Part Name	Material	Mass	Volume
1	Disartic Knee Top Link Bracket With Socket Attachment-1	[SW]Titanium	0.151837 kg	3.30081e-005 m^3
2	Residuum-1	[SW]Rubber	8.65506 kg	0.00865506 m^3
3	Socket to fit top link with bracket-1	[SW]PE Low/Medium Density	0.536364 kg	0.000584911 m^3

Appendix VI (Continued)

4. Load & Restraint Information

Restraint	
Restraint-1 <Residuum-1>	on 1 Face(s) fixed.
Description:	

Load	
Force-1 <Disartic Knee Top Link Bracket With Socket Attachment-1>	on 1 Face(s) apply force -20.201 N along circumferential. with respect to selected reference Face< 1 > using uniform distribution
Force-2 <Disartic Knee Top Link Bracket With Socket Attachment-1>	on 1 Edge(s) apply force -1.2013 N normal to reference plane with respect to selected reference Edge< 1 > using uniform distribution
Force-3 <Disartic Knee Top Link Bracket With Socket Attachment-1>	on 1 Edge(s) apply force -4.0594e-006 N normal to reference plane with respect to selected reference Edge< 1 > using uniform distribution
Force-4 <Disartic Knee Top Link Bracket With Socket Attachment-1>	on 1 Edge(s) apply force 1.1425 N normal to reference plane with respect to selected reference Top Plane using uniform distribution

Appendix VI (Continued)

5. Study Property

Mesh Information	
Mesh Type:	Solid mesh
Mesher Used:	Standard
Automatic Transition:	On
Smooth Surface:	On
Jacobian Check:	4 Points
Element Size:	1.0754 in
Tolerance:	0.053772 in
Quality:	High
Number of elements:	13803
Number of nodes:	22393
Time to complete mesh(hh;mm;ss):	00:00:14
Computer name:	INTELC2D

Solver Information	
Quality:	High
Solver Type:	FFEPlus
Option:	Include Thermal Effects
Thermal Option:	Input Temperature
Thermal Option:	Reference Temperature at zero strain: 298 Kelvin

Appendix VI (Continued)

6. Contact

Contact state: Touching faces - Bonded

7. Results

7a. Stress2 (von Mises)

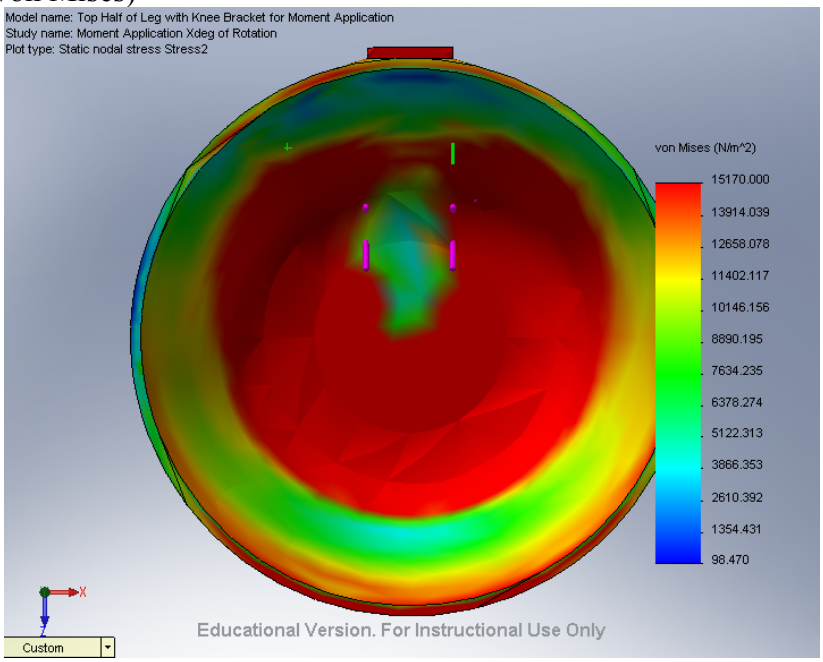

7a. Strain1 (-Equivalent-)

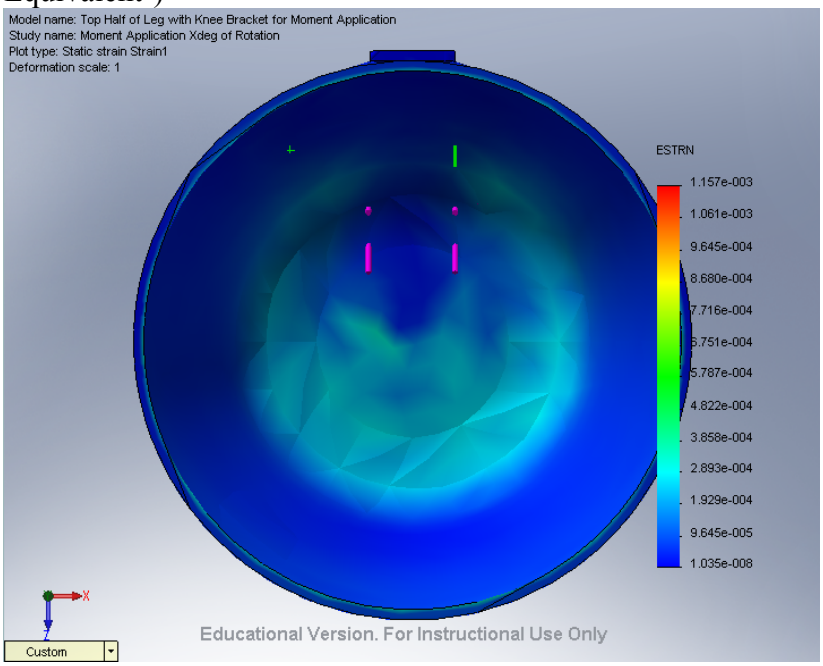

Appendix VI (Continued)

7b. Default Results

Name	Type	Min	Location	Max	Location
Stress2	VON: von Mises stress	2.49959 N/m^2 Node: 12454	(0.295982 in, 0.127197 in, 1.62194 in)	3.91105e+006 N/m^2 Node: 2652	(1.13819 in, -0.945371 in, 0.071128 in)
Strain1	ESTRN: Equivalent strain	1.03548e-008 Node: 5103	(0.946526 in, -2.36945 in, 0.071128 in)	0.00115734 Node: 21022	(0.941113 in, -1.36445 in, 2.35248 in)

8. Appendix

Material name:	[SW]Titanium
Description:	
Material Source:	Used SolidWorks material
Material Library Name:	SolidWorks Materials
Material Model Type:	Linear Elastic Isotropic

Appendix VI (Continued)

Property Name	Value	Units	Value Type
Elastic modulus	1.1e+011	N/m^2	Constant
Poisson's ratio	0.3	NA	Constant
Shear modulus	4.3e+010	N/m^2	Constant
Mass density	4600	kg/m^3	Constant
Tensile strength	2.35e+008	N/m^2	Constant
Yield strength	1.4e+008	N/m^2	Constant
Thermal expansion coefficient	9e-006	/Kelvin	Constant
Thermal conductivity	22	W/(m.K)	Constant
Specific heat	460	J/(kg.K)	Constant

Material name: [SW]Rubber

Description:

Material Source: Used SolidWorks material

Material Library Name: solidworks materials

Material Model Type: Linear Elastic Isotropic

Property Name	Value	Units	Value Type
Elastic modulus	6.1e+006	N/m^2	Constant
Poisson's ratio	0.49	NA	Constant
Shear modulus	2.9e+006	N/m^2	Constant
Mass density	1000	kg/m^3	Constant
Tensile strength	1.3787e+007	N/m^2	Constant
Yield strength	9.2374e+006	N/m^2	Constant
Thermal expansion coefficient	0.00067	/Kelvin	Constant
Thermal conductivity	0.14	W/(m.K)	Constant

Appendix VI (Continued)

Material name: [SW]PE Low/Medium Density

Description:

Material Source: Used SolidWorks material

Material Library Name: solidworks materials

Material Model Type: Linear Elastic Isotropic

Property Name	Value	Units	Value Type
Elastic modulus	1.72e+008	N/m^2	Constant
Poisson's ratio	0.439	NA	Constant
Shear modulus	5.94e+007	N/m^2	Constant
Mass density	917	kg/m^3	Constant
Tensile strength	1.327e+007	N/m^2	Constant
Thermal conductivity	0.322	W/(m.K)	Constant
Specific heat	1842	J/(kg.K)	Constant